U.S. Department of the Interior
U.S. Geological Survey

Miocene Extension and Post-Miocene Transpression Offshore of South-Central California

Structure and Tectonics of the Central Offshore Santa Maria and Santa Lucia Basins, California: Results from the PG&E/EDGE Seismic Reflection Survey

Bulletin 1995–Y, Z

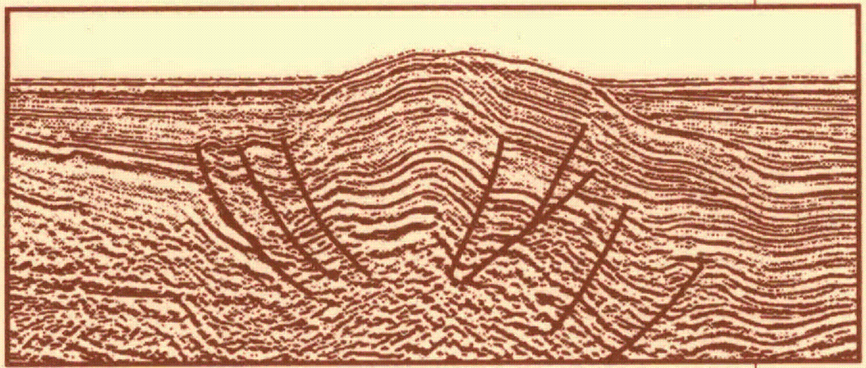

Geophysical section offshore Santa Maria basin

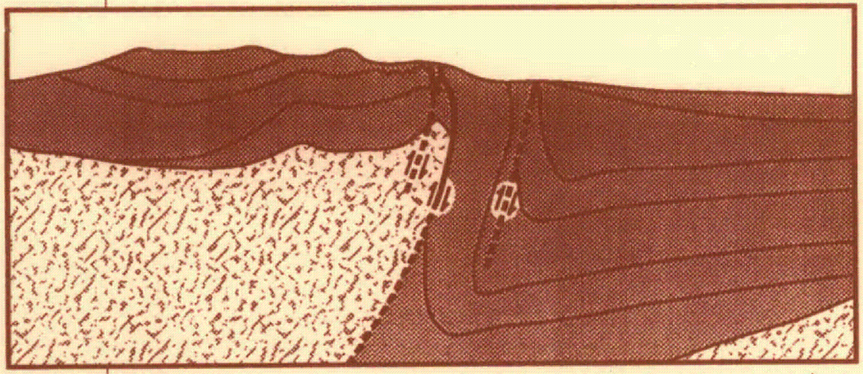

Geologic section onshore Santa Maria basin

USGS
science for a changing world

Availability of Publications of the U.S. Geological Survey

Order U.S. Geological Survey (USGS) publications from the offices listed below. Detailed ordering instructions, along with prices of the last offerings, are given in the current-year issues of the catalog "New Publications of the U.S. Geological Survey."

Books, Maps, and Other Publications

By Mail

Books, maps, and other publications are available by mail from—

USGS Information Services
Box 25286, Federal Center
Denver, CO 80225

Publications include Professional Papers, Bulletins, Water-Supply Papers, Techniques of Water-Resources Investigations, Circulars, Fact Sheets, publications of general interest, single copies of permanent USGS catalogs, and topographic and thematic maps.

Over the Counter

Books, maps, and other publications of the U.S. Geological Survey are available over the counter at the following USGS Earth Science Information Centers (ESIC's), all of which are authorized agents of the Superintendent of Documents:

- Anchorage, Alaska–Rm. 101, 4230 University Dr.
- Denver, Colorado–Bldg. 810, Federal Center
- Menlo Park, California–Rm. 3128, Bldg. 3, 345 Middlefield Rd.
- Reston, Virginia–Rm. 1C402, USGS National Center, 12201 Sunrise Valley Dr.
- Salt Lake City, Utah–2222 West, 2300 South (books and maps available for inspection only)
- Spokane, Washington–Rm. 135, U.S. Post Office Building, 904 West Riverside Ave.
- Washington, D.C.–Rm. 2650, Main Interior Bldg., 18th and C Sts., NW.

Maps only may be purchased over the counter at the following USGS office:

- Rolla, Missouri–1400 Independence Rd.

Electronically

Some USGS publications, including the catalog "New Publications of the U.S. Geological Survey" are also available electronically on the USGS's World Wide Web home page at **http://www.usgs.gov**

Preliminary Determination of Epicenters

Subscriptions to the periodical "Preliminary Determination of Epicenters" can be obtained only from the Superintendent of Documents. Check or money order must be payable to the Superintendent of Documents. Order by mail from—

Superintendent of Documents
Government Printing Office
Washington, DC 20402

Information Periodicals

Many Information Periodicals products are available through the systems or formats listed below:

Printed Products

Printed copies of the Minerals Yearbook and the Mineral Commodity Summaries can be ordered from the Superintendent of Documents, Government Printing Office (address above). Printed copies of Metal Industry Indicators and Mineral Industry Surveys can be ordered from the Center for Disease Control and Prevention, National Institute for Occupational Safety and Health, Pittsburgh Research Center, P.O. Box 18070, Pittsburgh, PA 15236–0070.

Mines FaxBack: Return fax service

1. Use the touch-tone handset attached to your fax machine's telephone jack. (ISDN [digital] telephones cannot be used with fax machines.)
2. Dial (703) 648–4999.
3. Listen to the menu options and punch in the number of your selection, using the touch-tone telephone.
4. After completing your selection, press the start button on your fax machine.

CD-ROM

A disc containing chapters of the Minerals Yearbook (1993–95), the Mineral Commodity Summaries (1995–97), a statistical compendium (1970–90), and other publications is updated three times a year and sold by the Superintendent of Documents, Government Printing Office (address above).

World Wide Web

Minerals information is available electronically at **http://minerals.er.usgs.gov/minerals/**

Subscription to the catalog "New Publications of the U.S. Geological Survey"

Those wishing to be placed on a free subscription list for the catalog "New Publications of the U.S. Geological Survey" should write to—

U.S. Geological Survey
903 National Center
Reston, VA 20192

Miocene Extension and Post-Miocene Transpression Offshore of South-Central California

By CHRISTOPHER C. SORLIEN, CRAIG NICHOLSON, and BRUCE P. LUYENDYK

Structure and Tectonics of the Central Offshore Santa Maria and Santa Lucia Basins, California: Results from the PG&E/EDGE Seismic Reflection Survey

By KATE C. MILLER and ANNE S. MELTZER

Chapters Y and Z are issued as a single volume
and are not available separately

U.S. GEOLOGICAL SURVEY BULLETIN 1995

EVOLUTION OF SEDIMENTARY BASINS/ONSHORE OIL AND GAS INVESTIGATIONS—
SANTA MARIA PROVINCE

Edited by Margaret A. Keller

U.S. DEPARTMENT OF THE INTERIOR
BRUCE BABBITT, Secretary

U.S. GEOLOGICAL SURVEY
Charles G. Groat, Director

UNITED STATES GOVERNMENT PRINTING OFFICE, WASHINGTON: 1999

For sale by
U.S. Geological Survey
Information Services
Box 25286
Denver Federal Center
Denver, CO 80225

Chapter Y

Miocene Extension and Post-Miocene Transpression Offshore of South-Central California

By CHRISTOPHER C. SORLIEN, CRAIG NICHOLSON, and BRUCE P. LUYENDYK

U.S. GEOLOGICAL SURVEY BULLETIN 1995–Y

EVOLUTION OF SEDIMENTARY BASINS/ONSHORE OIL AND GAS INVESTIGATIONS—SANTA MARIA PROVINCE

Edited by Margaret A. Keller

CONTENTS

PLATE

FIGURES

TABLE

Miocene Extension and Post-Miocene Transpression Offshore of South-Central California

By Christopher C. Sorlien[1], Craig Nicholson[2], and Bruce P. Luyendyk[3]

Abstract

A complex Neogene history characterizes the offshore Santa Maria basin and the northwest margin of the western Transverse Ranges, California. This history includes the transition from subduction to a transtensional and then transpressional plate boundary, including about 90° of clockwise rotation of the western Transverse Ranges. We use seismic reflection data to document the geometry of structures that accommodated this deformation and offshore well data to date and correlate the sediments which were affected by the different tectonic episodes.

The offshore Santa Maria basin is flanked by two systems of anastamosing to en-echelon moderately east-dipping faults, including the Santa Lucia Bank Fault and newly mapped West Basin Fault to the west, and the Offshore Lompoc, Purisima, and Hosgri Faults to the east. Between these two systems, northeast-striking cross faults downdrop the basement toward the south, from 2 km beneath the offshore Santa Maria basin to 8 km in the western Santa Barbara Channel. There is no significant fault boundary between the western Santa Barbara Channel and the offshore Santa Maria basin in upper Miocene and younger sediments, suggesting that these two provinces either rotated together, or no significant rotation occurred in this area since about 12 Ma. Normal separation of Miocene horizons indicates early and middle Miocene extension, while little-deformed upper Miocene sediments across the axis of the basin suggest slowed rates of extension. Subsequent contraction, revealed by folding and faulting, initiated at the beginning of the Pliocene but was most important toward the end of early Pliocene time.

Reflections (and refractions) from the top of oceanic crust (the Monterey Microplate) have been traced from the Pacific Ocean basin to beneath the offshore Santa Maria basin. We suggest that if subducted Monterey Microplate slab now forms the lower crust, it must have formed the lower crust at the time of microplate capture. Microplate capture occurred at about the same time as initiation of basin formation and rotation of the western Transverse Ranges Province. Thus, capture of the slab resulted in its motion with the Pacific Plate away from North America. The western Transverse Ranges and onshore and offshore Santa Maria basin were carried above the slab, resulting in the rifting of these provinces away from the Peninsular Ranges. In this model, no large-scale lateral slip on high-angle faults along and west of offshore Santa Maria basin is required or expected. Deposition, erosion, and tectonic denudation adequately explain contrasting stratigraphy between inferred crustal terranes. After a late Miocene period of relative inactivity, faults bounding the offshore Santa Maria basin were reactivated by Pliocene and Quaternary transpression. Most of the folding associated with this later episode is localized to either bends in the basin-bounding faults, to intersections with cross faults, or to transpressive regions associated with small block rotation; many faults preserve normal separations of Miocene horizons.

[1]Institute for Crustal Studies, University of California, Santa Barbara, CA 93106; home office: 61 Western Highway, Tappan, NY 10983.

[2]Institute for Crustal Studies, University of California, Santa Barbara, CA 93106.

[3] Department for of Geological Sciences and Institute for Crustal Studies, University of California, Santa Barbara, CA 93106.

Approved for publication May 20, 1999

INTRODUCTION

Geographic and Tectonic Setting

The southern offshore Santa Maria basin and western Santa Barbara Channel are critical areas to the understanding of the evolution of the Neogene California transform margin. This study area is located across and adjacent to several physiographic and structural provinces, including the western Transverse Ranges, the onshore and offshore Santa Maria basin, the Coast Ranges, and the California Continental Borderland (fig. 1). These provinces contain contrasting stratigraphic sections and structural styles, as well as different structural trend. Offshore Santa Maria basin is only lightly overprinted by subsequent deformation; therefore, the record of basin formation during the Miocene is preserved. Deposition of sediment across structures permits timing of Neogene deformation.

The original plate tectonic model for the Tertiary evolution of western North America includes orthogonal subduction of the Farallon Plate, approach of the Pacific-Farallon spreading centers to the subduction zone, and initiation of a transform boundary during late Oligocene time (Atwater, 1970). Regional tectonic models for the California margin proposed that strike-slip faults accommodated plate motion, that subduction-related stratigraphic belts were rearranged by strike-slip motion, and that extension and contraction were related to transtension or transpression along these faults (Howell and others, 1987; Vedder, 1987; McCulloch, 1987, 1989a; Sedlock and Hamilton, 1991). Recently, details of the breakup of the Farallon Plate have been studied, and the existence and continuing early Miocene spreading (and subduction?) of the Monterey and Arguello Plates has been recognized (Lonsdale, 1991; Severinghaus and Atwater, 1991). Abundant paleomagnetic data indicate Neogene clockwise rotation (90°+) of the western Transverse Ranges (Luyendyk and others, 1980, 1985; Luyendyk, 1991). The capture of the Monterey Plate by the Pacific Plate was completed by about 19 Ma (Lonsdale, 1991), a timing that approximately coincides with the initiation of this rotation. A mechanism linking microplate capture to large-scale extension of western North America and to rotation of the western Transverse Ranges has been proposed (Nicholson and others, 1994; Bohannon and

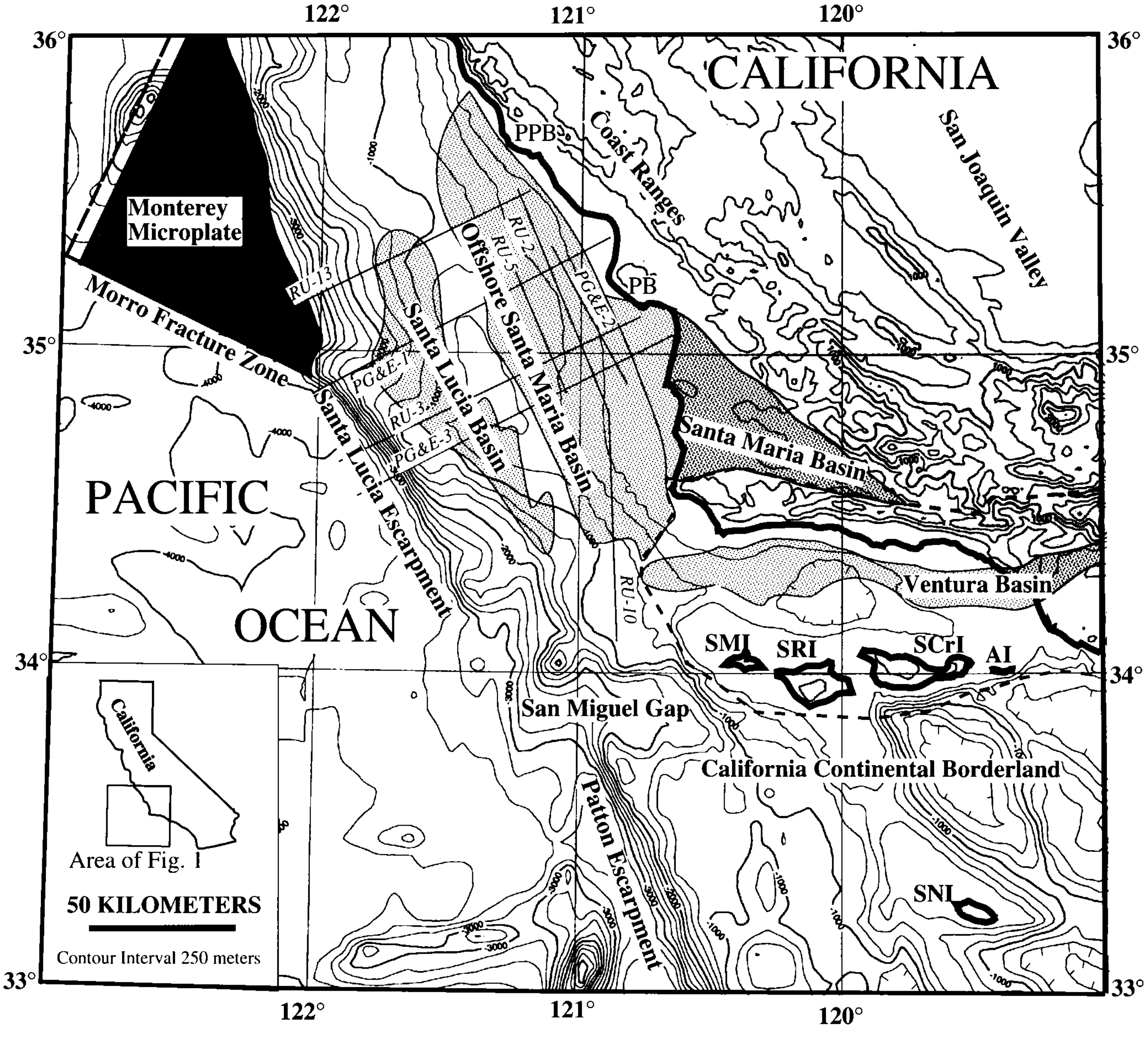

Figure 1. Map showing geographic features nearshore and offshore south-central California. EDGE (RU) and PG&E seismic reflection profile locations are also shown. Basins discussed in text are shown in stipple pattern as they appear today; their Miocene extent was likely different. Western Transverse Ranges are outlined by heavy dashed line. The seamount on the west-northwest edge of the Monterey Microplate outlined by the dashed line is interpreted to be a fossil spreading center (Lonsdale, 1991; Atwater, 1989). AI, Anacapa Island; PB, Point Buchon; PPB, Point Piedras Blancas; SCrI, Santa Cruz Island; SMI, San Miguel Island; SNI, San Nicolas Island; SRI, Santa Rosa Island.

Parsons, 1995; see also Tennyson, 1989). Large-scale extension accommodated by detachment faults has been proposed across the inner California Continental Borderland, located between the rotating western Transverse Ranges and the Peninsular Ranges (Yeats, 1976; Kamerling and Luyendyk, 1985; Legg, 1991; Crouch and Suppe, 1993). Miocene extension has been proposed for offshore Santa Maria basin (McCulloch, 1987, 1989a; Clark and others, 1991), but the timing, magnitude, and location of this extension has not been incorporated into a regional tectonic model.

In this chapter, we present a comprehensive regional study of the deep structure and stratigraphy of southern offshore Santa Maria basin and its "boundary" with the western Transverse Ranges. This work is based on the abundant seismic reflection and well data that exist in the study area, many of which are now publicly available. We integrate geologic and geophysical data to document the geometry, history of deformation, and structural style of this region. A two-dimensional map restoration of the southwest California margin is constructed in an attempt to relate Neogene structure to tectonic models. This map preserves area so that its predictions for net extension and its finite displacement for different areas can be compared to the individual structures. Other tectonic models utilize much larger fault blocks or "terranes" with the result that apparent motions become a problem and it is difficult to compare predicted motions to individual structures. Thus, this paper provides tests and outlines potential tests for a microplate slab capture mechanism for rotation of the western Transverse Ranges and parts of onshore and southern offshore Santa Maria basin (see Nicholson and others, 1994, vs. Bohannon and Parsons, 1995).

ACKNOWLEDGMENTS

We owe thanks to an unusually large number of people for technical help, logistical help, and geologic and geophysical discussions. The following individuals provided significant technical and logistical support, provided pre-prints of their work, and/or were valued for geologic and geophysical discussions.

Jim Crouch; John Crowell; Ed Edwards; Carl Evans; Jim Galloway; Jean-Pierre Gratier; Caroline Isaacs; Dale Julander; Bill Lettis; Margaret Keller; Jeff Kennedy; Calvin Lee; Mark Legg; Pat McCrory; Drew Mayerson; Art Sylvester; Rob Skillen; Rick Stanley; Lynn Tennyson; Frank Victor; Elaine Weed; Jack Williams; Richard Willingham; Julie Zweig; Mitch Lyle provided the site survey for ODP site CA-9.

The Minerals Management Service staff, several credited above, provided access to public well information and public high resolution seismic data, as well as insight into offshore geology.

An earlier version of this manuscript was edited by Ken Bird, Steve Lewis, and Scott Starratt. The current version is quite different, so we are responsible for any errors or omissions. This version was reviewed by Drew Mayerson, and edited by Margaret Keller, C. Powell, and Julia Thomas; we thank them for their efforts.

The excellent maps of, as well as geologic discussions with, Tom Dibblee Jr. and Helmut Ehrenspeck were important to understanding of western Transverse Ranges geology.

Robin Weeks and Stan Cisowski were part of the work on rotation of Santa Maria basin.

Tanya Atwater provided discussions of plate interactions.

Aaron Martin provided computer assistance.

Bob Bohannon and Jon Childs provided the data for USGS-105. Jon also provided processing suggestions, preliminary velocity analysis, and the data for the other USGS profiles.

Ken Bird and Ron Heck provided much assistance with stratigraphy and structural interpretations.

This project was funded by the American Chemical Society/Petroleum Research Fund, ACS PRF21194-AC2 to B. P. Luyendyk and ACS PRF24539-AC2-C to Luyendyk and C. Nicholson. Institute for Crustal Studies Contribution number 0184-44TC.

DATA ANALYSIS

Reprocessing

The structure and stratigraphy of the offshore Santa Maria basin was studied using public multichannel and single-channel seismic reflection profiles (fig. 2). These profiles were correlated to about 25 offshore wells. Regional structure was mapped using these data and multichannel industry data (lines and well locations shown in figure 3).

Serious noise problems contaminated initial stacks of seismic reflection profiles in the offshore California region. The strongest acoustic impedance contrasts are expected to be those between air and water, water and sediment, top of volcanic rocks, metamorphic rocks, thick chert horizons, and certain unconformities. Multiple reverberations between any of these layers are possible, while extra bounces of sound energy in the water layer are common. In addition, reflections from out-of-plane structure (sideswipe) are possible, as well as noise sources such as passing ships and fin whale calls (Larner and others; 1983; Hutchinson and Lee, 1989).

To help distinguish the primary reflections from coherent noise, a careful velocity analysis was performed every 1 km (profiles RU-10 and USGS-105) or 2 km. Common midpoint (CMP) gathers were corrected for normal move-out (NMO) with a velocity part way between the primary and multiple velocities. Much of the multiple energy was then removed using frequency-wavenumber (f-k) filters. Because some high-amplitude noise remains after f-k filtering, median amplitude stacking was applied. Median amplitude stacking sorts samples from each trace at each 4 millisecond (ms) time increment by amplitude and keeps only samples near the median amplitude value. At a given traveltime, strong events that are present on only a couple traces are eliminated, while weaker events which are flat on a moved-out CMP gather are retained. In order to effectively use median amplitude stacking, for correlation of sequences across faults and for identifying important events at deep levels, relative amplitude is preserved as much as possible through the processing stream. For display purposes, to reduce clipping, a 10- or 25-percent amplitude equalization was applied to the stacked section.

Stacking velocity is higher for dipping reflections than for flat reflections, so that one must choose, for example, between choosing stacking velocities for dipping fault-plane reflection and flat strata. Dip Moveout (DMO), a partial prestack migration, was done on profile USGS-105 before velocity analysis so that dipping and flat reflections would have more similar stacking velocities. There was only a marginal improvement. The rest of the processing sequence was relatively standard and includes such steps as trace editing, spherical divergence correction, constant and time-varying bandpass frequency filtering, and predictive and spiking deconvolution. The actual processing sequence is given in the side panels to the plates in Sorlien (1994a).

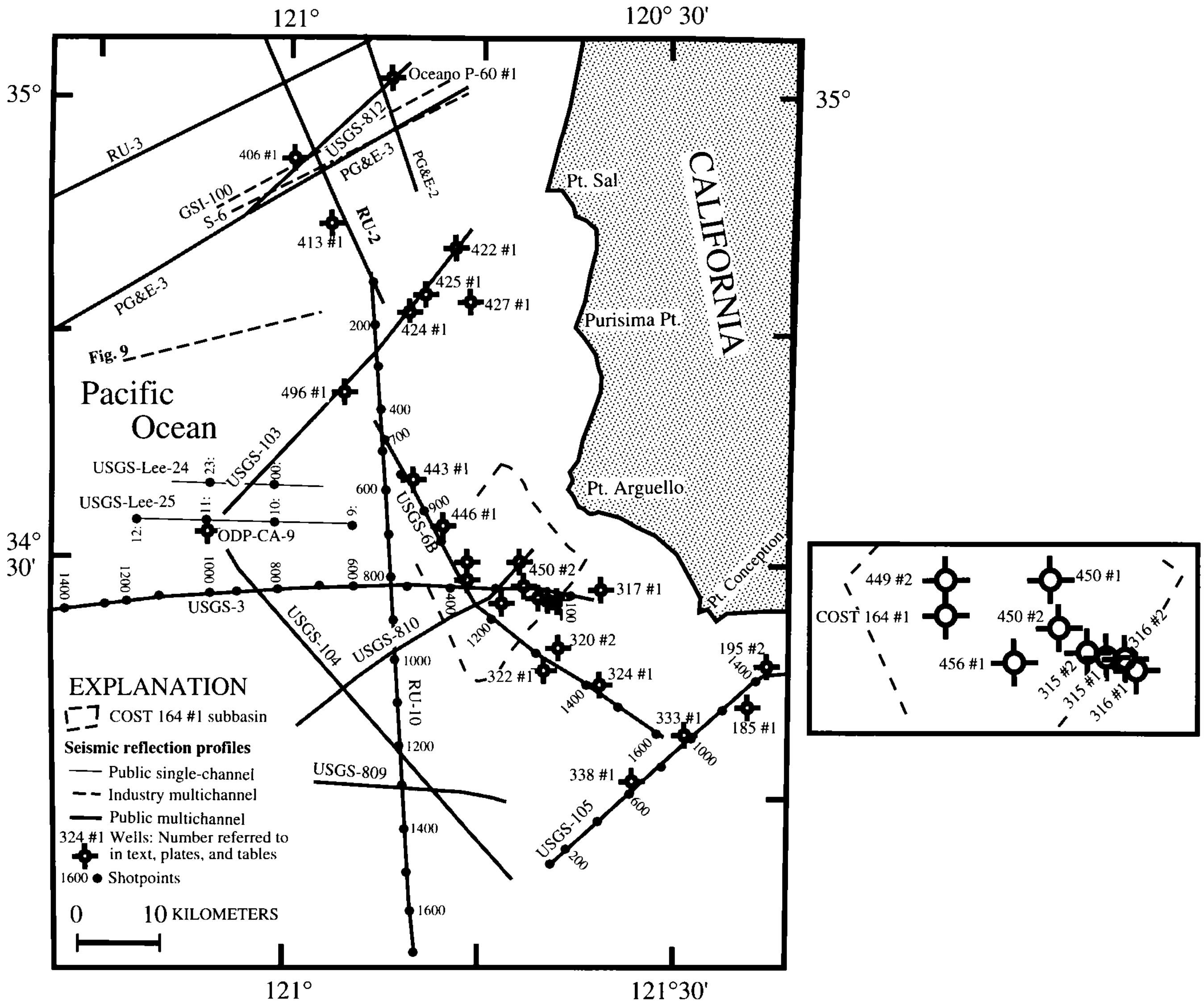

Figure 2. Location of wells and seismic reflection profiles, offshore south-central California, discussed in this report. The location of published interpretations of seismic reflection profiles used by us for stratigraphic correlation are also shown (PG&E, 1988; Bird and others, 1990; Clark and others, 1991; Meltzer and Levander, 1991). USGS-809 and USGS-810 are presented in Sorlien, (1994a). Closely-spaced wells are shown at a larger scale and identified next to map; dashed line outlining COST 164 #1 subbasin is also shown as reference. Shotpoints for profiles shown in plate 1 are given. Time shown for USGS-Lee-24 and USGS-Lee 25.

For migration, the stacking velocities from subhorizontal reflections were smoothed so that the corresponding interval velocities correspond to velocities in wells. Layers of constant or smoothly varying interval velocity were used below 3 to 4 s (all times in this chapter are two-way traveltime). This approach preserves detailed interval velocity information from shallow subhorizontal reflections and avoids artifacts related to abrupt changes in the longer migration distances at depth.

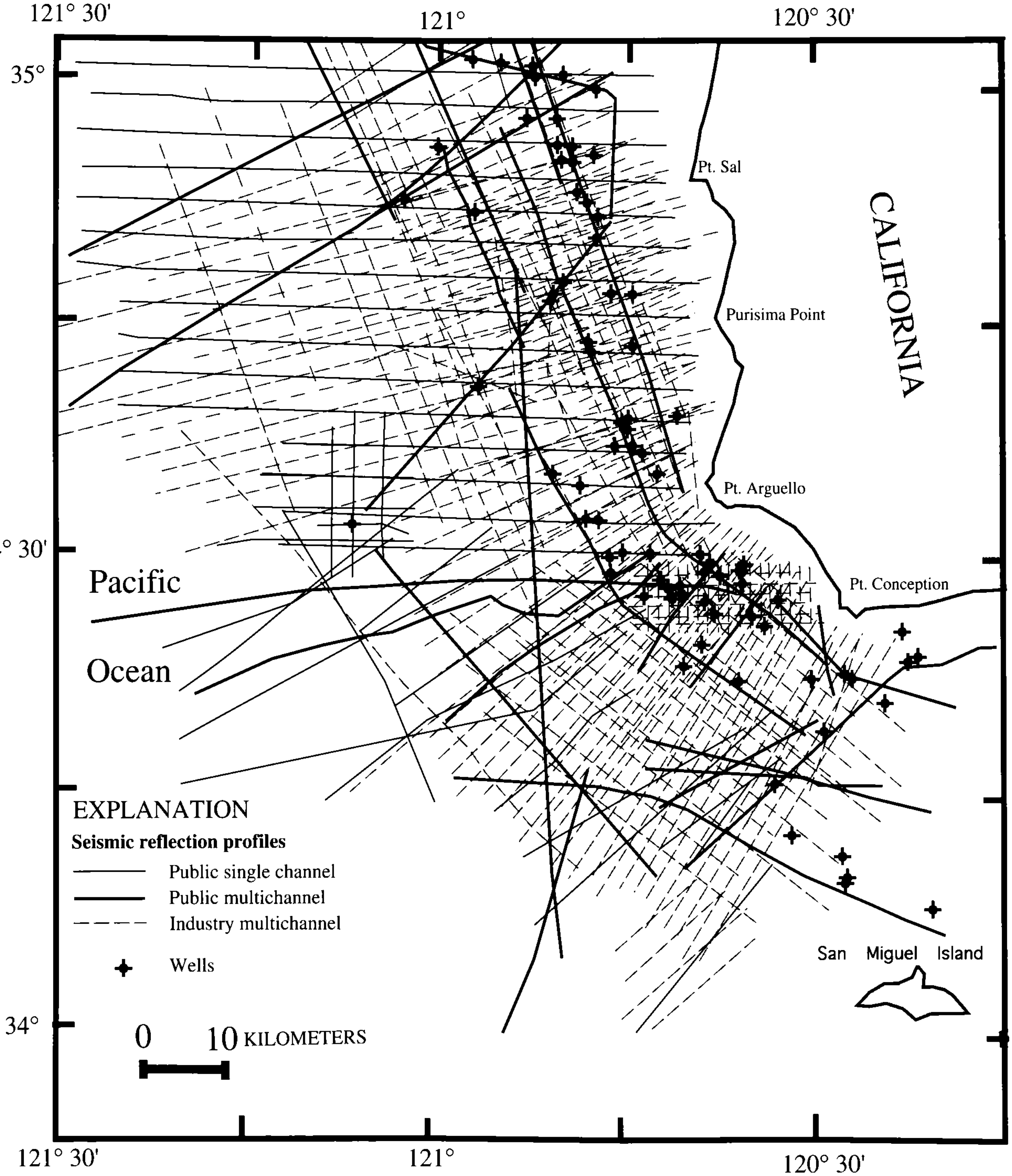

Figure 3. Location of tracklines for seismic reflection data from offshore south-central California used in construction of fault map (fig. 5); does not include closely spaced sections used to map southern Hosgri Fault (fig. 11). Precisely navigated industry multichannel profiles constrain location of offshore faults in most areas. Exploration wells located more than 5 km from coast are shown. For more detail, see table 1 and cross sections (pl. 1).

Because realistic interval velocities are used, multiples are overmigrated. Migrated reflections are always compared to the nonmigrated data in order to distinguish primary reflections from artifacts. The time sections were migrated with either 80 or 90 percent of the velocities used for the depth section.

Interpretation

Reprocessing the profiles allows deep structure to be interpeted because of improvement in signal-to-noise and because multiples and other coherent noise can be more easily identified on shot and CMP gathers than on stacked profiles. In our judgment, reflections in low signal-to-noise data in the basement, at traveltimes as much as 6 s, can be meaningfully interpreted. Although reviewers and others may not agree with this approach, we propose our deep interpretations as hypotheses that can be tested by acquisition of new data; our interpretation may aid in locating future tracklines. We interpret faults on discontinuities cutting primary reflections, on interpreted fault-plane reflections, and to explain tilting and folding of the mapped horizon. The interpretation that basin-bounding discontinuities are faults also explains the vertical offset of basement that is required by well control. Such indicators as sediments thickening toward the interpreted fault and folding in the hanging wall favor an interpretation of normal-separation faults over alternate interpretations such as buttress unconformities.

Once the geometry of deeper structures was interpreted, the response of sedimentation to fault and fold activity provided the timing; this timing in turn constrains regional tectonic models. For example, consistent thickening of a dated sequence from footwall to hanging wall across a fault indicates extension at that time, and thinning or erosion across a fold crest dates shortening. Care was taken to distinguish extensional highs that are the tips of tilted blocks from folds that result from contraction, because syntectonic sediments can onlap both types of structure.

Wells and Stratigraphy

Petroleum test wells provide the stratigraphic control for interpreting the seismic reflection profiles. Logs from dozens of abandoned hydrocarbon test wells located in the offshore Santa Maria basin and the Santa Barbara Channel are now publicly available. Available information includes that from the deep stratigraphic test well COST 164 #1 (fig. 2). This is an important correlation well because of (1) its central location within the transitional area between Santa Maria basin and Santa Barbara Channel and (2) the fact that detailed stratigraphic studies of the well have been published (fig. 4; table 1; Cook, 1979; Isaacs and others, 1983, 1989). The age control for other wells is provided by paleontology, by correlation to onshore deposits, or from published information (see table 1). We have also correlated to published interpreted seismic reflection profiles to provide additional stratigraphic control (fig. 2; PG&E-3 in PG&E, 1988; USGS-812 in Bird and others, 1990; and S-6 and GSI-100 in Clark and others, 1991). This age control was extended by correlating the gamma, spontaneous potential (S.P.), and lithologic (mud) logs of 17 wells (table 1). Several other wells with more limited information and published correlations of additional wells were incorporated (see Bird and others, 1990; Clark and others, 1991). Velocity analysis of subhorizontal reflections allowed well information in depth to be converted to time and placed onto adjacent seismic reflection profiles (fig. 2; table 1). This method of time-depth conversion gave similar results to those obtained directly from check-shot surveys (three wells) and sonic logs (COST 164 #1). In particular, we have compared velocities derived from the sonic logs and check shot survey for well 496 #1 (fig. 2) to velocity analysis of profile USGS-103 (table 1). Reflections corresponding to formation tops were regionally interpreted between wells on our grid of reprocessed time profiles (fig. 2), and on several of the industry profiles (fig. 3). This procedure serves as an internal check in the reliability of stratigraphic information and well-log correlations.

The regional deposition and erosion of sediments records local and regional tectonic events. Pre-Neogene rocks include Franciscan Complex or Point Sal Ophiolite basement, and Cretaceous and Paleogene forearc sediments (fig. 4). During the late Eocene and Oligocene, the nonmarine Sespe Formation was deposited on Santa Rosa Island and in the central and eastern Santa Ynez Mountains (Dibblee, 1966; Weaver and Doerner, 1969). This time interval is represented by a major unconformity in the onshore and offshore Santa Maria basin (Dibblee, 1950; Crain and others, 1985), much of central California (Page, 1981; Namson and Davis, 1990, Hall, 1991), and the outer California Continental Borderland (Lee, 1992). Marine deposition resumed in the western Transverse Ranges Province near the end of Oligocene time with the shallow marine sandstone of the Vaqueros Formation (Dickinson and others, 1987; Miles and Rigsby, 1990). Abrupt deepening of the same area and deposition of the Rincon Shale occurred near the beginning of Miocene time; in the western Santa Ynez Mountains the base of the Rincon Shale is earliest Miocene, about 24 Ma (Stanley and others, 1994). It has been interpreted that this rapid subsidence was delayed for the onshore and offshore Santa Maria basin (McCrory and others, 1995). In particular, the area near Point Sal subsided rapidly starting 17.7 Ma (Stanley and others, 1991a; McCrory and others, 1995).

Early Miocene tectonic activity has been related to deposition of two lithologically distinct congomerates or breccias, the Lospe Formation and the San Onofre Breccia (Stuart, 1976, 1979; Stanley and others, 1991b). The Lospe Formation is the oldest regionally preserved sediment above the mid-Cenozoic unconformity in the onshore Santa Maria basin, (McLean, 1991). Tuffs correlated to the Tranquillon Volcanics and interbedded with Lospe Formation have been dated at 17.4-17.7 Ma near Point Sal (Stanley and others, 1991a). In wells

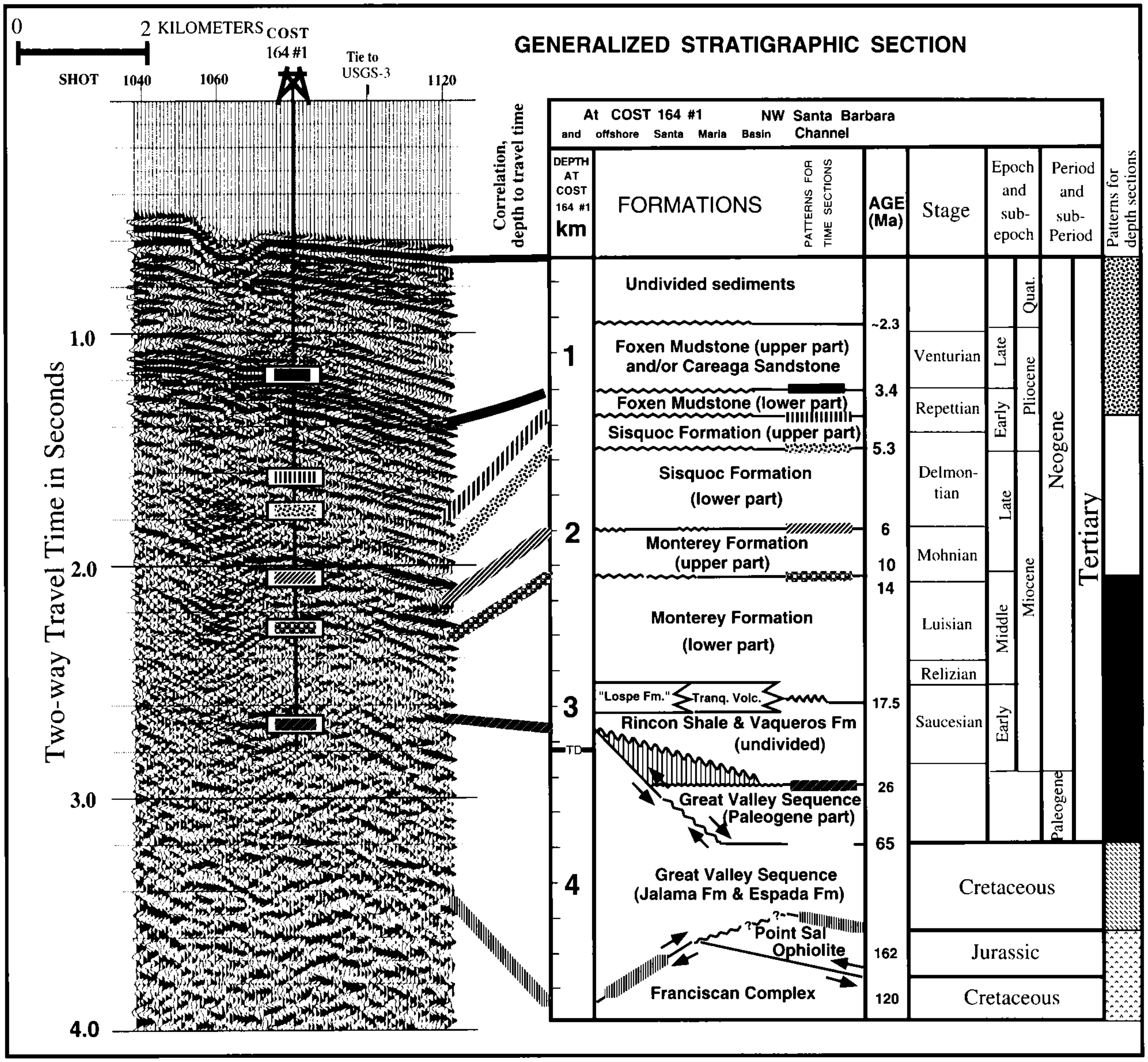

EXPLANATION

Formations at COST 164 #1 (patterns and shading correspond to interpreted time profiles on plate 1).

Undivided upper Pliocene and Quaternary sediments

Foxen Mudstone (lower part)

Sisquoc Formation (upper part)

Sisquoc Formation (lower part)

Monterey Formation (upper part)

Monterey Formation (upper part)

Espada Formation

Unconformity or other sequence boundary

Missing section (erosion and nondeposition)

Other formations named on figure are present in western Santa Barbara Channel and the western Santa Ynez Mountains.

Figure 4. Stratigraphic section at COST 164 #1 well, located in a subbasin between offshore Santa Maria basin and Santa Barbara Channel, offshore south-central California. Migrated data from seismic profile USGS-6B are shown. Patterns for the depth sections in plate 1 are shown in right column for reference. Well bottoms in late Jurassic-early Cretaceous Espada Formation; the Franciscan Complex or Point Sal ophiolite basement interpreted to be on a strong reflector near 3.4 s. Left of Formations column are rocks present in COST 164 #1 well, and right of that column shows other rocks present in southeastern part of study area. The Rincon Shale and Vaqueros Formation have not been found in most or all wells drilled in offshore Santa Maria basin, while Point Sal ophiolite is present there, at least locally. Upper paired arrows indicate hypothetical thrusting related to erosion of the Great Valley Sequence, followed by normal slip during deposition of the Rincon Shale and Vaqueros Formation. Lower pairs of arrows indicate subduction of the Franciscan Complex beneath generally older rocks.

Table 1. Approximate depth and traveltime to formation tops for selected wells, offshore south-central California. [Accuracy of data varies. Distance between the reference level and sea surface is subtracted (Kelly Bushing (KB) or derrick floor), converted to meters, then converted to time using velocity analysis from processing. This method of time conversion was supplemented and confirmed using check-shot surveys from three wells and using transit times for the COST 164 #1 well. Check-shot surveys are now publicly available that were not available when these correlations were done. Depths are true vertical depth from the sea surface. Traveltimes are rounded to the nearest 10 ms. Location of the wells shown on figure 2.]

Well See fig. 2 for location	Horizon	Depth, in meters	Two-way Travel time in seconds	Comments
P-60 (Oceano)	Seafloor	168	0.227	Travel times from sonic log.
	Top Sisquoc Formation	1027	1.221	
	Top Monterey Formation	1662	1.762	Rocks near bottom of well may be
	Top volcanic rocks	2142	2.035	Franciscan Complex or lower
	Bottom of well	2434	2.142	Miocene breccia and volcanic rocks.
413 #1	Seafloor	309	0.418	Travel times from VSP.
	Top Sisquoc Formation	781	0.976	Oldest upper Neogene sand:
	Top Monterey Formation	1163	1.416	629 and 693 m.
	Top volcanic rocks	1391	1.596	
	Bottom of well	1489	1.618	
496 #1	Seafloor	366	0.494	Travel time from check-shot survey.
	Top early Pliocene sediments	560	0.690	First samples in lower Pliocene.
	Top Sisquoc Formation	651	0.820	No late Neogene sand below 560 m.
	Top of Miocene sediments	743	0.922	
	Top Monterey Formation	1000	1.240	
	Top lower part Monterey Formation	1145	1.360	
	Top Franciscan Complex	1383	1.482	Volcanic rocks from 1383 m to 1815 m.
	Bottom of well	1815	1.660	
424 #1	Seafloor	177	0.209	Travel times from sonic log.
	Top Sisquoc Formation	446	0.540	Oldest upper Neogene sand near 377 m.
	Top of Miocene sediments	612	0.740	
	Top Monterey Formation	871	1.014	
	Top volcanic rocks	1030	1.167	
	Top Franciscan Complex	1073	1.192	Top metasediments noted on mud log.
	Bottom of well	1201	1.260	
443 #1	Seafloor	271	0.366	Travel time from velocity analysis of USGS-6B and from check-shot survey in 443 #2.
	Top Sisquoc Formation	966	1.160	
	Top Miocene sediments	1103	1.310	
	Top Monterey Formation	1335	1.500	Oldest late Neogene sand near 975 m.
	Top lower part Monterey Formation	1479	1.620	
	Top Cretaceous sediments	1489	1.630	
	Top Franciscan Complex	2082	1.970	Serpentine below 2082 m.
	Bottom of well	2115	2.115	
COST 164 #1	Seafloor	447	0.604	Travel time from sonic information.
	Sequence Boundary	855	1.100	Early-late Pliocene unconformity?
	Top lower Pliocene sediments	1208	1.470	McDougall and others (1979).
	Top Sisquoc Formation	1351	1.590	From Isaacs and others (1989).
	Top Miocene sediments	1540?	1.750	
	Top Monterey Formation	1986	2.000	Travel time could be greater.
	Top lower part Monterey Formation	2235	2.250	Compositional change. From Isaacs and others (1989).
	Top Cretaceous sediments	3018	2.650	Espada Formation, (Cook and others, 1979).

Table 1. Approximate depth and traveltime to formation tops for selected wells, offshore south-central California. [Accuracy of data varies. Distance between the reference level and sea surface is subtracted (Kelly Bushing (KB) or derrick floor), converted to meters, then converted to time using velocity analysis from processing. This method of time conversion was supplemented and confirmed using check-shot surveys from three wells and using transit times for the COST 164 #1 well. Check-shot surveys are now publicly available that were not available when these correlations were done. Depths are true vertical depth from the sea surface. Traveltimes are rounded to the nearest 10 ms. Location of the wells shown on figure 2.]—Continued

Well See fig. 2 for location	Horizon	Depth, in meters	Two-way Travel time in seconds	Comments
446 #1	Early-late Pliocene unconf.	907	1.120	Travel times from VELANS USGS-6B.
	Top Sisquoc Formation	1080	1.280	Base sand-conglomerate a few meters above top Sisquoc Formation.
	Top of Miocene sediments	1230	1.410	
	Top Monterey Formation	1430	1.590	
	Top lower part Monterey Formation	1650	1.770	
	Top "Lospe" Formation	1670	1.780	
	Serpentine	1940	1.950	From mud log.
	Bottom of well	1953	1.960	
449 #2	Early-late Pliocene unconf.	1000	1.210	Near base multicolor sand.
	Top Sisquoc Formation	1170	1.370	Travel times from VELANS USGS-6B.
	Top of Miocene sediments	1430	1.600	0.1 s added to TWTT for correlation along USGS-Lee-26 to USGS-6B.
	Top Monterey Formation	1810	1.910	
	Top lower part Monterey Formation	2070	2.090	
	Bottom of well	2297	2.210	Bottoms in lower part Monterey Formation.
450 #2	Top Sisquoc Formation	1290	1.390	Travel times from VELANS USGS-3.
	Top Monterey Formation	2330	2.180	
	Bottom of well	2784	2.410	
456 #1	Top early Pliocene sediments	1230	1.420	Travel times from VELANS USGS-810.
	Top Sisquoc Formation	1550	1.660	Depths are true vertical depth; well is deviated.
	Top Miocene sediments	1910	1.810	
	Top Monterey Formation	2060	2.000	
	Top lower part Monterey Formation	2370	2.200	Bottoms in lower part Monterey Formation; deep travel times not precise.
	Bottom of well (TVD)	2841	2.420	
322 #1	Top Sisquoc Formation	1680	1.830	Travel times from VELANS USGS-6B.
	Top Miocene sediments	1810	1.870	Added 0.05 s to travel times given here to account for water depth to tie with USGS-6B.
	Top Monterey Formation	2010	2.060	
	Top lower part Monterey Formation	2180	2.170	
	Top Cretaceous sediments	2230	2.200	
320 #2	Sandstone	1560	1.750	Travel times from VELANS USGS-6B.
	Top Sisquoc Formation	1784	1.900	Subtracted 0.05 s to travel times given here to account for water depth to tie with USGS-6B.
	Top Miocene sediments	1910	2.030	
	Top lower part Monterey Formation	2250	2.223	
324 #1	Top Sisquoc Formation	1490	1.720	Travel times from VELANS USGS-6B.
	Top Miocene sediments	1620	1.820	Upper part Monterey Formation is thin (part is missing?)
	Top Monterey Formation	1830	2.000	
	Top lower part Monterey Formation	1900	2.050	
	Top of Paleogene sediments	2160	2.250	Mud log shows interbedded sand, siltstone, and volcanics below the Monterey Formation.
	Top of Cretaceous sediments	3650	3.070	

Table 1. Approximate depth and traveltime to formation tops for selected wells, offshore south-central California. [Accuracy of data varies. Distance between the reference level and sea surface is subtracted (Kelly Bushing (KB) or derrick floor), converted to meters, then converted to time using velocity analysis from processing. This method of time conversion was supplemented and confirmed using check-shot surveys from three wells and using transit times for the COST 164 #1 well. Check-shot surveys are now publicly available that were not available when these correlations were done. Depths are true vertical depth from the sea surface. Traveltimes are rounded to the nearest 10 ms. Location of the wells shown on figure 2.]—Continued

Well See fig. 2 for location	Horizon	Depth, in meters	Two-way Travel time in seconds	Comments
	Early-late Pliocene unconf.	1320	1.470	Travel times from VELANS USGS-105.
333 #1	Top Sisquoc Formation	1570	1.700	Deviated well; depths are true vertical.
	Top of Miocene sediments	1690	1.920	
	Top Monterey Formation	1920	1.960	Same as Hornafius (1991).
	Top lower part Monterey Formation	2240	2.200	
	Tranquillon bentonite	2420		Hornafius (1991).
	Top Eocene	2540	2.410	Hornafius (1991).
	Early-late Pliocene unconf.	820	1.040	Travel times from VELANS USGS-105.
338 #1	Top Sisquoc Formation	980	1.220	Deviated well; depths are true vertical.
	Top Monterey Formation	1130	1.360	Paleogene volcanics (?) on mudlog.
	Pre-Monterey Formation early Miocene	1380	1.560	Bottoms in Paleogene or Cretaceous sandstone.
	Top Paleogene sediments	1410	1.580	
	Base sand	1340	1.430	Incomplete well logs used.
185 #1	Top Sisquoc Formation	1620	1.690	Travel times from VELANS USGS-105.
	Top Monterey Formation	1985	2.000	Deviated well; depths are true vertical.
	Top lower part Monterey Formation	2280	2.150	
	Top Vaqueros Formation	2647	2.320	Sand on mudlog.
	Top Paleogene sediments	2768	2.370	
	Slickensides	3600	2.770	From mud log.
	Base main sand	670	0.810	Incomplete well logs used.
195 #2	Top Sisquoc Formation?	~1680	1.670	Travel times from VELANS USGS-105.
	Top Monterey Formation	2150	2.020	Deviated well; depths are true vertical.
	Top lower part Monterey Formation	2540	2.310	
	Top Rincon Shale?	2670	2.380	
	Top Vaqueros Formation	2940	2.510	
	Top Paleogene sediments	2963	2.530	

located off of the crest of older structures in the offshore Santa Maria basin, a multicolor conglomerate, sandstone, or volcanic rocks overlie the mid-Cenozoic unconformity. These rocks have been correlated to the Tranquillon Volcanics or Obispo Formation and Lospe Formation; this correlation has some support from paleontology (Crain and others, 1985; Hornafius, 1991; Clark and others, 1991; McCrory and others, 1995). The San Onofre Breccia underlies volcanic sediments on the northern Channel Islands (Avila and Weaver, 1969; McLean and others, 1976; Stuart, 1976, 1979; Scholl, 1960). The San Onofre Breccia and part of the (synchronous?) Rincon Shale contain blue schist clasts, thought to be derived from fault scarps, which may record tectonic denudation of the Catalina Schist (Avila and Weaver, 1969; McLean and others, 1976; Stuart, 1976, 1979; Yeats, 1976; Bohannon and Geist, 1991; Crouch and Suppe, 1993).

Volcanism was most active between about 18 and 15-13 Ma in the study area (fig. 2 and Santa Cruz and Santa Rosa Islands (compilation in Weigand and Savage, 1993). Older K-Ar dates include Oligocene ages on San Miguel Island, while the intrusions which extend from San Luis Obispo to Morro Bay are dated at 22.7±0.9 to 27.2±0.8 Ma (Kamerling and Luyendyk, 1985; Vedder and others, 1991, recalculated from Turner, 1970). The San Miguel Volcanics mapped on Santa Rosa and San Miguel Islands are stratigraphically above the Rincon Shale (Weaver, 1969). The age determination on the uppermost Rincon Shale is late Saucesian Stage (early Miocene) on Santa Rosa Island (Bereskin and Edwards, 1969) and

Saucesian Stage or younger (inferred to be early Saucesian Stage by Weaver and Doerner, 1969) on San Miguel Island. Therefore, the Oligocene dates for the overlying volcanic rocks are suspect.

Thus, during late-early to middle Miocene time volcanic flows, tuffs and breccias were deposited near volcanic centers, thick sandstone of the Lospe Formation and Point Sal Formation (Santa Maria basin), or Beechers Bay Formation (Santa Rosa Island) was deposited near the edges of adjoining basins, and the biogenic shale of the Monterey Formation was deposited in more distal parts of deep basins (Dibblee, 1950; Weaver, 1969; Hornafius, 1991, McCrory and others, 1995; Stanley and others, 1996). An upward decrease in the terrigenous content of the Monterey Formation occurs at 7,400 feet or 2,256 m in the well COST 164 #1; this change corresponds to the top of the lower part of the Monterey Formation (top unit "B" in Isaacs and others, 1989). Because this change is relatively distinct in well logs and often corresponds to a strong seismic reflection, a fault map was constructed on this horizon where possible. This level corresponds roughly with the approximately late-middle Miocene (13 $\pm$1 Ma to 10 $\pm$1 Ma) hiatus or condensed phosphatic section found in other wells and onshore sections, or to the organic shale member of the Monterey Formation (Isaacs and others, 1983; Hornafius, 1984, 1985, 1991; Arends and Blake, 1986; Barron, 1986; Bohacs, 1990; DePaolo and Finger, 1991; Flower and Kennett, 1993). This phosphatic interval corresponds to deposition on structurally controlled bathymetric highs, while laterally, diatoms accumulated in deeper water (R.E. Garrison, oral commun., 1992; see Hornafius, 1991). Today, the resulting cherts are present in offshore wells, especially southeast of COST 164 #1, and probably correspond to the strong reflection that we mapped. Deposition of the cherts and siliceous shale of the upper Monterey Formation continued through much of late Miocene time (DePaolo and Finger, 1991; Barron, 1986; Arends and Blake, 1986; Flower and Kennett, 1993). About 6 Ma, an increased input of fine terrigenous material was added to the biosiliceous components during deposition of the Sisquoc Formation (Isaacs, 1981; discussion in Dumont and Barron, 1995). Finally, Pliocene and Quaternary shale, siltstone, and sandstone were deposited.

In the offshore area, identification of the top of Miocene sediments is difficult. It can be difficult to correlate because stages based on benthic foraminifera can be time transgressive (D.W. Weaver, oral commun., 1993) and because the top of Miocene sediments is not a formation top and need not have lithostratigraphic significance. Diatom assemblages (and other planktonic microfossils) allow the top Miocene and top early Pliocene to be identified (Clark and others, 1991; Blake, 1991). East of the well COST 164 #1, we place the top of Miocene sediments just below the top of the Sisquoc Formation; top Miocene is significantly shallower in the interpretation of Crain and others (1985; fig. 4; table 1). An early-late Pliocene (top Repettian-base Venturian stage) sequence boundary was interpreted on the reflection profiles by correlation to Clark and others (1991) and from age control in a few wells (table 1).

DISCUSSION OF SEISMIC REFLECTION PROFILES

We reprocessed several multichannel seismic reflection profiles that traverse the southern offshore Santa Maria basin and western Santa Barbara Channel. The area south and west of Santa Maria basin contains a shallow unconformity which appears as the top of acoustic basement on all reflection profiles, including the state-of-the-art RU-10 profile and industry data. However, our reprocessing allows interpretation of reflections originating in the lower and middle crust on both RU-10 and the lower-fold USGS profiles. Also, clearer images of the Neogene basin sediments have been produced.

RU-10 Profile

RU-10 is a nearly north-south profile which was shot to image the deep structure between the rotated western Transverse Ranges and the presumed nonrotated offshore Santa Maria basin (figs. 1, 2; pl. 1). It traverses proposed terrane boundaries between crustal blocks containing different stratigraphic sections (Howell and others, 1987; McCulloch, 1987, 1989a). RU-10 was acquired using a powerful array of airguns shooting every 50 m and recording 180 channels. The data were then sorted into 45-fold CMP gathers at 12.5-m intervals. To filter certain types of coherent noise, f-k filters were applied to the shot gathers, followed by an adjacent trace sum and sort to 45-fold CMP gathers at 25-m intervals. In a separate processing scheme, all traces were retained and f-k filtering was applied only on CMP gathers.

RU-10 is oblique to the axis of the offshore Santa Maria basin, crossing its southwest margin. Consequently, upper Miocene and younger sediments onlap or downlap (to the south) the top of the lower part of the Monterey Formation along RU-10 (pl. 1). This boundary in turn onlaps a strong reflection which corresponds to Miocene volcanic rocks exposed at the sea floor at the south end of RU-10 (Vedder, 1990). This onlap can be explained as deposition onto a paleo-high located to the south or southwest, with later subsidence or tilt reversal explaining today's deepening to the southwest. Alternatively, the observed pattern may be downlap related to distal sedimentation from a sediment source located to the northeast. Only a thin veneer of Quaternary sediments, and locally no Quaternary sediments, are present on a gently-sloping surface beneath about a kilometer of water.

We interpret that faults cross RU-10 at both high angles and low angles and that these faults produce reflections. On the north third of RU-10 and southern RU-2, the middle crust (about 2 to 5 s or 2 to 10 km) is dominated by a south-dipping reflection fabric, the central third of RU-10 has crossing south- and north-dipping reflections, and the south end of RU-10 has mostly north-dipping reflections in the middle crust (pl. 1; Nicholson and others, 1992). The upper Miocene and younger sediments are little deformed and produce coherent reflections, while the middle Miocene and older sediments are disrupted and therefore poorly imaged, perhaps in part due to moderate out-of-the-plane-of-the-section dips. A strong reflection from a sequence boundary caps the deformed section (top lower part Monterey Formation or older rocks). The relief on this strong reflection is consistent with our interpretation of the faults beneath it and can be explained as back-tilting with minor, younger folding.

Correlation of the stratigraphy in well COST 164 #1 with seismic reflection profile USGS-3 indicates that thick lower Monterey Formation or equivalent age sediments and Cretaceous sediments extend west to the intersection (tie) with profile RU-10. Interpretation of Paleogene sediment on RU-10 is speculative because these sediments are not present at COST 164 #1. However, the south end of RU-10 is on trend with the northern Channel Islands, where a thick Paleogene section is present (Weaver, 1969). Significant layered section is imaged below the strong reflection (top lower part Monterey Formation or older rocks) toward the south end of RU-10 (S.P. 1250; pl. 1). The faults which separate thick pre-Miocene sediment from thin pre-Miocene sediments have only minor effect on upper Miocene sediment.

USGS-3 Profile

USGS-3 profile provides three-dimensional control to profile RU-10 and passes close to numerous wells within the Point Arguello oil field to the east (pl. 1). It passes south of well COST 164 #1 and crosses the transitional subbasin that separates the offshore Santa Maria basin from the Santa Barbara Channel (figs. 1, 2). Lack of geologic control west of COST 164 #1 limits stratigraphic interpretation to correlations based on seismic character or continuity of the shallow subhorizontal reflections. USGS-3 was recorded to 7.8 s in 1979. Hydrophone group spacing was 100 m along a 2.6-km streamer producing 24-channel shot gathers at 50-m intervals; 24-fold CMP gathers are also located at 50-m intervals. A deep-water delay on the western portion of USGS-3 allowed processing to 8.8 and 9.8 s. Although the recording geometry for these lines was much less favorable for multiple reduction than that for RU-10, a substantial improvement was achieved beneath areas with thick (greater than 2 km) sediments and shallow (less than 500 m) water.

A broad zone of east-dipping normal-separation faults is interpreted on east-dipping reflections along the central part of profile USGS-3 (pl. 1). These faults affected early and middle Miocene sediments; these sediments are thickest near and west of the COST well. An escarpment along the Santa Lucia Bank Fault forms the west margin of offshore Santa Maria basin, but the bathymetric expression dies well north of USGS-3 (fig. 1). These faults interpreted between S.P. 1100 and 700 are part of the wider West Basin-Santa Lucia Bank Fault System (pl. 1, profile USGS-3). A (middle?) Miocene angular unconformity is observed between S.P. 960 and about S.P. 840. Although not very clear, the structure below the unconformity is interpreted to be a series of west-tilted blocks into east-dipping normal separation faults.

The sea floor along USGS-3 was deformed by long-wavelength folds after early Pliocene time. The more pronounced fold (near S.P. 1100-1200, pl. 1) forms a steeper (5°) upper slope bounded by nearly flat platforms. This fold scarp can be seen on bathymetric maps to be northwest-trending (U.S. Geological Survey National Ocean Survey, 1989). The assymmetry of the fold suggests that it is southwest verging. Faults are interpreted on reflections that dip east beneath this fold (pl. 1, profile USGS-3). Similar low-angle faults are found where this northwest-trending slope crosses other multichannel lines (Bird and others, 1990; PG&E, 1988; McIntosh and others, 1991). We call these faults the Santa Lucia Slope Fault System.

Upper Miocene and lower Pliocene sediments thicken dramatically eastward toward the Point Arguello Oil Field (Crain and others, 1985). The thickest sediments are near the crest of a broad long-wavelength, low-amplitude fold (east of S.P. 280, profile USGS-3, pl. 1). We interpret that Miocene extension was followed by mainly post-early Pliocene contraction and basin inversion on a system of northeast-dipping blind faults. These faults merge with the North Channel Fault System to the east and therefore can be considered to be its westward continuation. Along trend in the northern Santa Barbara Channel, a similar interpretation of late Miocene and early Pliocene transtension has been made for the Hondo field–Santa Ynez unit (McGroder and others, 1994).

Deep, west-dipping reflections that we interpret to be primary underlie well COST 164 #1 and the Point Arguello Oil Field (pl. 1, profile USGS-3). The reflection beneath this well is near 3.5 s or 5 km; we interpret this reflection to be the top of Franciscan Complex or Point Sal Ophiolite basement (pl. 1, profile USGS-3; labelled "basement" on reflection profiles and depth sections). By definition, a Franciscan/Espada contact must be a fault unless the fault was eroded away before Espada deposition. Minor post-Miocene thrust reactivation of this west-dipping system is interpreted. A high-amplitude reflection is imaged near 5 s at the east end of USGS-3 (pl. 1). Other data, which we do not show except for their location in figure 3, image an important imbricate zone of west-dipping reflections in this area. A related southwest-dipping fault is also present on USGS-105, and this system will be further discussed in the section on USGS-105.

USGS-6B Profile

Northwest-trending USGS-6B profile extends 50 km along the late Neogene depositional axis from the southern offshore Santa Maria basin to the western Santa Barbara Channel, crossing the gradational intervening pre-Miocene stratigraphic boundary across and southeast of the subbasin near

COST 164 #1 (fig. 2; pl. 1). Nine wells are located within 2.5 km of USGS-6B, including the stratigraphic test well COST 164 #1. Along the northwestern part of this profile, Point Sal Ophiolite or metamorphosed Franciscan Complex basement is interpreted at a depth of less than 2 km (by correlation to wells 496 #1, 424 #1, and 443 #1, fig. 2, table 1). Above the basement, erosional remnants of late Jurassic–Early Cretaceous Espada Formation and Late Cretaceous Jalama Formation have been drilled. (pl. 1, profile USGS-6B; table 1). Little is known about the basement south of Point Arguello because offshore wells bottom in thick Paleogene and Cretaceous sediments. These wells are as deep as 4 km, supporting our interpretation that basement is below 6 km depth (pl. 1, profile USGS-6B).

The contrast in total sedimentary thickness along USGS-6B is related to the following two observations or interpretations: thick Cretaceous and Paleogene sediments in Santa Barbara Channel form a northwest-tapering wedge onto Amberjack High, and post-Miocene sediments form a southeast-thickening wedge into the Santa Barbara Channel. The southeast thickening of the post-Miocene sediments is related to sediment supply and/or a broad warping or folding, not to erosion (pl. 1). We interpret that Oligocene erosion near the Amberjack High is responsible for the abrupt northwest thinning of the Paleogene sediment (pl. 1). We interpret that Paleogene and Cretaceous sediments are concordant, and both are folded together above gently southeast-dipping faults before deposition of the Vaqueros Formation. Paleogene sediments were removed by erosion after deposition of the Eocene Sacate Formation and before deposition of the latest Oligocene-earliest Miocene Vaqueros Formation (Dibblee, 1950; Miles and Rigsby, 1990; Dickinson and others, 1987; Hornafius, 1991; Stanley and others, 1994).

Miocene extension also has affected sedimentation along USGS-6B. Lower and middle Miocene sediments are more than twice as thick, and upper Miocene and lower Pliocene sediments are about twice as thick, in the sub-basin near COST 164 #1 than to the northwest and southeast (fig. 2; pl. 1). The northwest margin of this subbasin is a strong reflector. This reflector projects upward to a northeast-striking fault that has been previously mapped in the shallow subsurface (Chevron, 1982). We interpret the reflector to be a southeast-dipping fault that was most active during Miocene extension (Relizian and Luisian Stages, fig. 4). This fault and other northeast-striking faults along the Amberjack High (fig. 5) have been reactivated (pl. 1, profile USGS-6B; Crain and others, 1985). However, none of the northeast-striking faults appear to be significant in upper Miocene and younger sediments; therefore, no important post-12-Ma structural boundary exists between the presumed rotated Santa Barbara Channel and the offshore Santa Maria basin. The observed contrasts in the sediments between the two basins can be explained by deposition and erosion, and therefore large-scale lateral transport does not have to be invoked to explain these contrasts.

Several reflections from the midcrust can be interpreted along USGS-6B, despite a low signal-to-noise ratio. Strong, gently south-southeast-dipping reflections beneath the COST well are interpreted to be from basement near 4.5 km (fig. 4; pl. 1). Corresponding reflections dip west on USGS-3, indicating a true southwest dip. Additional reflections dip northwest in the midcrust along the northwest end of USGS-6B (pl. 1). The strongest of these reflections is below 5 s or about 10 km depth near S.P. 800. These reflections can be character correlated with subhorizontal to very gently north-dipping reflections on profile RU-10 a couple kilometers to the west (Nicholson and others, 1992). On 1:1 depth sections, apparent dips of northwest 18° and north 02° were measured on profiles 6B and RU-10 respectively, resulting in a true dip of about 30° due west. Color displays of the seismic attribute reflection strength (the envelope of amplitude) that we did for this project support a fault interpretation for this west-dipping reflection because the interpreted fault separates significantly different reflection strength character at both shallow (above 5 s) and deep (below 5 s). Logically, this structure is associated with the west-dipping imbricate system of reflections which underlies the region west and southwest of Point Arguello.

USGS-105 Profile

USGS-105 profile crosses the western Santa Barbara Channel from the west of San Miguel island to just south of the North Channel Fault (figs. 1, 2; pl. 1). USGS-105 was recorded in 1990 to 12 s, with hydrophone groups spaced at 50-m intervals on a 2.4-km streamer; 44-channel shot gathers were recorded at 50-m intervals to produce 22-fold CMP gathers located at 25-m intervals.

A broad, gently north-dipping fold limb dominates the shallow structure of the western Santa Barbara Channel (pl. 1, profile USGS-105). This fold is interpreted to have no forelimb at deeper levels, and only a short southwest-dipping forelimb at shallow levels. The low-angle faults partially responsible for this structure are also imaged. These faults are not parallel to the 9-km-long north-dipping backlimb, but they flatten downdip to become parallel to Cretaceous and Paleogene bedding. Short wavelength folding is apparent along this backlimb. These folds are overlapped by post-Sisquoc Formation sediments and have the same amplitude in Miocene Monterey Formation as in Miocene-Pliocene Sisquoc Formation. This observation can be explained by their formation during an early (mid?) Pliocene compressional episode. A 200-m-thick sequence overlaps these folds, which is in turn onlapped by upper Pliocene(?) and Quaternary sediments. These post-early Pliocene sediments are progressively tilted; the older sediments dip more steeply north than do the younger ones. This progressive north tilting is continuous over at least a 100 km length of southern Santa Barbara Channel (Sorlien and others, 1995; Seeber and Sorlien, unpub. data).

The progression from short wavelength folding to longer wavelength folding is not limited to profile USGS-105. Short wavelength folds truncated by an unconformity are imaged on profiles located west of San Miguel Island. This unconformity is in turn folded by long wavelength folds, with deposition of subhorizontal (Quaternary?) sediments in the resulting synclines. One explanation for this progression is that a shallow decollement became relatively inactive, and then slip on a deeper northeast-dipping low-angle fault caused the broad antiformal warping of the northern Channel Islands ridge (Seeber and Sorlien, unpub. data).

A northeast-verging fold near S.P. 330, profile USGS-105, is located above southwest-dipping discontinuities that are interpreted to be the causative faults. These faults are likely part of the Santa Cruz Island Fault System and therefore are expected to have a left-lateral component of slip (Pinter and Sorlien, 1991). To the southwest of this fold, short wavelength folds are cut by steeply dipping faults; these faults are on trend with sinistral strike-slip faults on northern Santa Rosa Island (Sorlien, 1994b). Unfortunately, Miocene rocks are at the sea floor on the Channel Islands ridge (Vedder, 1990), and hence post-Miocene activity on faults that cut the ridge cannot be evaluated. However, the sea floor is deformed above folds imaged in the Miocene section, and ample evidence exists for late Quaternary faulting and uplift on the islands (Colson and others, 1995; Pinter and others, 1995).

Although Miocene extension affected the western Santa Barbara Channel, Miocene sediments are relatively thin beneath its axis. In fact, Miocene sediments are less than 1 km thick along the axis of the western Santa Barbara Channel, while Miocene sediments and volcanics are several times thicker in the northern Channel Islands and are somewhat thicker along the mainland coast (pl. 1, profile USGS-105; Dibblee, 1950; Weaver, 1969). The present deep basin is due to deposition of post-Miocene sediments in combination with preservation of pre-Miocene sediments. The form of the Miocene basin bore little resemblance to the present basin.

RESULTS FROM MAPPING AND WELLS

Fault Pattern

In order to understand the geometry of the deep structures related to basin formation, a fault map (fig. 5) was constructed over a large region of offshore south-central California using the data located in figure 3. This map was constructed on the sequence boundary at the top of the lower part of the Monterey Formation (fig. 4). This horizon is at a deeper structural level than any previously published map. The middle Miocene horizon chosen for the map has been drilled by most wells, is fairly easy to correlate from both lithologic descriptions or electrical logs, and corresponds to a strong reflector in most areas (fig. 4). Around the edges of the basin, the map level onlaps older sequence boundaries; where this occurs, the map is carried on the older horizon. For example, where Pliocene sediments unconformably overlie lower Eocene sediments, the map continues on the unconformity, but is shown as top Paleogene on cross sections, or as top lower Monterey or older where the age of the underlying rocks is unknown. Faults are mapped if they are important just below the map horizon (locally acoustic "basement"), even if they do not significantly offset it. In addition to the mapped faults, unmapped flat to gently dipping faults are present beneath the mapped horizon. For example, subhorizontal faults underlie the western Santa Barbara Channel and the eastern margin of the offshore Santa Maria basin, as seen on the cross sections in figure 6.

Figure 6 is a simplified block diagram constructed from the fault map (fig. 5). Although designed to appear as an oblique view toward the north-northwest, the map and cross sections are drawn to the same scale. The location of faults on figure 6 matches figure 5, but the relief of fault scarps and folds is exaggerated. The relief of the map surface is as seen today on that horizon; dotted folds on the block surface indicate structures only seen at shallower structural levels.

Santa Lucia Bank and West Basin Fault Systems

The Santa Lucia Bank Fault is part of a 30-km-wide anastamosing to en-echelon pattern of faults along the west margin of the offshore Santa Maria basin. It is distinguished from other north-striking, east-dipping faults by a somewhat more linear trace, and in the north by a somewhat steeper (but still moderate) dip (figs. 5, 6). The Santa Lucia Bank Fault had been proposed to have accommodated up to 280 km of late Miocene dextral slip (Sedlock and Hamilton, 1991). Lateral motion on this fault was inferred based largely on its long linear trace, presumed steep dip, and the termination of magnetic anomalies against it (McCulloch, 1987, 1989a). In fact, dense published magnetic coverage does not extend across most of the Santa Lucia Bank Fault (McCulloch and Chapman, 1977), and we interpret the dip of this fault to be gentle to moderate along its southern part (fig. 6). The large amount of strike-slip motion previously proposed for offshore faults is based on regional tectonic models (Sedlock and Hamilton, 1991).

Our detailed mapping and interpretation provides new information on the geometry of this fault system. Faults within this system retain inherited Miocene normal separations at deep levels and were reactivated by post-early Pliocene shortening discontinuously along strike. A Miocene subbasin of the offshore Santa Maria basin is bounded on the west by a newly mapped fault or family of faults here called the West Basin Fault; this system underlies the Queenie structure (figs. 5, 6; Clark and others 1991). West of Point Sal, the footwalls of the Santa Lucia Bank and West Basin Faults form separate acoustic basement highs, with a western subbasin located between the highs (figs. 5, 6). North-northeast-striking splays or strands near 34°45' N. are present both east and west of the Santa Lucia Bank Fault (figs. 7, 8, 9). These previously unrecognized structures are associated with gravity lows above the hanging-wall basins, and with gravity highs above the acoustic basement highs (fig. 10).

We used single-channel profiles to interpret the geometry of folding in the upper Pliocene-Quaternary sediments. This geometry was used to infer east dip on the West Basin Fault System (figs. 7, 8). Also, scans of the data were stretched on a computer, resulting in sections with less vertical exaggeration (fig. 7*B*). At this revised scale, an east-dipping fault-plane reflection is observed that is not as apparent on the unstretched profile. This geometry agrees with the east-dipping fault-plane reflections that were interpreted as faults on multichannel industry profiles. Figure 9 is a tracing of reflections on a migrated industry profile that crosses the Santa Lucia Bank and West Basin Faults, as well as a north-northeast-striking splay between the two systems (figs. 5, 6). The strong east-dipping reflections are interpreted to originate from moderately east-dipping fault planes; pre-Miocene(?) prerift sediments are backtilted into the faults. The faults have a true dip of approximately 35° assuming an interval velocity

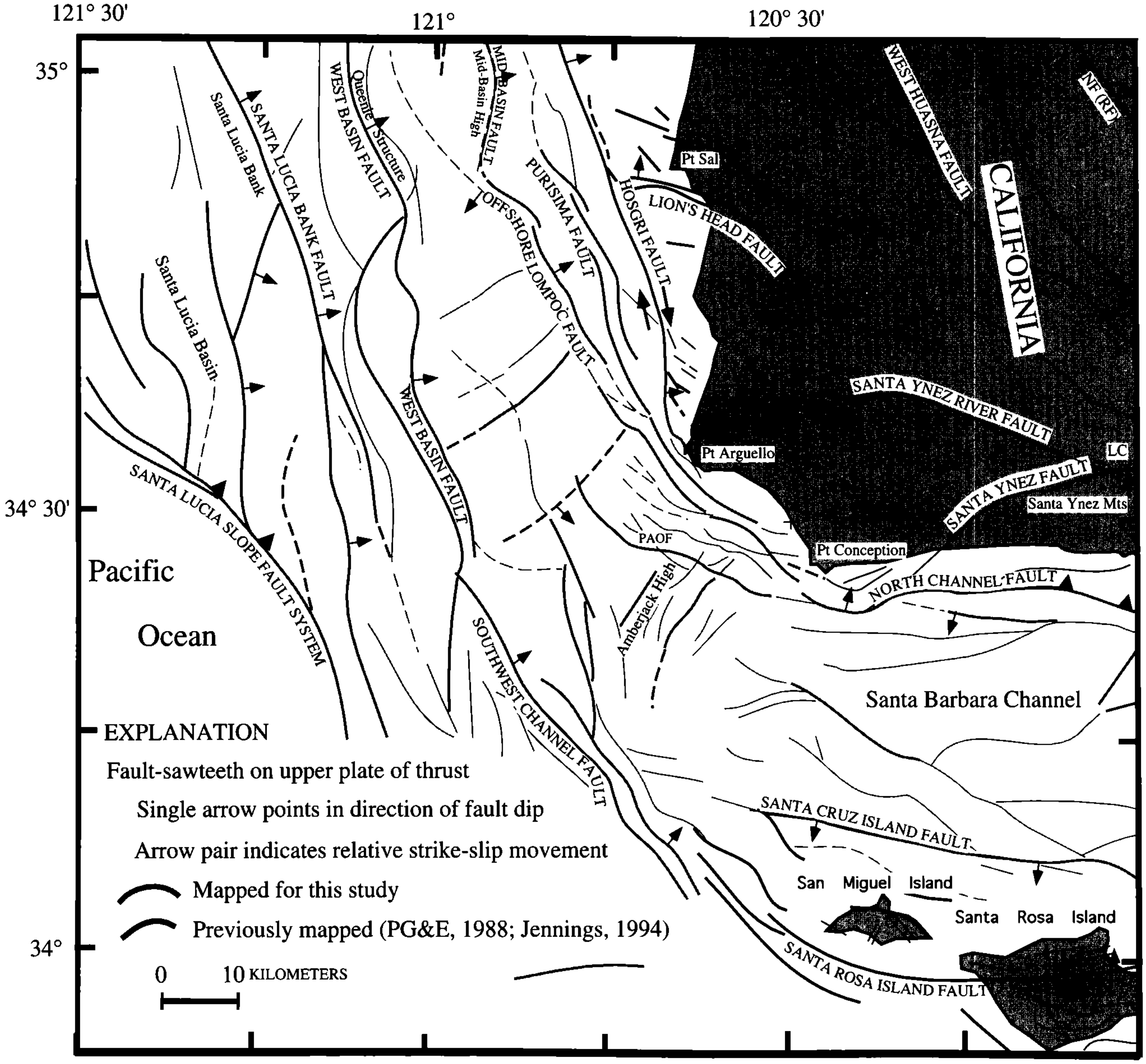

Figure 5. Map showing faults on a late-mid Miocene horizon, or sequence boundary (top lower part Monterey Formation; see table 1), south-central California. Where this surface onlaps an older surface, the fault map is carried on the older surface. Most north-striking faults are east dipping. Faults that we interpret to have been more important during Neogene time are drawn with a thicker line than those judged less important. LC is Lake Cachuma; NF(RF) is the Nacimiento Fault (Rinconada Fault).

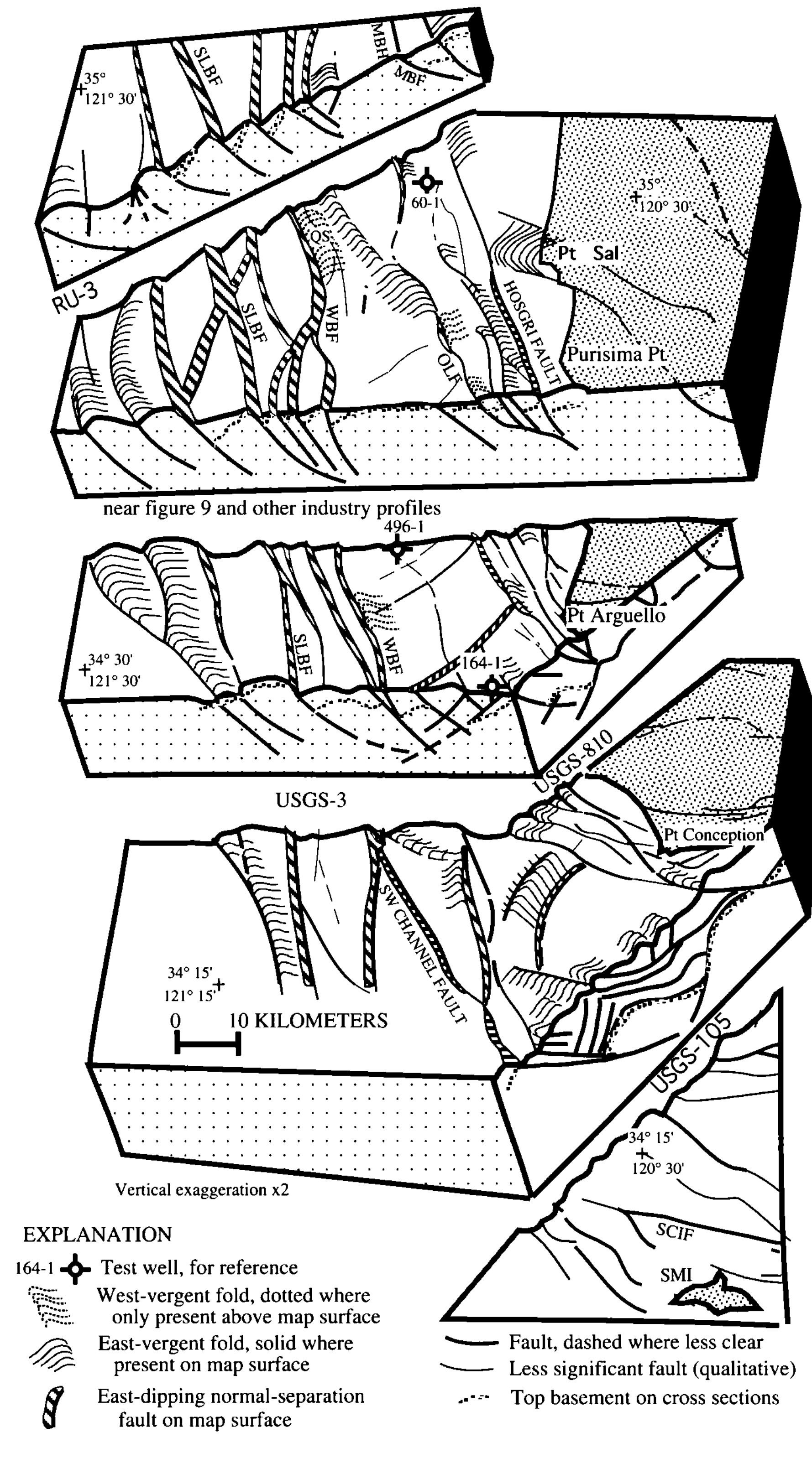

Figure 6. Block diagram of study area, offshore south-central California, showing interpretation of faults in the subsurface. Surface is the same as in figure 5 (late mid-Miocene horizon; top lower part Monterey Formation or older). Cross-sections are labelled with names of nearby or coincidental seismic reflection profiles; industry data was used to extend beyond the end of profile USGS-105, profile USGS-810 (Sorlien, 1994a), and figure 9. MBF, Mid-Basin Fault; MBH, Mid-Basin High; SLBF, Santa Lucia Bank Fault; WBF, West Basin Fault; OLF, Offshore Lompoc Fault; SCIF, Santa Cruz Island Fault; SMI, San Miguel Island.

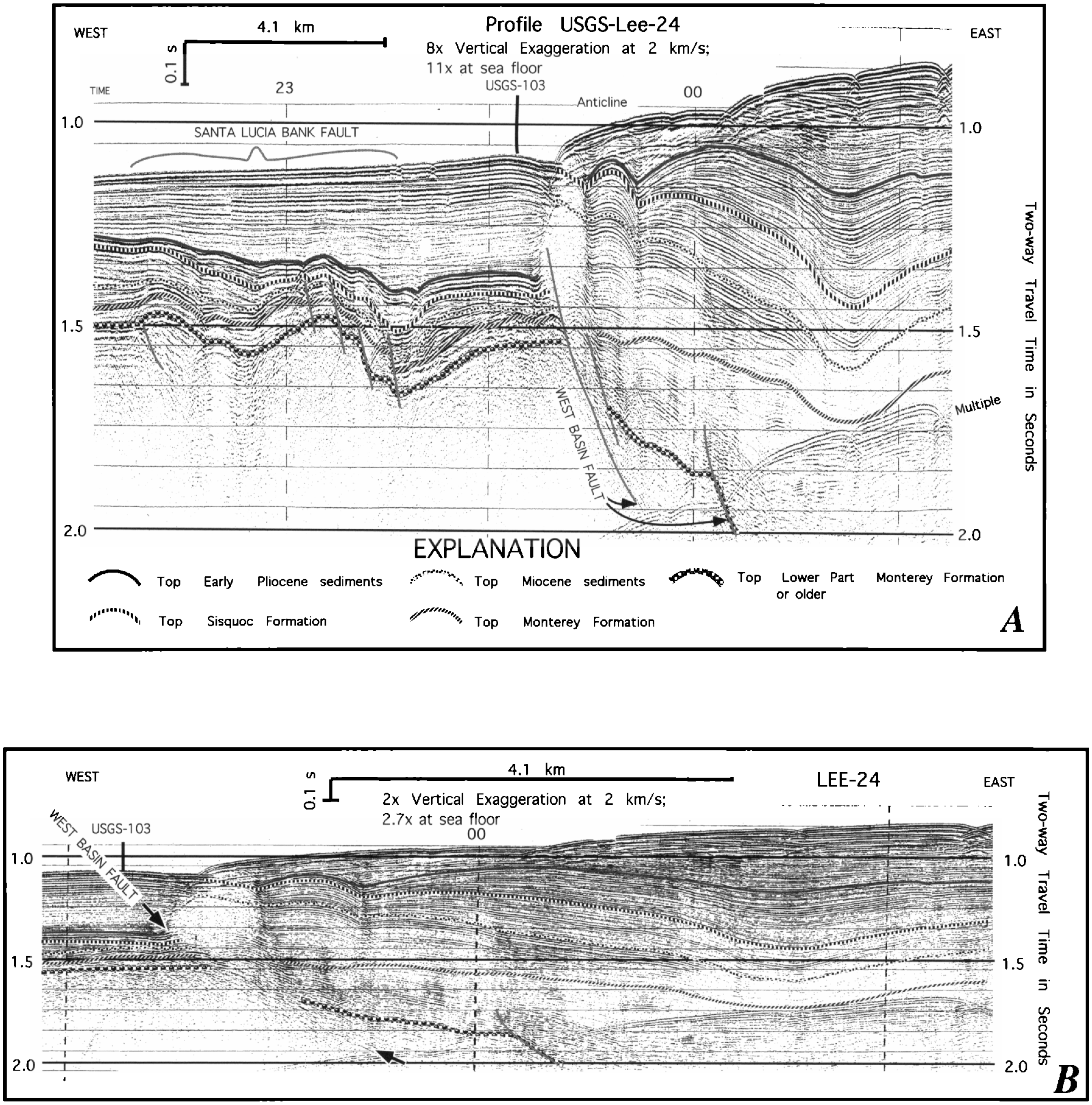

Figure 7. USGS-Lee-24 single-channel seismic profile, offshore south-central California. *A*, scan of original data. An industry strike line allowed correlation of the interpretation to well 496 #1 near shot-time 00:30. Vertical separation of strata is up to the east in the shallow section and down to the east in the deep section. Lower Pliocene sediments thin slightly over the anticline (near shot-time 00); erosion into top of lower Pliocene strata immediately adjacent to West Basin Fault, suggests that much folding is quite young. Remnants of the Santa Lucia Bank Fault are overlapped by upper Pliocene (?) sediments; this fault is interpreted as a single western strand (shot-time ~22:40), and four closely-spaced eastern strands (shot-time 23:10). Although the Santa Lucia Bank Fault does not appear to be a major structure from this point south, it has likely transferred displacement to the West Basin Fault and a fault to the west of this figure. *B*, east half of *A* scan stretched to be less vertically exaggerated. Note gently to moderately dipping fault-plane reflections related to the west strand of the West Basin Fault (indicated by arrows) ; the east strand is drawn as a gray curve.

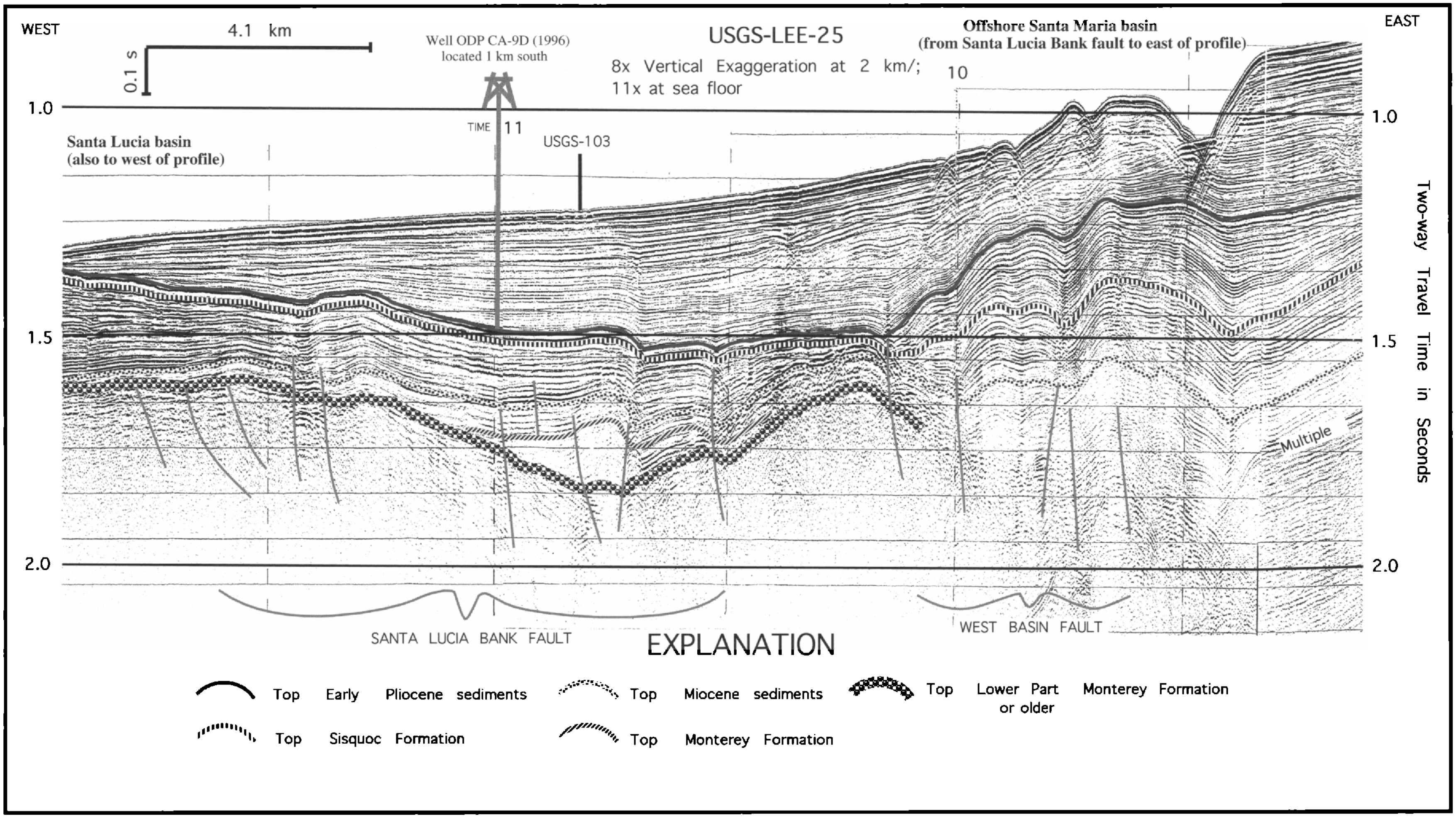

Figure 8. USGS-Lee-25 single-channel seismic profile, parallel to and 4 km south of USGS-Lee-24. This is the most northern location where Pliocene sediments can be correlated directly across the West Basin (shot-time 09:30-10:10) and Santa Lucia Bank Faults (west of shot-time 10:30), offshore south-central California.

of 4 km/s. This is a reasonable velocity for pre-Miocene sediment, as seen in the sonic logs of wells.

It is possible that moderately dipping (45° or more) pre-Miocene sediments are present, but not imaged beneath the eastern part of figure 9. The stacking velocity of moderately dipping reflections is dramatically increased from that expected for flat reflections (Yilmaz, 1987). Unless a processor specifically increases the stacking velocity abruptly at the unconformity, the dipping reflections will not stack in. The use of too-low velocities is likely the case here because a strong pegleg multiple does stack in. Evidence for moderately dipping reflections along this trend was seen during processing of USGS-103 (fig. 2; K. Bird, C. Sorlien and E. McWayne, unpub. data, 1994).

Post-Miocene reactivation of these faults is represented by folding and basin inversion along the east half of the profile shown in figure 9; the strong reflection near 1 s (marked "u") is probably from the early/late Pliocene unconformity. Figures 7 and 8 show that a local angular unconformity or onlap surface is present on the folds and that the most important folding occurred toward the end of early Pliocene time. The most significant folding and reverse separation is localized to profile USGS-Lee-24; normal separation is retained on Miocene horizons on all profiles (figs. 7, 8, 9).

The Santa Lucia Bank Fault proper (the fault that bounds the east edge of the acoustic basement high) is overlapped by Pliocene sediments west of Point Arguello (fig. 8; pl. 1). This strand continues southward into the California Continental Borderland below a shallow unconformity. Within a 40-km-wide zone, north- to northwest-striking, east-dipping faults diminish in throw while others increase. Slip, possibly including Quaternary slip, is likely transferred to parallel faults to the east and west (figs. 5, 6). McCulloch (1987) correctly noted that southward continuations of the Santa Lucia Bank Fault System are visible on side-scan sonar records and that one of these lineaments crosses a submarine canyon at a right deflection (offset?) of the canyon (EEZ Scan, 1986).

Major strands of the West Basin Fault split off and form the southwest end of the basin beneath the Santa Barbara Channel. This fault system continues southeast into the outer California Continental Borderland (figs. 1, 5). For convenience, the main southeast-striking strand is called the Southwest Channel Fault. The Southwest Channel Fault is clearly imaged west of San Miguel Island as an important northeast-dipping fault, with substantial normal separation of Miocene(?) sediments. Previous mapping in the younger sediments above the Southwest Channel Fault interpreted the Santa Lucia Bank Fault System to die out to the southwest of Point Arguello in a series of east-southeast-striking splays (PG&E, 1988; McCulloch, 1989b). A large blank area near 34°15′ N., 120°45′ W. on these compiled fault maps is an artifact of a lack of data in that area, the edge of McCulloch's (1987, 1989a) fault map, and of the geology. In this area, post-middle Miocene sediments onlap or downlap onto the westward continuation of the northern Channel Islands platform. Offsets of this surface were continuously removed by erosion until deposition resumed during the Quaternary. Therefore, the apparent lack of offset is due to erosion of the sediments and does not represent a lack of fault activity. Because of the lack of upper Neogene sediments, important Miocene faults must be interpreted

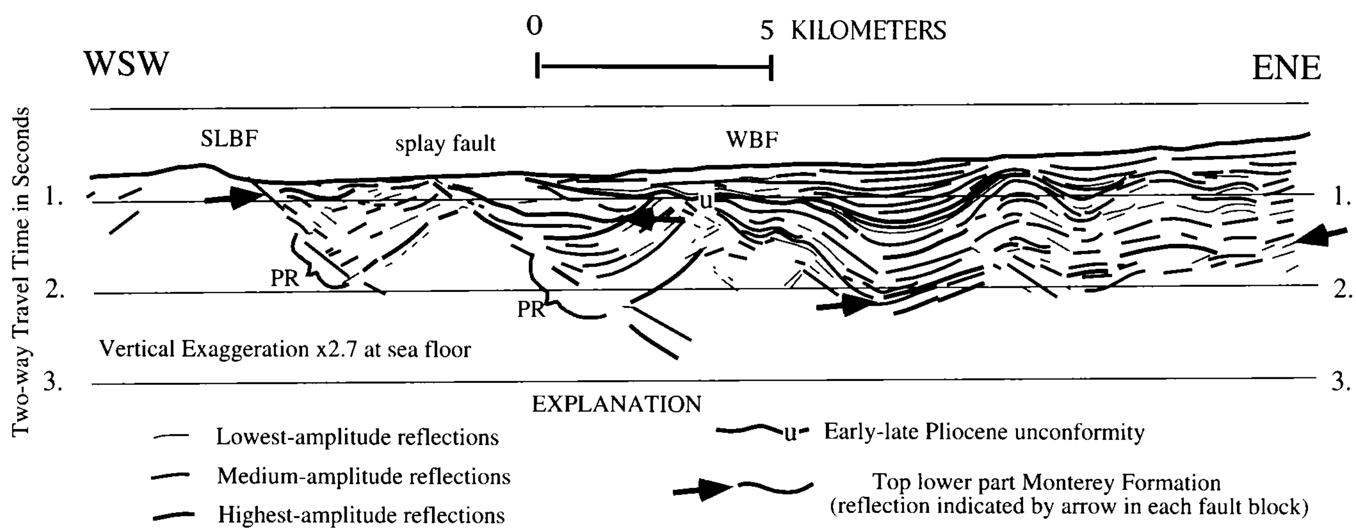

Figure 9. Hand-traced line drawing of primary reflections from migrated industry multichannel seismic reflection section offshore south-central California (see figure 2 for location). Obvious multiples were not traced. SLBF, Santa Lucia Bank Fault; WBF, West Basin Fault. The splay fault strikes north-northeast. The folds at WBF and 5 km east of WBF combine toward the north to form the Queenie structure. Note the large normal separation of the lower part Monterey Formation and older strata, tilted blocks of pre-rift sediments (PR), and east-dipping fault-plane reflections. These east-dipping reflections are shown as they appear on the original data, and were not added to the figure as an interpretation.

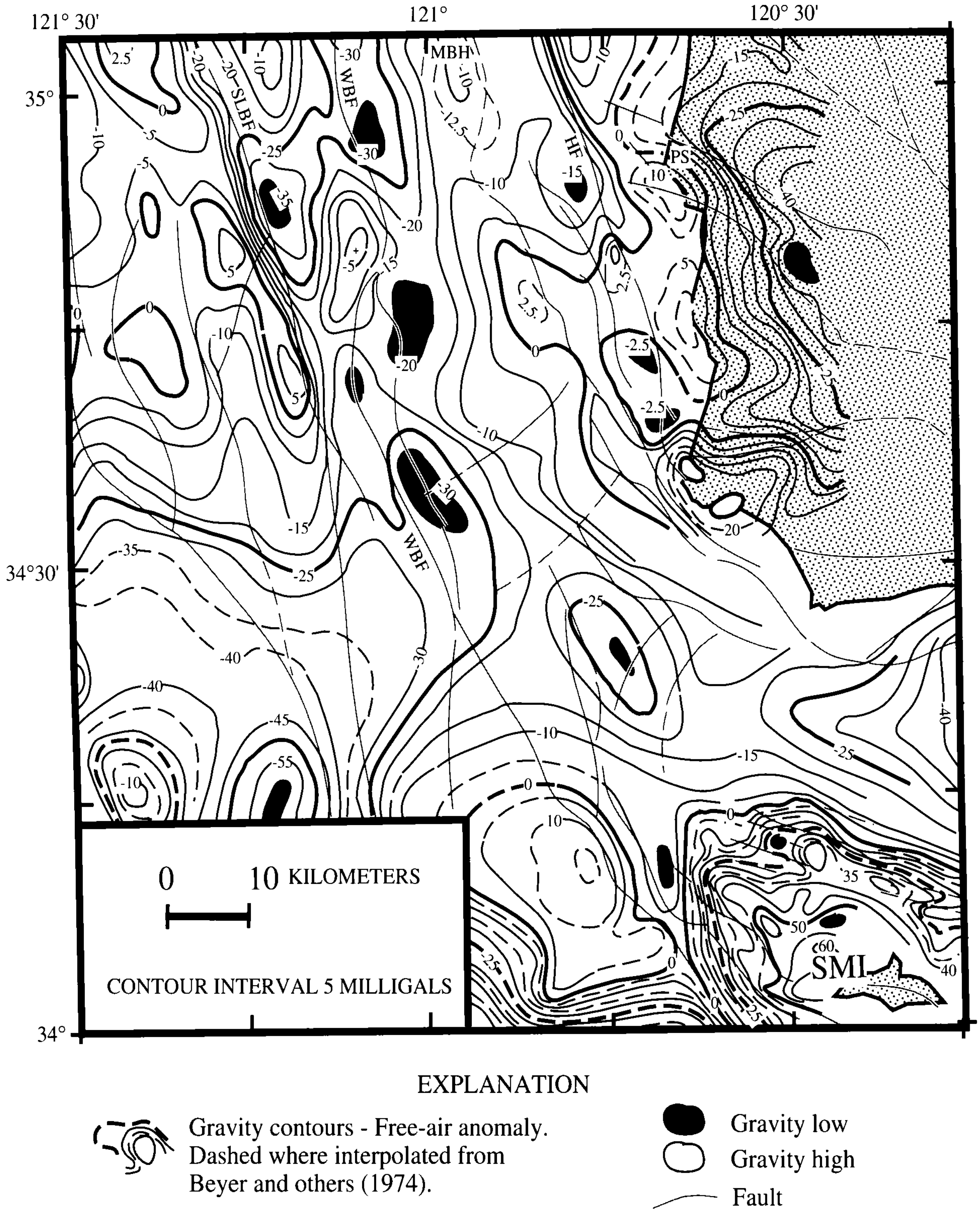

Figure 10. Free-air gravity map, near and offshore south-central California. Major faults from figure 5 are shown in the gray. Note that north-northeast-striking, east-dipping faults linking Santa Lucia Bank (SLBF) and West Basin (WBF) Faults are associated with hanging-wall gravity lows, and that the Mid-Basin (MBH) high of McCulloch (1987, 1989a) is associated with a gravity high. Free-air gravity is not corrected for bathymetry. Certain features, such as the gradient along the Santa Lucia Bank Fault, are associated with a sea floor topography, while others, such as the gradient across the Hosgri Fault (HF) northwest of Point Sal (PS), are largely due to a subsurface density contrast. Gravity contours redrawn after Beyer and others (1974) and McCulloch and others (1989).

in low signal-to-noise data below the map horizon if they are to be mapped.

Santa Lucia Slope Fault System

McCulloch (1987, 1989a) mapped a northwest-striking thrust fault in the outer slope between Santa Lucia Bank and the Santa Lucia Escarpment. This thrust fault is part of a belt of gently to moderately east-to-northeast-dipping faults that fold and fault the sea floor (figs. 1, 6; pl. 1). Lineaments imaged by side-scan sonar along this trend are consistent with faulting of the sea floor (EEZ Scan, 1986). The location of thrust earthquakes that occurred in 1969 and the attitude of the gently northeast-dipping nodal planes of their focal mechanisms are consistent with the location and attitude of these faults (Gawthrop, 1978). Faults split off from the northwest-striking Santa Lucia Slope Fault Zone and continue due northward along the west margin of Santa Lucia basin (figs. 5, 6). One of these faults is an important east-dipping normal-separation fault that backtilts a crustal block; Santa Lucia Bank is the east tip of this block.

The only stratigraphic control for timing of folding in the hanging wall of the Santa Lucia Slope Fault System comes from a regional correlation of Pliocene sediments across the West Basin and Santa Lucia Bank Faults along Lee 25 (fig. 8). The backlimb of this fold is onlapped by upper Pliocene sediments. The backlimb of this fold is between 7 and 10 km long on profiles USGS-3 and USGS-Lee-25, yet dips only about 1° on USGS-Lee-25, assuming an interval velocity of 2 km/s for late Pliocene sediment (fig. 8; pl. 1).

Northeast-Striking Faults

Northeast-striking middle Miocene and older acoustic basement highs which cross the axis of the offshore Santa Maria basin have been previously mapped (Willingham and others, 1991; Crain and others, 1985). We interpret these structures to be associated with northeast-striking, mostly southeast-dipping normal-separation faults (figs. 5, 6). The basin-bounding faults and the southeast-dipping cross faults break the deep horizons into rectangular blocks with map-view dimensions of ~10 km (northwest-southeast) by ~20 km (northeast-southwest).

Hosgri–Purisima–Offshore Lompoc–Mid-Basin Fault System

Offshore and onshore Santa Maria basins are separated by a broad system of mostly east-dipping faults, the Hosgri–Purisima–Offshore Lompoc–Mid-Basin Fault System. The Offshore Lompoc–Mid-Basin Fault(s) forms the west edge of the fault zone, the Hosgri Fault forms its east edge (Hoskins and Griffiths, 1971), and the Purisima Fault cuts the intervening sedimentary subbasin (see McCulloch, 1987, 1989a; figs. 5, 6). Quaternary slip on the Offshore Lompoc and Purisima Faults had been interpreted to be reverse (or thrust) (Payne and others, 1979; Crouch and others, 1984). However, all that can be said from seismic reflection profiles is that these faults exhibit reverse separation of the post-Miocene strata. At shallow levels, right-stepping en-echelon transpressional folds and faults of the Lompoc and Purisima trends converge and interconnect in map view southward with the Hosgri Fault (PG&E, 1988; Sorlien and others, 1996). These folds and discontinuous faults lie above continuous faults cutting middle Miocene and older horizons (fig. 6).

Stratigraphic separation of the Miocene map horizon, fold vergence, and structural style all vary along the strike of these faults in our new interpretation (fig. 6). These observations can be explained by an interacting system of strike-slip, oblique-slip, and perhaps reverse-slip fault strands which reactivate a preexisting Miocene extensional system. We interpret the Mid-Basin Fault of McCulloch (1987, 1989a) to be an east-dipping low-angle normal fault (profile RU-3 cross section on fig. 6). This fault has been interpreted as an unnamed detachment by Crouch and Suppe (1993; their fig. 9) on a profile located near Point Buchon. The footwall of the Mid-Basin Fault is the Mid-Basin High; this high is the tip of a crustal block which has been backtilted into the West Basin Fault.

The east-dipping strand of the Mid-Basin Fault continues into the Offshore Lompoc Fault across a right step located west of Point Sal (fig. 5). Southwest-dipping strands of the Offshore Lompoc Fault continue to the northwest where they are imaged on published seismic reflection sections that cross the Queenie structure (Clark and others, 1991). A large associated northeast-verging fold can be explained as the result of transpression in a restraining bend (a northwest-striking fault segment) of a system with a significant dextral component (fig. 6).

Northeast-striking structures cannot be traced east of the Offshore Lompoc Fault, suggesting either important strike-slip on the Offshore Lompoc Fault System or formation of the northeast-striking structures as cross faults between existing basin-bounding faults. While an important strike-slip component is possible on the Offshore Lompoc Fault, it is distinctly different in geometry from the Purisima and Hosgri faults. The Offshore Lompoc Fault generally lacks the subvertical hanging-wall fault strands that characterize the Purisima Fault and the Hosgri Fault in the shallow subsurface.

Hosgri Fault

We define the Hosgri Fault to be a distinctive steeply to moderately east-dipping strand or strands in the top 1 to 2 s (1 or 2 km) and do not interpret its geometry or slip farther downdip. The Hosgri Fault is the best studied of the wider fault system, in part due to its proximity to Diablo Canyon nuclear powerplant (PG&E, 1988). Despite this previous study, disagreement prevails about virtually every aspect of the Hosgri Fault, while little is published about the Purisima and Offshore Lompoc–Mid-Basin faults. Previous interpretations for Quaternary slip on the Hosgri Fault have included reverse slip (Namson and Davis, 1990), thrust and reverse slip (Crouch and others, 1984), or strike-slip (PG&E, 1988; Willingham and others, 1991; Hall and others, 1994; Hanson and Lettis, 1994; Steritz and Luyendyk, 1994). Estimates for the amount of Neogene lateral displacements along the Hosgri Fault have ranged from more than 80 km (Hall, 1975), to 115 km (Graham and Dickinson, 1978), to as high as 140 km (Hornafius, 1984). Alternatively, Neogene lateral displacements along the Hosgri–San Simeon–San Gregorio Fault System have been estimated at between 5 and 20 km (Willingham, 1978; Sedlock and Hamilton, 1991; Underwood and others, 1995).

We used high-resolution multichannel seismic reflection data (see fig. 11 for trackline locations) to locally map the Hosgri Fault in the shallow subsurface. The Hosgri Fault proper projects onshore near Point Arguello, but the wider fault system continues southeastward into the western Santa Barbara Channel (figs. 5, 11; see Roush, 1983; Steritz and Luyendyk, 1994). Mapping using the data from profiles located in figure 3 indicates that the faults between Point Arguello and Point Conception are interconnected in three dimensions. Therefore, in this area we refer only to the Hosgri–Purisima–Offshore Lompoc Fault System. There is a complex interference pattern between this fault system and west-striking faults of northern Santa Barbara Channel such as the North Channel Fault (fig. 5) of Yerkes and others (1981). In detail, the southwestern strand of the Hosgri–Purisima–Offshore Lompoc Fault System (at K on fig. 11) is segmented by bends as it alternatively reactivates west-striking and then northwest-striking Miocene faults along strike. We agree with the Steritz and Luyendyk (1994) interpretation that the fault system is truncated by an east-west fault, the North Channel Fault, in northwestern Santa Barbara Channel (fig. 5).

North Channel Fault

Major east-west fault systems bound Santa Barbara Channel to the north and south; both fault systems interact with the fault systems which flank the offshore Santa Maria basin. The North Channel Fault System parallels the coast a few kilometers offshore and was thought to be active as a reverse fault (fig. 6; Yerkes and others, 1981). This structure has recently been interpreted to be a hanging-wall fault-propagation fold above an underlying ramp of the major San Cayetano Fault (blind, low-angle thrust fault ramps are not mapped in fig. 5, and the surface trace of the San Cayetano Fault is east of fig. 5; Namson and Davis, 1992). A deep fault-plane reflection has been interpreted, and the deep fault has been locally mapped beneath north-central Santa Barbara Channel (Hornafius and Luyendyk, 1995). The North Channel Fault trend curves to the northwest near Point Conception, and the Point Arguello Oil Field is located in a broad fold in the hanging wall of related northeast-dipping faults.

Northern Channel Islands Faults

A broad zone of west-northwest-striking faults was mapped between the northern Channel Islands (including San Miguel and Santa Rosa Islands on fig. 5) and Santa Barbara Channel (Junger, 1979). This zone includes the westward continuations of the Santa Cruz Island and Santa Rosa Island Faults, which each run east-west down the axis of their namesake islands and continue offshore. Both the north branch of the Santa Cruz Island Fault (onshore) and the east half of the Santa Rosa Island Fault dip north with normal separation on Miocene and older rocks and generally reverse (north-side-up) separations on Pleistocene terrace deposits. Both the Santa Cruz Island Fault and the Santa Rosa Island Fault have an important Quaternary sinistral component, as shown by offset canyons, ravines, and striations, and both are probably strike-slip faults (Patterson, 1979; Pinter and Sorlien, 1991; Sorlien, 1994b; Colson and others, 1995).

The main Quaternary strand of the Santa Cruz Island Fault dips south for at least 40 km in the area north of Santa Rosa Island to the northwest of San Miguel Island (fig. 5; McWayne and Sorlien, 1994). This fault segment has south-side-up separation of Quaternary sediments where they are present, and it controls the location of the shelf break north of Santa Rosa Island. Farther west, the Santa Cruz Island Fault no longer forms a distinctive narrow fault zone, but instead a zone of partially blind south-dipping faults is present (pl. 1, line USGS-

Figure 11. Shallow subsurface (top 100 m) fault map of the southern Hosgri Fault north of Point Arguello, and the Hosgri-Purisima-Lompoc Fault system to the south of Point Arguello, California. For maps of associated folding, see PG&E (1988) and Cummings and Johnson, (1994). Locations of migrated 3-s to 4-s multichannel reflection profiles are indicated by thin gray lines. Lower hemisphere equal-area plots show fault and striation measurements. Upper left plot includes latest slip on three major strands of Honda Fault; middle plot includes measurements of scattered faults, and lower plot is last slip on a fault that cuts tip of Point Arguello. Important observations include: Out-of-plane reflections mask a diffuse Hosgri Fault (A); folding above shallow decollements (B); an arcuate southwest-dipping reverse (?) fault (C); east-dipping fault-plane reflections (D); subhorizontal striations on last-active surfaces of Honda Fault (F), 10-20 m of normal separation of the Monterey Formation across a fault aligned with the offshore Hosgri Fault (G); horizontal striations on last-active surfaces of a north-striking fault (H); southwest-dipping shear zone in Monterey Formation which is likely related to offshore southwest-dipping zones (I); diffuse disturbed zone (J) becomes a discrete northeast-dipping fault (J′); and a fault bends as it reactivates northwest and west-striking faults (K).

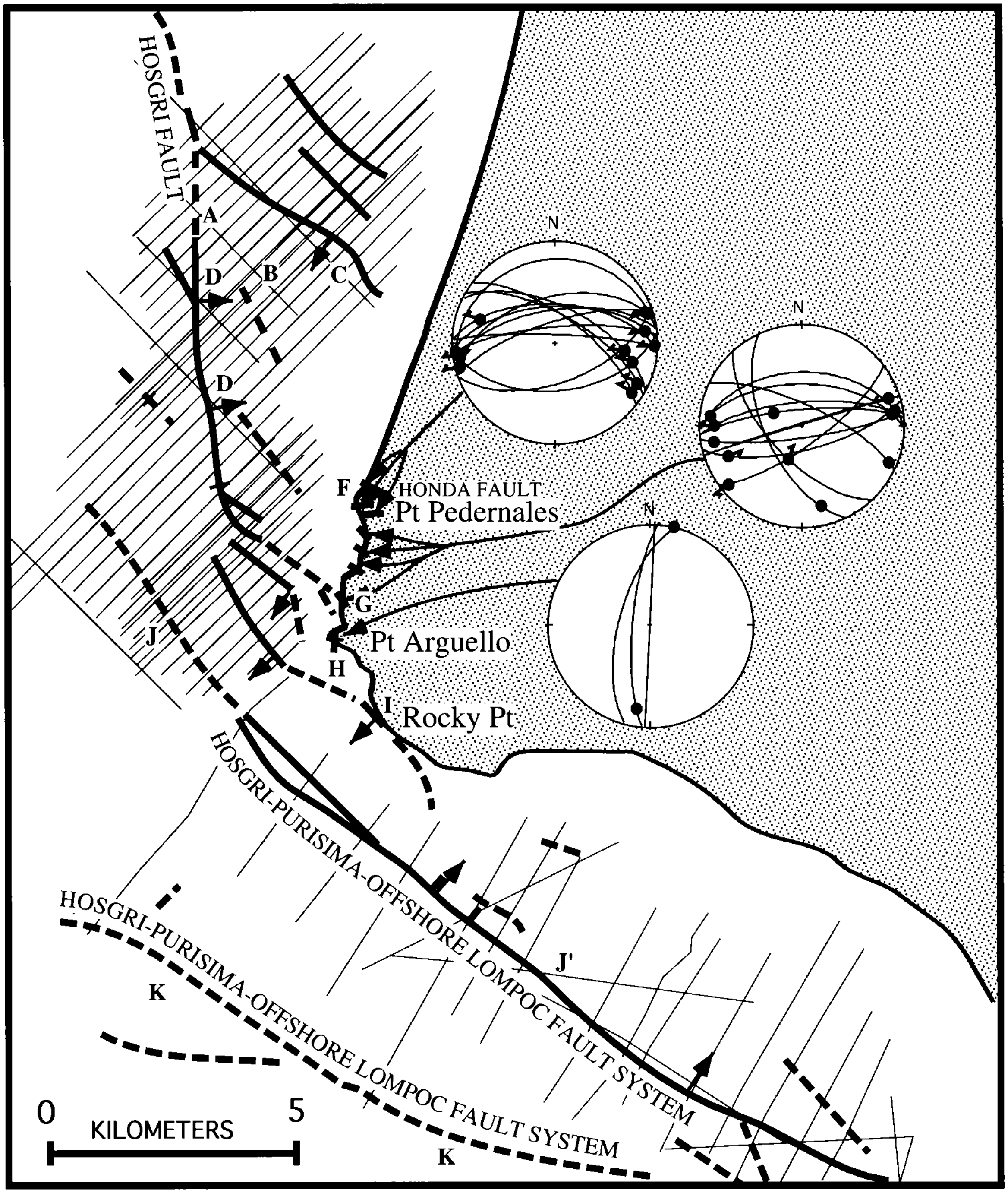

EXPLANATION

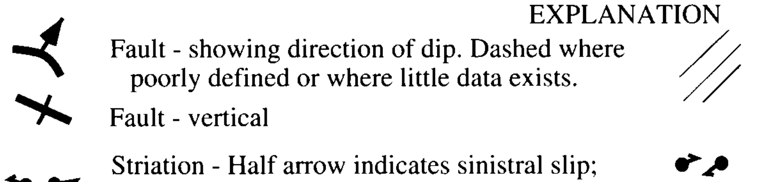

Fault - showing direction of dip. Dashed where poorly defined or where little data exists.

Fault - vertical

Striation - Half arrow indicates sinistral slip; arrows pointing toward center of circle indicate a reverse component of slip.

Multichannel high-resolution seismic reflection profiles

Striation - Half arrow indicates dextral slip; arrows pointing away from center of circle indicate a normal component of slip.

105, S.P. 300-500). The Santa Cruz Island Fault is well defined and continuous for a distance of over 100 km, east of, and not inclusive of, USGS-105.

DISCUSSION

Models for Formation of Structures

Oligocene Erosion and Miocene Rifting

The west North American margin has been active for the entire Cenozoic and has been affected by subduction, transtension, and then transpression (Atwater, 1970, 1989). As stress and strain patterns changed, faults in older rocks have been reactivated (Clark and others, 1991). We have constructed a regional two-dimensional (map view) block model and reconstructed this model to early Miocene time. Before this could be done, the timing, type, and magnitude of motions within and between crustal blocks had to be estimated.

The regional mid-Cenozoic unconformity and nonmarine deposition discussed in the "Wells and Stratigraphy" section occurred as Pacific-Farallon spreading centers approached western North America and younger crust was being subducted (Atwater, 1989; Lonsdale, 1991). We have interpreted northeast-striking thrust faults to be associated with this erosion along profile USGS-6B, especially beneath the Amberjack High (fig. 5; pl. 1). However, more onshore and offshore work is required, especially between Point Conception and Point Arguello, before the existence of Oligocene thrust faults is confirmed.

We have discussed a geometry of gently to moderately dipping faults which commonly preserve normal separation of Miocene sediments. Prerift sediments are backtilted into the border faults, forming half-grabens, with limited syn-rift (early and middle Miocene) sediments thickening westward into the faults (fig. 9). The available dates and correlations (discussed in the "Wells and Stratigraphy" section) indicate subsidence at about 25 Ma in the western Transverse Ranges and about 18 or 17 Ma in onshore and offshore Santa Maria basin (McLean, 1991; McCrory and others, 1995; Stanley and others, 1994). Logically, subsidence of hanging walls accompanies rapid extension. Subsidence in backtilted half-grabens will be maximum in the hanging-walls adjacent to listric faults (see Xiao and Suppe, 1992; Shelton, 1984). The tips of the backtilted blocks (or crests of roll-over anticlines) may not subside. Extension across south- and southeast-dipping faults such as the Santa Ynez River Fault and faults parallel to Amberjack High (fig. 5) is expected to cause subsidence of the hanging wall (the Santa Ynez Mountains block and Santa Barbara Channel), as seen by the rapid subsidence at about 24 Ma (Stanley and others, 1994). Subsidence of the footwall (onshore and offshore Santa Maria basin) might be delayed (western Transverse Ranges) (see Tennyson, 1992; Tennyson and Beeman, 1993). Thus, the Lospe Formation may record the first subsidence of Santa Maria basin, but need not record the time of initial extension (M.E. Tennyson, oral commun., 1994).

Large normal separations across certain faults are limited to pre-late Miocene sediments. Near Point Buchon (fig. 1), hanging-wall strands of the Mid-Basin Fault are overlapped by upper Miocene sediments and probably by middle Miocene sediments (fig. 9 in Crouch and Suppe, 1993). Several of the northeast-striking faults are also overlapped by upper Miocene sediment, with only minor reactivation. Extension must locally have been rapid if most of it occurred during early and middle Miocene time. Slower extension continued at least to the end of the Miocene because upper Miocene sediments thicken in the hanging walls of faults (figs. 7, 8; Clark and others, 1991).

Extension can be estimated across moderately dipping faults along the west margin of the offshore Santa Maria basin from fault dip and vertical separation. The acoustic basement has about 2 km of normal vertical separation across the Santa Lucia Bank Fault System and an additional 2 km across the West Basin Fault System. Qualitative comparison with the Offshore Lompoc and Purisima–Hosgri Faults results in similar estimates. Using a 35° dip estimated from figure 9, the horizontal extension of acoustic basement (west) or the base of Miocene sediments (east) across offshore Santa Maria basin would be slightly more than 10 km.

This estimate of 10 km of Miocene extension may be a minimum amount. West of the Hosgri Fault, a trough in the hanging wall of the Mid-Basin Fault may contain Paleogene and Cretaceous sediments (Vedder and others, 1991; Crouch and Suppe, 1993). If these sediments are erosional remnants, then large-scale extension is not required. If these sediments are, in part, tectonic slivers, then they might restore tens of kilometers against Paleogene and Cretaceous sediments on Santa Lucia Bank (Hoskins and Griffiths, 1971). This extension would be accommodated by gently dipping faults inferred, but not drawn on plate 1, to separate Franciscan Complex from Cretaceous sediments. The backtilted, parallel reflections seen on figure 9 are interpreted to be pre-Miocene, prerift sediments (D. Mayerson, national assessment of undiscovered resources, Pacific offshore region, offshore Santa Maria basin, Jan. 12, 1994, presentation, Camarillo). These imaged blocks, the nonimaged moderately to steeply dipping blocks of presumed Paleogene and Cretaceous sediments, and erosion of these sediments must all be taken into account before a quantitative pre-Miocene reconstruction of offshore Santa Maria basin can be attempted.

Shortening and Basin Inversion

There is general agreement that post-Miocene contraction has occurred along the southern and central California margin (Page, 1981; Namson and Davis, 1988, 1990, 1992; Yeats, 1983 and 1988; Crouch and others, 1984; Davis and others, 1989; Edwards and Heck, 1994; McGroder and others, 1994; Crouch and Suppe, 1993). Northeast-southwest to north-northeast–south-southwest shortening continues to the present (Feigl and others, 1990, 1993, Harris and Segall 1987; Yerkes and Lee, 1987; PG&E, 1988; Mount and Suppe, 1992; Shen and Jackson, 1993). However, several recent papers have suggested late Miocene through Pliocene contraction in the offshore Santa Maria basin (Meltzer and Levander, 1991, Miller, 1993) or even middle to late Miocene contraction (Henrys and others, 1993). These latter conclusions are based on mis-ties to the only two wells used for stratigraphic control in those studies, the Oceano P-060 #1 and COST 164 #1 wells, and the assumption that a diagenetic marker represents top of the Monterey Formation (Meltzer, 1988). The regional correlations of Meltzer and Levander (1991) mis-tie the intersecting published profiles of Clark and others (1991) and PG&E (1988). The latter interpretations are part of regional stratigraphic correlation that is controlled by about 50 wells (Clark and others, 1991).

The timing of shortening is given by the age of sediments which thin over or onlap onto compressional folds. These relations are clearly imaged on single-channel profiles which cross the west margin of offshore Santa Maria basin (figs. 7, 8). On profile USGS-3, onlap of upper Pliocene sediments from east to west supports an initiation of growth of the hanging-wall fold above the Santa Lucia Slope Fault System toward the end of early Pliocene time (fig. 8; pl. 1, profile USGS-3). Post-Miocene shortening can also be inferred in the Point Arguello Oil Field and in northwestern Santa Barbara Channel (pl. 1, profiles USGS-3 and USGS-105; Edwards and Heck, 1994). In fact, in northwestern Santa Barbara Channel, transtension may have locally continued through early Pliocene time (McGroder and others, 1994).

Folding Significance: Transpression, Rotation, and Total Shortening

The location and orientation of post-Miocene folds can now be related to the deeper structure of the Miocene border fault system, and fault kinematics can be inferred. North- to north-northwest-striking basin-bounding faults and northeast-striking cross faults form the deep framework of the offshore Santa Maria basin which is now being reactivated by late Pliocene and Quaternary north-northeast to northeast shortening. Regionally, fold axis trends are west-northwest in the onshore Santa Maria basin and north-northwest to northwest in the offshore Santa Maria basin (PG&E, 1988). This contrast could be explained by contrasting late Pliocene-Quaternary stress and strain fields across the Hosgri Fault System, or by the following alternative hypothesis: The regional stress field in the onshore and offshore Santa Maria basin is roughly the same, with north-northeast- to northeast-directed compression (Mount and Suppe, 1992). Basement ramps associated with existing normal separation faults serve as buttresses against which thick hanging-wall sediments are folded (see Clark and others, 1991). The trend of the fold will be parallel to the underlying ramp even if slip is oblique. Folds are amplified in left bends (northwest- to west-northwest-striking border-fault segments) and disappear in right bends (north-northeast-striking border-fault segments). For example, the Queenie structure (fig. 5), the largest amplitude fold in western offshore Santa Maria basin, dies out abruptly to the north as the West Basin Fault curves to a more northerly strike (fig. 6), and the fold at time 00 on profile USGS-Lee-24 dies out over a short distance to the north and south (fig. 7). This localization of shortening is compatible with north-northeast shortening and with distributed right-lateral regional shear on the north-south border-fault systems.

The bends in the West Basin Fault and Offshore Lompoc Fault tend to occur near their intersections with the northeast-striking cross faults. Small block rotation within offshore Santa Maria basin may contribute to localization of folding and bending of the border faults. In this model, post-Miocene dextral slip on border faults is accompanied by sinistral reactivation of northeast-striking cross faults and clockwise rotation of the rectangular crustal blocks between. The north and south corners of these blocks pull away from basin-bounding faults, while east and west corners overlap them (see Nicholson and others, 1986).

The average rate of shortening across offshore Santa Maria basin is related to the timing of shortening and the rate of dip slip on faults and to the dip of these faults.

One of the largest folds along the southern segment of the West Basin Fault is imaged on profile USGS-Lee-24 (fig. 7). The fold in the hanging wall of the West Basin Fault appears impressive because of vertical exaggeration (fig. 7*A*), but the steepest average dips of the east limb are only about 4°. The early/late Pliocene unconformity has about 240 m of vertical separation across the fault. These numbers should be increased by 50 percent to account for erosion across the crest of the fold; sediment compaction is not corrected. Erosion is estimated from the thickness of the upper part of the lower Pliocene sediments on the east flank of the fold, compared with the corresponding thickness across the crest of the fold, with the difference being due to erosion during slip on the fault. This adjusted 360-m separation represents about 510 m of shortening and 630 m of dip-slip component on a 35°-dipping fault. If this adjusted slip is averaged over 3.5 Ma, the average rate of dip-slip motion is about 0.2 mm/year. Estimates for post-Miocene shortening on the Queenie structure (fig. 5), located above another north-northwest-striking segment of the West Basin Fault, are as high as about 550 m (Clark and others, 1991).

It is possible to estimate the strike-slip component of slip on the West Basin Fault from the shortening in its restraining bends. North-northeast-striking segments of the West Basin Fault south of the Queenie structure have minimal post-Miocene dip-slip motion. North-northeast-striking (23°) strike-slip fault segments therefore link two north-northwest-striking (336°) oblique-slip segments. The strike-slip motion on the north-northeast-striking segments is 510 m/(cos 43)=700 m.

This will be a minimum estimate if the bends in the West Basin Fault have increased in amplitude during post-early Pliocene time.

The bed length of a Pliocene reflection was measured on a 1:1 depth section along the eastern 50 km of profile USGS-3 (fig. 2; pl. 1) to estimate shortening due to folding (fig. 8). Shortening in the plane of the section due to folding is less than 1 percent or between zero and a few hundred meters.

Post-early Pliocene upper crustal shortening across the offshore Santa Maria basin does not average more than a fraction of a millimeter per year, since folding is both localized and low amplitude (fig. 7). The Santa Lucia Slope Fault System (fig. 5) may accommodate an additional kilometer of shortening due to faulting and folding. This shortening can be measured from the depth section (pl. 1, line USGS-3) by comparing present bed length of the early/late Pliocene unconformity to the horizontal distance. An estimate of about 0.7 km of shortening can be made by simple balancing of the cross-sectional area below the interpreted early/late Pliocene sequence boundary. The excess area is calculated above the straight line shown on profile USGS-3, plate 1. A depth to detachment of about 15 km is used. This depth is a little less than the depth of the top of the subducted oceanic slab interpreted from seismic reflection and refraction experiments farther east (Nicholson and others, 1992, K. Bird, C. Sorlien, and E. McWayne, unpub. interpretation of profile USGS-103) and about the same as the depth to this high-velocity interface along strike to the north (Howie and others, 1993). Sediment compaction and a possible preexisting normal-separation scarp makes 0.7 km a minimum estimate of shortening.

Fault-Related Folds

Fault-related fold theory has been applied to California to estimate slip on blind faults from the geometry of folds (Namson and Davis, 1990; Shaw and Suppe, 1994). Slip is equal or greater than the width (downdip direction) of the backlimb for a fault-bend fold (Suppe, 1983). Only part of this slip is absorbed by faulting and folding along the hanging-wall fold trend; the rest continues on a decollement toward the foreland.

Slip is estimated from the distance between the intersections of axial surfaces with the fault for a fault propagation fold. All slip is absorbed in the hanging-wall fold (Suppe and Medwedeff, 1990; Mitra, 1990). Predictions of both models include no progressive tilting because dip is acquired instantaneously by kinking through active axial surfaces (Suppe and others, 1992). The uplift rate is constant above fault ramps in these models (Sorlien and others, 1995).

Wide gently dipping backlimbs of folds are present beneath the western Santa Barbara Channel, offshore Santa Maria basin, and southwestern Santa Lucia basin. Examples are seen on profile USGS-Lee-24 (~6 km, 3°; fig. 7), profiles USGS-Lee-25 and USGS-3 (7 to 10 km, 1-2°; fig. 8; pl. 1), and USGS-105 (9 to 10 km; 6°; pl. 1). Reflections interpreted to be from the faults responsible for these wide backlimbs are best imaged along the West Basin Fault and beneath western Santa Barbara Channel (figs. 7, 9; pl. 1, line USGS-105). Slip would be 9 to 10 km if the fold in western Santa Barbara Channel is a fault-bend fold, and 7 or 8 km if it is a fault-propagation fold related to the shallow, imaged faults. The entire slip 7 or 8 km of slip predicted from a fault-propagation fold model would have to be absorbed by shortening along the trend of the structure; it would be difficult to account for more than a kilometer or two of this slip. Seeber and Sorlien (unpub. data) have interpreted the 9- to 10-km-wide backlimb on profile USGS-105 (fig. 2; pl. 1) to be part of a 20-km-wide fold limb that becomes apparent farther east.

It is possible to form wide gently dipping backlimbs by small slip on a listric fault (Sorlien and others, 1995). Curved faults are common in extended areas (Xiao and Suppe, 1992; Yin and Dunn, 1992; Wernicke and Axen, 1988), and curved (listric and antilistric) detachment faults are present in the inner California Continental Borderland (Nicholson and others, 1993). Our interpretation that post-Miocene contraction reactivates existing Miocene normal faults is consistent with a listric model for compressional folding (see also Erslev, 1986; Clark and others, 1991; McClay and Buchanan, 1992; Mitra, 1993). Thrust slip on a listric fault will also cause progressive rotation of fold backlimbs (Sorlien and others, 1995). Older sediments dip more steeply north than do younger sediments along at least a 100 km length of southern Santa Barbara Channel (pl. 1, profile USGS-105; Seeber and Sorlien, unpub. data).

Kinematics and Structural Style

In a region of oblique deformation, the strain often partitions between coexisting thrust and strike-slip faults (Fitch, 1972; Mount and Suppe, 1987, 1992; Lettis and Hanson, 1991; Molnar, 1992). Evidence for post-Miocene oblique-reverse-dextral slip at slow rates has been discussed above. Therefore, it is possible that strike-slip and reverse faults may both be present in the study area.

Here, we present an argument for post-Miocene strike-slip motion on the Hosgri Fault. While the wider Hosgri-Purisima-Lompoc Fault System may have been oblique-reverse-dextral since the end of Miocene time, the steeply dipping hanging-wall strands in the top 1 to 2 km are being discussed here. With northeast-southwest shortening (or northeast-southwest-oriented maximum principal stress axis), dextral shear is expected on north-striking faults, and reactivation of older structures will be important in the older strata. However, in post-Miocene sediments, the Hosgri and Purisima Faults formed as new faults. As sediments are deposited, active faults will extend upward, essentially creating new fault surface. The sea floor serves as a free surface which cannot support shear stress, requiring that one of the principal stress axes be vertical. For reverse faulting, the minimum principal stress axis is vertical and the fault should dip about 30° (Anderson, 1951). Under a stress field consistent with strike-slip faulting, new faults near the sea floor should be vertical. In this model, subvertical strands of the Hosgri and Purisima Faults which cut the hanging-wall of the underlying east-dipping faults indicate strike-slip motion. We do not mean to imply what the slip might be at depth, as we cannot interpret whether the higher angle faults cut across or merge with low-angle east-dipping faults.

Other evidence exists for strike-slip motion on other coastal faults aligned with and north of the Hosgri Fault. Evidence for strike-slip motion on the San Simeon Fault (near Point Piedras Blancas in fig. 1) is compelling, and this slip is transferred to the offshore Hosgri Fault if displacement is conserved (PG&E, 1988; Lettis and others, 1990; Hall and others, 1994; Hanson and Lettis, 1994). Seismic reflection data and gravity data do not support cumulative post-Miocene reverse slip on the Hosgri Fault south of Point Sal. Gravity anomalies are consistent with an east-side-up reverse separation north of the intersection of the Hosgri Fault with the Lion's Head Fault (figs. 5, 10), while normal separation of the top of the Miocene has been proposed south of that intersection (Willingham and others, 1991; Steritz and Luyendyk, 1994). Normal separation of (eroded) top Sisquoc Formation also occurs north of the intersection with the Lion's Head Fault, with large reverse separation of top Monterey Formation (Sorlien and others, 1996). Our mapping indicates that the Hosgri Fault projects to the coast at Point Arguello. Subhorizontal striations are present on the last-active surface of a north-striking fault that cuts the tip of Point Arguello (fig. 11). Other high-angle faults in this area also are strike-slip faults. For example, the last active surfaces of the Honda Fault at Point Pedernales (fig. 11) record horizontal striations, interpreted from the striations as left-lateral on two or three fault surfaces, on several distributed fault strands.

Plate Tectonics

Geologic Evolution and Tectonics

Using marine magnetic anomalies and bathymetry recorded in the Pacific Plate oceanic crust, a carefully documented model has been presented for the evolution of oceanic crust in the northeast Pacific Ocean (Lonsdale, 1991; Atwater, 1989; Severinghaus and Atwater, 1991). During magnetic anomaly 10 time (30 Ma), the northern part of the Farallon Plate broke up, with the formation of the Monterey and Arguello Microplates (Lonsdale, 1991; Atwater, 1989), which are separated by the Morro Fracture Zone (fig. 1). First contact of the Pacific and North American Plates occurred north of the Monterey Microplate, near the Pioneer Fracture Zone; hence the maximum cumulative Neogene transform motion must have occurred north of the Monterey Microplate. A remnant of the Monterey Microplate and a fossil Monterey-Pacific spreading center are preserved west of central California (Lonsdale, 1991; Severinghaus and Atwater, 1991).

The Pacific-Monterey spreading center died about 19 Ma, while to the south of the Morro Fracture Zone, spreading continued at least to chron 5D (17.5 Ma), concluding with the subduction of, or extinction of, the Pacific-Arguello spreading center near the then active trench (fig. 12; Lonsdale, 1991; Severinghaus and Atwater, 1991). The transform boundary has lengthened by triple junction migration and microplate capture through Neogene time (Lonsdale, 1991; Atwater, 1989; Tennyson, 1989; Nicholson and others, 1994; Bohannon and Parsons, 1995).

Rifting of Baja away from mainland Mexico and a change in motion of the Pacific Plate have both been proposed as an explanation for initiation of crustal shortening in California. At about 5.5 Ma, initiation of spreading at the mouth of the Gulf of California occurred, but a significant amount of Pacific-North America Plate motion continued on faults located to the west of Baja California until at least 4 Ma (Lonsdale, 1989). Although 100 km of displacement occurred prior to 4 Ma in the Gulf of California, it was not until about 3.5 Ma that the offshore faults became inactive and the full (or nearly full) plate motion stepped inland to the Gulf of California (Lonsdale, 1989). Slip on the southern San Andreas Fault accelerated at this time (Crowell, 1979). Motion on the southern San Andreas Fault initiated the left step or restraining bend in the larger transform system at the present latitude of the Transverse Ranges; the amplitude of the restraining bend of the San Andreas Fault increased with time because of left slip on the Garlock Fault (see Bohannon and Howell, 1982; Atwater, 1989). The timing of initiation of sea floor spreading in the Gulf of California corresponds to the initiation of contraction in offshore Santa Maria basin.

Terranes

"Terranes are fault-bounded geologic entities of regional extent, each characterized by a geological history that is different from adjacent terranes. Such geologic histories are determined from stratigraphic successions preserved within terranes ..." (McWilliams and Howell, 1982).

On the basis of structural orientation, stratigraphic sequences, and paleomagnetic data, coastal California was previously divided into several distinct tectonostratigraphic terranes (Howell and others, 1987; Vedder, 1987; McCulloch, 1987, 1989a). The different pre-Neogene stratigraphic assemblages are best understood in terms of subduction-related belts. From originally inboard to outboard, these belts are (1) Cretaceous arc-related plutons intruded into Paleozoic metamorphic rocks, (2) late Jurassic through Paleogene forearc sediments, (3) late Jurassic through Cretaceous accretionary prism melange structurally below Jurassic ophiolite, and (4) Paleogene melange. It has previously been inferred that large lateral motion on strike-slip faults has rearranged these originally linear belts (Howell and others, 1987). However, the present distribution of basement and sedimentary rocks can be explained by subduction processes, onlap, erosion, tectonic denudation during extension, and filling of extensional basins. Therefore, the terrane concept must be modified to fit new information on the geometry and sediment distribution along terrane boundaries.

Model for Neogene Terranes

The traditional names for tectono-stratigraphic terranes have been retained in figure 13*A*. In south-central California, many of the structural and stratigraphic boundaries are transitional; therefore, to place distinct terrane boundaries at these features is misleading. For that reason, we characterized a number of fault blocks as transitional. Other boundaries that are shown as distinct in figure 13*A* are actually the result of erosion and are therefore gradual, or are the result of hanging wall over footwall relations across broad zones of gently dipping faults (Lee, 1992; Bohannon and others, 1993; Sorlien and others, 1993). Where lateral motion is involved, that motion might be the motion of sheets of crust detached above subhorizontal faults (Bohannon and Geist, 1991, in press; Crouch and Suppe, 1993).

In our reinterpretation, terranes are characterized as footwall or hanging wall (fig. 13*A*). This geometry is best seen to the southeast of our study area, where Cretaceous arc rocks and older country rocks (Santa Ana terrane) are in the hanging-wall of an east-dipping detachment fault above the tectonically denuded accretionary rocks of the Catalina terrane (Bohannon and Geist, 1991, in press; Nicholson and others, 1993; Crouch and Suppe, 1993). Although the surface trace of the Catalina–Santa Ana terrane boundary appears to coincide with the Coronado Bank and Newport Inglewood Faults, the boundary in cross section is actually across a family of gently east-dipping faults (Crouch and Suppe, 1993; M. Legg and others, unpub. data). High-angle faults such as the Newport–Inglewood Fault may have formed above relatively unimportant synthetic and antithetic Miocene faults and are not themselves important to the basement boundary. Large-scale extension across gently dipping faults results in backtilted prerift rocks being laterally distributed downdip. The map location of a terrane boundary depends on how far downdip it is placed. For example, the contact between footwall Catalina Schist and hanging-wall granite might be downdip of and east of the contact between Catalina Schist and hanging-wall Great Valley Series strata. Downdip distribution of hanging-wall sediment may also be the case above the Mid-Basin–Offshore Lompoc Fault. Cretaceous sediments are expected to be in fault contact with Franciscan Complex rocks east of (downdip of) the location of Paleogene sediments if the sediments are backtilted down to the west.

The proposed terrane boundary between the Patton and San Simeon terrane, previously proposed to be along the Santa Lucia Bank Fault (McCulloch, 1987, 1989a), is now interpreted to be a hanging wall over footwall relation across a wide fault zone. Significant basement velocity contrasts across the Santa Lucia Bank Fault are not indicated by published models derived from wide-angle reflection/refraction data, and large basement density contrasts are also not required to explain the observed gravity anomalies (Trehu, 1991; Miller and others, 1992). The subtle decrease in velocity west of the Santa Lucia Bank Fault can be explained by lower Miocene, Paleogene, and/or Cretaceous sediments being present below top acoustic basement (see Miller and others, 1992, p. 19,968). Interpretation of both single-channel reflection data and multichannel profiles shows that "acoustic basement" beneath Santa Lucia Bank may actually be composed of sediments which dip too steeply to be imaged. It is likely that the Franciscan Complex is younger to the west and that the age contrast should be across pre-Neogene thrust faults (Howie and others, 1993). However, there are several candidate faults, including the Offshore Lompoc Fault, the West Basin Fault, the Santa Lucia Bank Fault, several faults farther west, and the Santa Lucia Slope Fault System. Changes in basement age or composition are inherited from subduction and do not require large northwest-southeast lateral motion.

The North Boundary of the Western Transverse Ranges

A terrane boundary has previously been placed along the boundary between the western Transverse Ranges and Santa Maria basin (onshore and offshore) (Howell and others, 1987). This boundary was proposed to explain stratigraphic contrasts across it and has been proposed to be the edge of rotated crust (Hornafius and others, 1986). Paleogene sediments are characteristic of the western Transverse Ranges, and their near absence characterizes the onshore and offshore Santa Maria basin. This contrast has been attributed to either faulting (Sylvester and Darrow, 1979; Up de Graff and Luyendyk, 1989) or to the existence of a paleo-high and onlap onto that high (Dibblee, 1950, 1982a). In detail, the outcrop and subcrop pattern of the Great Valley Series is not so simple. Remnant deep water Eocene sediments are present between the Offshore Lompoc and Hosgri Faults, and Cretaceous forearc sediments are present beneath onshore Santa Maria basin (Vedder and others 1991; McLean, 1991; Crouch and Suppe, 1993). The distribution of forearc sediments is consistent with Oligocene erosion and/or Miocene tectonic denudation removing a regionally continuous Paleogene section.

For there to be a rotation boundary between onshore and offshore Santa Maria basin and the western Transverse Ranges, there must be a fault. Along profile USGS-6B (pl. 1), a notable feature of the post-middle Miocene section (or even post-Luisian Stage, about 14 Ma) is the lack of major structures between the western Santa Barbara Channel and the offshore Santa Maria basin. The onshore boundary had been proposed to be along the Santa Ynez River Fault and its east continuation, the Santa Ynez Fault (fig. 5; Hornafius and others, 1986). Dibblee (1982a) suggested that there has been minimal lateral slip on the Santa Ynez Fault and questions the existence of a post-early Miocene Santa Ynez River Fault. The rocks exposed on either side of the Santa Ynez River can be explained without an important fault. The American Association of Petroleum Geologists (1959) cross section shows a blind south-dipping fault beneath the Santa Ynez River to not cut the Miocene Monterey Formation. A seismic reflection profile along the American Association of Petroleum Geologists (1959) cross section allows only minor vertical separation of the Monterey Formation across this Santa Ynez River Fault (unpub. interpretation by C. Sorlien, 1996, of UNOCAL profile). A south-dipping fault or active axial surface along the trend of the Santa Ynez River Fault is mapped in the offshore on figure 11 at C. Thus, the onshore north boundary of the western Transverse Ranges is very similar to the stratigraphy and structure along the offshore Amberjack High (fig. 5; pl. 1, line USGS-6B), with blind south-dipping faults, erosion of Paleogene sediment, and continuity of Neogene sediments. Erosion and deposition can adequately explain the stratigraphic boundary between the onshore and offshore Santa Maria basin and the western Transverse Ranges, and large lateral motion between the two provinces is not required.

Rotation Models

Background

Extensive paleomagnetic sampling of the Miocene Monterey Formation and early to middle Miocene volcanic flows indicate about 90° of clockwise rotation of the western Transverse Ranges since about 19 Ma (Kamerling and Luyendyk, 1979, 1985; Luyendyk and others, 1980, 1985; Hornafius and others, 1986; Liddicoat, 1990; Luyendyk, 1991). Rotation models incorporate the geologic tie, indicated by Eocene (Poway) conglomerate clasts, between Santa Rosa-southwestern Santa Cruz Islands and the San Diego area (Abbott and Smith, 1978, 1989; Kamerling and Luyendyk, 1985). Models indicate that the western Transverse Ranges rifted away from the Peninsular Ranges and rotated about 110° outward about an east hinge (Kamerling and Luyendyk, 1985; Crouch and Suppe, 1993). The resulting large-scale extension was accommodated by detachment faults in these models (Yeats, 1976; Kamerling and Luyendyk, 1985; Legg, 1991; Crouch and Suppe, 1993).

Certain existing models for rotation of the western Transverse Ranges assume that blocks to the north and south are nonrotated, and that space problems to the north and south are accommodated by dextral strike-slip on northwest-striking faults or by overriding of blocks to the north (Luyendyk and others, 1980, 1985; Luyendyk and Hornafius, 1987; Luyendyk, 1991; Crouch and Suppe, 1993). However, we have shown that blocks north of the western Transverse Ranges are extended and propose that these blocks have been variably clockwise rotated. Several other studies have shown that crustal blocks located north and east of Santa Maria basin have been clockwise rotated 40° and more (Greenhaus and Cox, 1979; Hornafius, 1985; Whidden and others, 1993; Omarzai, 1992). Therefore, we suggest that remagnetization of rocks before or during Pliocene folding can explain the nonrotated results at sites within the Santa Maria basin (Hornafius, 1985; Beebe, 1986).

Mechanics and New Tectonic Rotation Model

The existence of offshore microplates, and their early Miocene capture, has provided a mechanism for regional extension and clockwise rotation (Nicholson and others, 1994; Bohannon and Parsons, 1995). The Pacific Plate captured the Monterey Microplate and its subducted slab about 19 Ma (Lonsdale, 1991). Regional extension occurred before and during this capture (Tennyson, 1989). Material with the high velocity characteristic of oceanic crust is present in the lower crust beneath offshore Santa Maria basin (Trehu, 1991; Meltzer and Levander, 1991; Howie and others, 1993). High-amplitude reflections have been traced from the top of oceanic crust of the Monterey Microplate remnant in the deep Pacific Ocean basement continuously for 40 km landward of the fossil trench (Meltzer and Levander, 1991). A discontinuity that disrupts this reflection is aligned with the Morro Fracture Zone in the lower crust beneath Santa Lucia basin and offshore Santa Maria basin (McIntosh and others, 1991; Nicholson and others, 1992). We propose that the subducted slab of the Monterey Microplate, bounded on the south by the Morro Fracture Zone (fig. 1), is today located in the lower crust beneath Santa Lucia basin and offshore Santa Maria basin. We propose that it has been there since subduction ceased (see Nicholson and others, 1994).

Rotation of the western Transverse Ranges initiated about 20-17 Ma (Luyendyk, 1991). The 19-Ma reconstruction of Lonsdale (1991) places the Monterey Microplate directly adjacent to the back-rotated western Transverse Ranges (fig. 12). A direct cause and effect between capture of the Monterey Microplate and rotation of the western Transverse Ranges is proposed by the tectonic model of Nicholson and others (1994). The western Transverse Ranges and Santa Maria basin are shown as a single block in figure 12, resulting in in an apparent space problem, with part of the offshore Santa Maria basin located above the Pacific Plate. Other regional reconstructions also use very large blocks, making it difficult to relate predicted motions to individual structures and causing apparent motions and space problems (Nicholson and others, 1994; Bohannon and Parsons, 1995). In addition, other reconstructions do not model the Santa Maria basin side of the rotating block (Legg, 1991), do not backrotate the western

Transverse Ranges (McCrory and others, 1995), or do not show the reconstructed map at all (Crouch and Suppe, 1993). We have used smaller blocks, allowing displacements predicted by the model to be compared to fault systems. However, internal deformation within the blocks must still be seen as a predicted motion at the block boundary.

Our reconstruction (fig. 13*B*) locates the Monterey Plate farther north with respect to the western Transverse Ranges than do those of Sedlock and Hamilton (1991), Legg (1991), and Bohannon and Parsons (1995). This discrepency is partially the result of existing models using the Neogene slip estimates of 80 km or more for the Hosgri Fault (Hall, 1975). The cross-Hosgri Fault correlation of Hall (1975) has been questioned (V.M. Seiders, unpub. data, 1979; Tennyson and others, 1990; Sedlock and Hamilton, 1991; R. Stanley, oral commun., 1991), and estimates of 5 to 20 km of Neogene displacement exist (Willingham, 1978; Sedlock and Hamilton, 1991; Underwood and others, 1995).

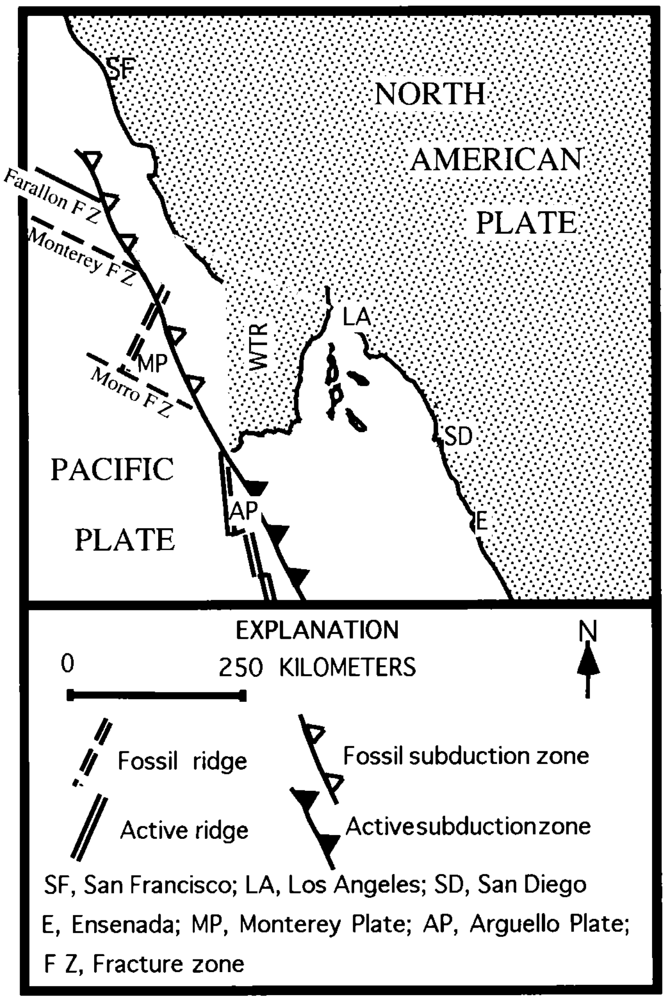

Figure 12. Position of the western Transverse Ranges (WTR), southern California, with respect to oceanic plates at 19 Ma. The central California coast and oceanic features are from Lonsdale (1991), and western Transverse Ranges are positioned where suggested by Lonsdale (1991). Overlap of rotated block with the subduction zone is partly due to use of a large single rotated block.

The Hosgri Fault terminates in northwestern Santa Barbara Channel (fig. 5; Steritz and Luyendyk, 1994). From this starting point of zero lateral slip, lateral slip can only be as much as the shortening east of the fault and extension west of the fault. Geologic maps and cross sections (Dibblee, 1950; 1988, a, b) and our interpretation suggest that north-south shortening along the coast is less than 10 percent, or less than 10 km, and therefore Neogene lateral slip on the Hosgri Fault is of this magnitude. We have not identified any piercing points across the West Basin–Santa Lucia Bank Fault System. However, many strands of these fault systems are overlapped by upper Pliocene sediments, and we estimate tens, not hundreds, of kilometers of oblique right-normal post-19 Ma slip across these faults.

In figure 13*A*, the south half of California west of the San Andreas Fault has been broken up into fault blocks. These identical fault blocks have been repositioned in the 19 Ma reconstruction (fig. 13*B*). This model uses a local reference frame, with the bounding rectangular frame being fixed to San Diego (Peninsular Ranges). Unlike previous models, block shapes and sizes do not change; therefore, the extension, displacement, and rotation can all be measured from this reconstruction, and space problems can be identified. The position of blocks, and thus the inferred cumulative strain on an individual block boundary, is also influenced by the need to minimize space problems throughout a model of interrelated blocks. A simplifying assumption that went into these figures is that post-Miocene shortening commonly has reactivated the Miocene extensional faults and that shortening almost everywhere has been less than earlier extension. Cumulative post-19 Ma extension is seen as overlap between fault blocks and the hanging-walls are on top of the footwalls across upper crustal faults in figure 13*B*.

Our reconstruction requires tens of kilometers of Miocene extension across the Santa Lucia basin and onshore and offshore Santa Maria basins. Restoration of the Paleogene and Cretaceous sediments preserved between the Mid-Basin and Hosgri Faults to Santa Lucia Bank is consistent with exposure of the Franciscan Complex by tectonic denudation above subhorizontal detachment faults (see Vedder and others, 1991; Crouch and Suppe, 1993; Hoskins and Griffiths, 1971). The Franciscan Complex basement beneath the central subbasin of offshore Santa Maria basin would then be analogous to the tectonically unroofed Catalina terrane (see Bohannon and Geist, 1991, in press; Crouch and Suppe, 1993).

The 19-Ma reconstruction (fig. 13*B*) suggests a mechanism for rotation of south-central California, including the western Transverse Ranges. Large-scale extension of the California margin had previously been linked to divergent motion of the Pacific Plate away from North America (McCulloch, 1987; Bohannon and others, 1993, Bohannon and Parsons, 1995; see Stock and Molnar, 1988). Plate motion was accommodated by spreading between the Pacific

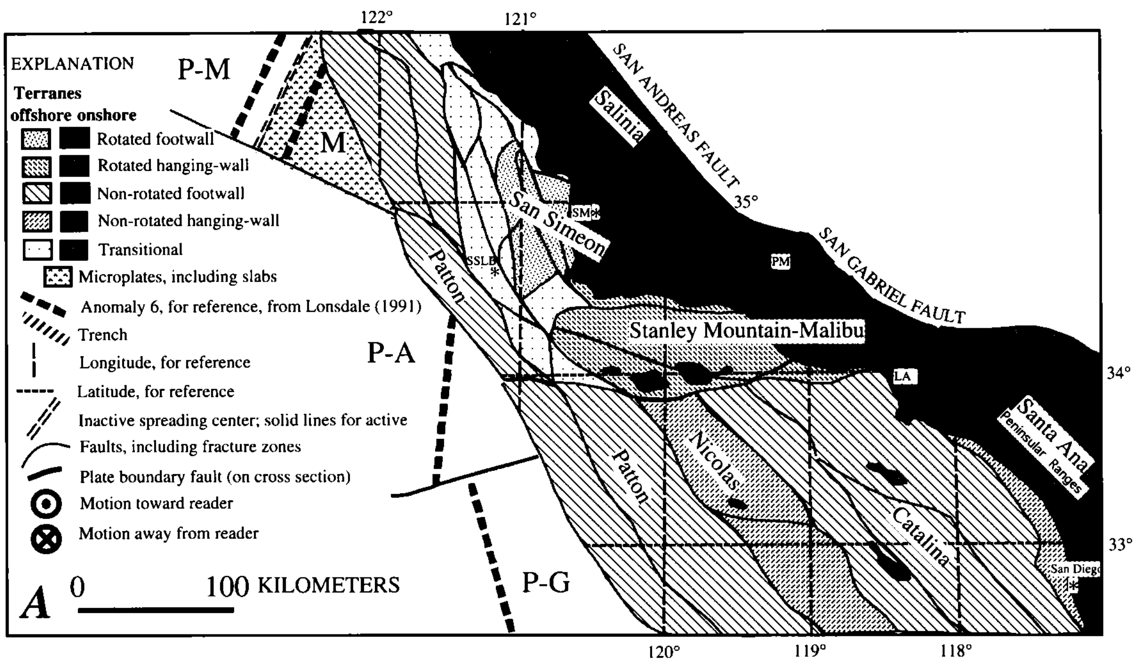

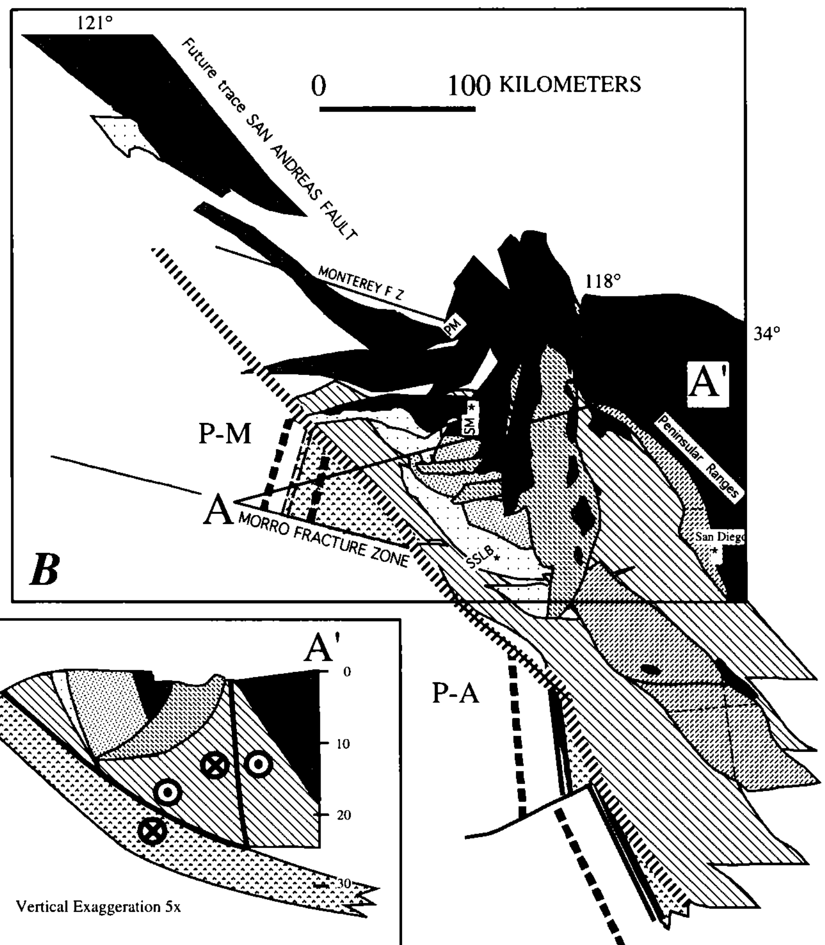

Figure 13. Neogene terranes of southwestern California. Every 1° of latitude and longitude is shown by thin black dashed lines. Asterisks are reference points for the reconstruction. LA, Los Angeles; M, Monterey Microplate remnant; P-M, Pacific Plate crust formed at the Pacific-Monterey spreading center; P-A, crust formed at the Pacific-Arguello spreading center; P-G, crust formed at the Pacific-Guadalupe spreading center; PM, Pine Mountain; SM, Santa Maria; SSLB=southern Santa Lucia Bank. *A*, Present distribution of fault blocks. *B*, 19 Ma reconstruction of Neogene terranes of southwestern California shows relative movement and rotation with respect to a fixed Peninsular Ranges block. There is 100 km, 140 km, and 350 km of displacement of a point on the Pacific Plate on the Morro Fracture Zone with respect to: Point Arguello, the Nicolas terrane, and the Peninsular Ranges (San Diego), respectively. Latitude and longitude lines and location names rotate with the blocks. Hanging-wall blocks are shown on top of footwall blocks; overlap indicates net extension since 19 Ma. Where individual fault blocks from the same terrane (fig. 13*A*) overlap, the block boundary is not drawn, for simplicity; the block boundary is retained in Sorlien (1994a). *C*, Cross section through figure 13*B* 19 Ma model.

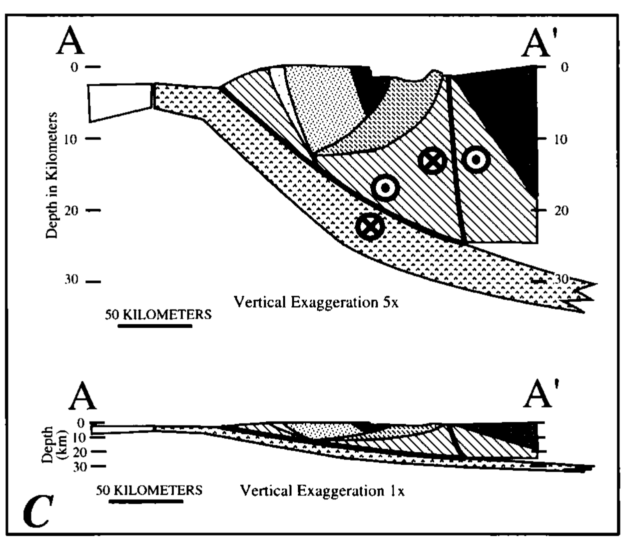

Plate and the Arguello and Monterey Microplates during early Miocene time. There is disagreement over whether the Monterey Microplate was subducting beneath the western Transverse Ranges, but there is agreement that subducted slab of either the Monterey or Farallon plates is present in the lower crust (Nicholson and others, 1994; Bohannon and Parsons, 1995). The end of spreading between the two microplates and the Pacific Plate at about 19 and 17 Ma (Lonsdale, 1991) resulted in the subducted slab of the Monterey Microplate following the Pacific Plate in a right-extensional motion away from the North American margin (Nicholson and others, 1994; Bohannon and Parsons, 1995). The upper-plate western Transverse Ranges were passively carried along and rifted away from the Peninsular Ranges (Nicholson and others, 1994). The plate boundary zone deformation then occurred on a series of low-angle faults, including the former subduction interface, with possible partitioned strike-slip on higher angle faults in areas predicted to be weak (fig. 13*C*).

While simply moving the subducted slab relatively to the northwest does not require rotation, clockwise rotation is expected if the then north end of the western Transverse Ranges was pinned to or buttressed against North America (see Nicholson and others, 1994). In addition, the subducted slab of former Monterey Microplate was oldest and coldest immediately north of the Morro Fracture Zone and was youngest and warmest immediately south of the Monterey Fracture Zone. The mechanically strong part of the slab is expected to be wider near the Morro Fracture Zone than just south of the Monterey Fracture Zone (see Severinghaus and Atwater, 1991). Therefore, the southern part of the slab might have exerted more traction on the upper plate than was the case farther north. In fact, for rotation of the upper plate or hanging wall to have occurred above a nonrotating slab, some decoupling is required.

Post-Miocene Tectonics

It is becoming apparent that clockwise rotation of at least part of the western Transverse Ranges continues today (Jackson and Molnar, 1990; Molnar and Gipson, 1994; Larson and Webb, 1992; Donnellan and others, 1993). This rotation may be associated with crustal shortening on many of the same low-angle faults which accommodated Miocene extension. Differential shortening across the south boundary of the western Transverse Ranges requires relative clockwise rotation of that block since mid-Pliocene time (relative to the borderland).

The new tectonic regime after Miocene time likely led to reactivation of Miocene detachment faults as large thrust faults. Large-area thrust faults have been proposed to explain the regionally continuous uplifting islands and mountain ranges in the western Transverse Ranges (Namson and Davis, 1988, 1992; Davis and Namson, 1994; Shaw and Suppe, 1994; L. Seeber and C. Sorlien, unpub. data).

CONCLUSIONS

Faults with moderate east dips bound the present-day offshore Santa Maria basin and preserve normal separation of Miocene horizons. To the west of the basin, the Santa Lucia Bank–West Basin Fault System is tens of kilometers wide, and it continues nearly due south into the outer borderland. To the east of the basin, the Hosgri Fault is a post-Miocene strike-slip fault above a family of moderately east-dipping faults. During Miocene extension on these boundary faults, all of the border faults of subbasins were also active.

The basement steps down to the southeast across northeast-striking faults from near 2 km depth in the offshore Santa Maria basin to near 8 km depth in the western Santa Barbara Channel. In the offshore Santa Maria basin, localized, limited post-Miocene shortening, and more important post-early Pliocene shortening, reactivated the border faults. The more important folds are associated with restraining bends for dextral slip on these faults. Post-Miocene shortening is estimated to be less than 1 km between the Offshore Lompoc Fault and the Santa Lucia Slope Fault System, with less than a kilometer of additional shortening across the latter structure. A sea floor fold scarp is seen above the Santa Lucia Slope Fault System, and sea-floor folding is interpreted above other structures.

Stratigraphic contrasts between crustal blocks in the offshore Santa Maria basin and Santa Lucia Bank areas can be explained by subduction processes, onlap, erosion, deposition in half-grabens, and possibly tectonic denudation from gently dipping faults; major lateral transport across hypothesized terrane boundaries is not required. We propose that inferred terrane boundaries are not major strike-slip faults, but are instead gently to moderately dipping faults which may be distributed several to tens of kilometers across strike. The thick Paleogene and Cretaceous sediments of the western Transverse Ranges are progressively more deeply eroded toward the northwest across several southeast-dipping transverse faults, while Neogene sediments thicken toward the southeast, resulting in a transitional stratigraphic boundary between the offshore Santa Maria basin and the Santa Barbara Channel. No important post-middle Miocene structural boundary separates the onshore and offshore Santa Maria basin from the western Transverse Ranges. The lack of an important late Neogene structural boundary, in addition to the continuity of structures and sediments from Santa Barbara Channel into offshore Santa Maria basin, suggests that blocks to the north of the rotated western Transverse Ranges have also been clockwise rotated.

Spreading (and subduction?) of microplates continued through much of early Miocene time along the south and south-central California margin. As the subducted slab of the Monterey Microplate was captured by the Pacific Plate after spreading stopped at 19 Ma, the upper-plate western Transverse Ranges were carried above it and rifted away from the Peninsular Ranges. Important syn-rotation extension occurred on the other side of the western Transverse Ranges, in offshore Santa Maria basin.

REFERENCES

Abbott, P.L., and Smith, T.E., 1978, Trace-element comparison of clasts in Eocene conglomerates, southwestern California and northwestern Mexico: Journal of Geology, v. 86, p. 753-762.

———1989, Sonora, Mexico, source of the Eocene Poway conglomerate of southern California: Geology, v. 17, p. 329-332.

American Association of Petroleum Geologists, Santa Maria Basin Sub-Committee of the American Association of Petroleum Geologists Committee on Stratigraphic Correlations; 1959, Correlation section across Santa Maria basin from outcrop in Santa Ynez Mountains northerly to outcrop north of the Santa Maria River, California: Pacific Section American Association of Petroleum Geologists.

Anderson, E.M., 1951, The dynamics of faulting: Oliver and Boyd, Edinburgh, 199 p.

Arends, R.G., and Blake, G.H., 1986, Biostratigraphy and paleoecology of the Naples Bluff coastal section based on diatoms and benthic foraminifera, *in* Casey, R.E, and Barron, J.A., eds., Siliceous microfossil and microplankton of the Monterey Formation and modern analogs: Pacific Section Society of Economic Paleontologists and Mineralogists, Los Angeles, p. 121-139.

Atwater, T., 1970, Implications of plate tectonics for the Cenozoic tectonic evolution of western North America: Geological Society of America Bulletin 81, p. 3513-3516.

——1989, Plate tectonic history of the northeast Pacific and western North America, *in* Winterer, E.L., Hussong, D.M., and Decker, R.W., eds., The Eastern Pacific Ocean and Hawaii: Boulder, Colorado, Geological Society of America, The Geology of North America, v. N, p. 21-72.

Avila, F.A., and Weaver, D.W., 1969, Mid-Tertiary stratigraphy, Santa Rosa Island, *in* Weaver, D.W., assisted by Doerner, D.P., and Nolf, B., Geology of the Northern Channel Islands: American Association of Petroleum Geologists and Society of Economic Paleontologists and Mineralogists Pacific Section, Special Publication, p. 48-67.

Barron, J.A., 1986, Upper diatom biostratigraphy for the Monterey Formation of California, *in* Casey, R.E., and Barron, J.A., eds., Siliceous microfossil and microplankton of the Monterey Formation and modern analogs: Pacific Section Society of Economic Paleontologists and Mineralogists, Los Angeles, p. 105-119.

Beebe, W.J., 1986, A paleomagnetic study of the southern Coast Ranges ophiolite, California, and tectonic implications: University of California, Santa Barbara, M.A. thesis,148 p.

Bereskin, S.R., and Edwards, L.N., 1969, Mid-Tertiary stratigraphy, southwestern Santa Cruz Island, *in* Weaver, D.W., assisted by Doerner, D.P., and Nolf, B., Geology of the Northern Channel Islands: American Association of Petroleum Geologists and Society of Economic Paleontologists and Mineralogists Pacific Section, Special Publication, p.68-79.

Beyer, L.A., Pisciotto, K.A., and Sasnett, N.B., 1974, Free-air gravity map of the California Continental Borderland, *in* Preliminary report on the geology of the Continental Borderland of southern California: U.S. Geological Survey Map MF-624.

Bird, K.J., McClellan, P.H., and Bruns, T.R., 1990, Case studies, Santa Maria province, California: American Association of Petroleum Geologists, Bulletin, v. 74, no. 5, p. 610 (abstract).

Blake, G.H., 1991, Review of the Neogene biostratigraphy and stratigraphy of the Los Angeles Basin and implications for basin evolution, *in* Biddle, K.T., ed., Active margin basins, AAPG Memoir 52: American Association of Petroleum Geologists, Tulsa, p. 135-184.

Bohacs, K.M., 1990, Sequence stratigraphy of the Monterey Formation, Santa Barbara County: Integration of physical, chemical, and biofacies data from outcrop and subsurface, *in* Keller, M.A., and McGowen, M.K., eds., Miocene and Oligocene petroleum reservoirs of the Santa Maria and Santa Barbara-Ventura basins, California: Society of Economic Paleontologists and Mineralogists Core Workshop No. 10, p. 139-200.

Bohannon, R.G., and Howell, D.G., 1982, Kinematic evolution of the junction of the San Andreas, Garlock, and Big Pine faults, California: Geology v. 10, p. 358-363.

Bohannon, R.G., and Geist, E.L., 1991, Tectonostratigraphy and Miocene extensional tectonism on part of the California Continental Borderland: A seismic reflection perspective, Geological Society of America, Abstracts with Programs, v. 23, no. 5, p. A479.

———, in press, Upper crustal structure and Neogene tectonic development of the California Continental Borderland: Geological Society of America Bulletin.

Bohannon, R.G., Geist, E.L., and Sorlien, C.C., 1993, Miocene extensional tectonism on California Continental Borderland between San Clemente and Patton escarpment: American Association of Petroleum Geologists Bulletin, v. 77, no. 4, p. 691 (abstract).

Bohannon, R.G., and Parsons, T., 1995, Tectonic implications of post-30 Ma Pacific and North American relative plate motions: Geological Society of America Bulletin, v. 107, no. 8, p. 937-959.

Chevron U.S.A. Inc./ Phillips Petroleum Company, 1982, Environmental Report (Exploration) Proposed exploratory wells, Federal OCS Leases 445, 446, 447, and 448.

Clark, D.H., Hall, N.T., Hamilton, D. H., and Heck, R.G., 1991, Structural analysis of late Neogene deformation in the central offshore Santa Maria basin, California: Journal of Geophysical Research, v. 96, no. B4, p. 6435-6457.

Colson, K.B., Rockwell, T.K., Thorup, K.M., and Kennedy, G.L., 1995, Neotectonics of the left-lateral Santa Rosa Island fault, western Transverse Ranges, southern California: Geological Society of America Abstracts with Programs, Cordilleran Section, v. 27, no. 5, p. 11.

Cook, H.A., editor, 1979, Geologic studies of the Point Conception deep stratigraphic test well OCS-CAL 78-164 no.1 outer continental shelf, southern California, United States: U.S. Geological Survey Open-File Report 79-1218.

Crain, W.E., Mero, W.E., and Patterson, D., 1985, Geology of the Point Arguello discovery: American Association of Petroleum Geologists Bulletin, v. 69, no.4, p. 537-545.

Crouch, J.K., Bachman, S.B., and Shay, J.T., 1984, Post Miocene compressional tectonics along the central California margin, *in* Crouch, J.K., and Bachman, S.B., eds., Tectonics and sedimentation along the California margin: Pacific Section Society of Economic Paleontologists and Mineralogists, Los Angeles, p. 37-54.

Crouch, J.K., and Suppe, J., 1993, Late Cenozoic tectonic evolution of the Los Angeles basin and inner California borderland: A model for core complex-like crustal extension: Geological Society of America Bulletin, v. 105, no. 11, p. 1415-1434.

Crowell, J. C., 1979, The San Andreas fault system through time: Journal of the Geological Society London, v. 136, p. 293-302.

Cummings, D., and Johnson, T.A., 1994, Shallow geologic structure. offshore Point Arguello to Santa Maria River, central California, *in* Alterman, I.B., McMullen, R.B., Cluff, L.S., and Slemmons, D.B., eds., Seismotectonics of the Central California Coast Ranges: Geological Society of America Special Paper 292, p. 211-222.

Davis, T.L., and Namson, J.S., 1994, A balanced cross-section of the 1994 Northridge earthquake, southern California: Nature, v. 372, p. 167-169.

Davis, T.L., Namson, J.S., and Yerkes, R.F., 1989, A cross section of the Los Angeles Area: Seismically active fold and thrust belt, the 1987 Whittier Narrows earthquake, and earthquake hazard: Journal of Geophysical Research, v. 94, no. B7, p. 9644-9664.

DePaolo, D.J., and Finger, K.L., 1991, High resolution strontium-isotope stratigraphy and biostratigraphy of the Miocene Monterey Formation, central California: Geological Society of America Bulletin, v. 103, p. 112-124.

Dibblee, T.W. Jr., 1950, Geology of southwestern Santa Barbara County, California: California Division of Mines and Geology Bulletin 150, 95 p.

——1966, Geology of the central Santa Ynez Mountains, Santa Barbara: California Division of Mines and Geology Bulletin 186, 99 p.

——1982a, Geology of the Santa Ynez-Topatopa Mountains, Southern California, *in* Davis, T.L., and Namson, J., eds., Evolution of the western Transverse Ranges: Society of Economic Paleontologists and Mineralogists, v. 48A, p. 1-16.

——1988a, Geologic map of the Tranquillon Mtn. and Point Arguello quadrangles, Santa Barbara County, California: *in* Ehrenspeck, H.E., ed., Dibblee Geological Foundation: Santa Barbara, California.

——1988b, Geologic map of the Lompoc and Surf quadrangles, Santa Barbara County, California, *in* Ehrenspeck, H.E., ed., Dibblee Geological Foundation: Santa Barbara, California.

Dickinson, W.R., Armin, R.A., Beckvar, N., Goodlin, T.C., Janecke, S.U., Mark, R.A., Norris, R.D., Radel, G., and Wortman, A.A., 1987, Geohistory Analysis of rates of sediment accumulation and subsidence for selected California basins, *in* Ingersoll, R.V., and Ernst, W.G., eds., Cenozoic Basin Development of Coastal California: Rubey Volume VI: Englewood Cliffs, New Jersey, Prentice Hall, p. 1-23.

Donnellan, A., Hager, B.H., King, R.W., and Herring, T.A., 1993, Geodetic measurement of deformation in the Ventura basin region, southern California: Journal of Geophysical Research, v. 98, no. B12, p. 21,727-21,739.

Dumont, M.P., and Barron, J.A., 1995, Diatom biochronology of the Sisquoc Formation in the Santa Maria basin, California, and its paleooceanographic and tectonic implications, *in* Keller, M.A., ed., Evolution of Sedimentary Basins/ Onshore Oil and Gas Investigations-Santa Maria Province: U.S. Geological Survey Bulletin 1995, p. K1-K17.

Edwards, E.B., and Heck, R.G., 1994, Structural model for Gato Canyon field, Santa Barbara Channel, California: Association Round Table, American Association of Petroleum Geologists Bulletin, v. 78, no. 4, p. 662, abstract.

EEZ SCAN 84 Scientific Staff, 1986, Atlas of the exclusive economic zone, western conterminous United States: U.S. Geological Survey Miscellaneous Investigation Series 1-1792.

Erslev, E.A., 1986, Basement balancing of Rocky Mountain foreland uplifts: Geology, v. 14, p. 259-262.

Feigl, K.L., King, R.W., and Jordan, T.H., 1990, Geodetic measurement of tectonic deformation in the Santa Maria fold and thrust belt, California: Journal of Geophysical Research, v. 95, no. B3, p. 2679-2699.

Feigl, K.L., Agnew, D.C., Bock, Y., Dong, D., Donnellan, A., Hager, B.H., Herring, T.A., Jackson, D.D., Jordan, T.H., King, R.W., Larsen, K.M., Murray, M.H., Shen, Z., and Webb, F.H., 1993, Space geodetic measurement of crustal deformation in central and southern California, 1984-1992: Journal of Geophysical Research, v. 98, no. B12, p. 21,677-21,712.

Fitch, T.J., 1972, Plate convergence, transcurrent faults, and internal deformation adjacent to southeast Asia and the western Pacific: Journal of Geophysical Research, vol. 77, no. 23, p. 4432-4460.

Flower, B.P, and Kennett, J.P., 1993, Relations between Monterey Formation deposition and middle Miocene global cooling: Naples Beach section, California: Geology, v. 21, p. 877-880.

Gawthrop, W.H., 1978, Seismicity and tectonics of the central California coastal region: California Division of Mines and Geology Special Report 137, p. 45-56.

Graham, S.A., and Dickinson, W.R., 1978, Apparent offsets of on-land geologic features across the San Gregorio-Hosgri Fault trend: California Division of Mines and Geology Special Report 137, p. 13-23.

Greenhaus, M.R., and Cox, A., 1979, Paleomagnetism of the Morro Rock-Islay Hill Complex as evidence for crustal block rotations in central coastal California: Journal of Geophysical Research, v. 84, 2393-2400.

Hall, C.A., Jr., 1975, San Simeon-Hosgri Fault system, coastal California: economic and environmental implications: Science, v. 190, p. 1291-1294.

———1991, Geology of the Point Sur-Lopez Point region, Coast Ranges, California: A part of the southern California allochthon: Geological Society of America, Special Paper 266, 40 pages.

Hall, N.T., Hunt, T.D., Vaughan, P.R., 1994, Holocene behavior of the San Simeon fault zone, south-central coastal California, *in* Alterman, I.B., McMullen, R.B., Cluff, L.S., and Slemmons, D.B., eds., Seismotectonics of the Central California Coast Ranges: Geological Society of America Special Paper 292, p. 167-189.

Hanson, K.L., and Lettis, W.R., 1994, Estimated Pleistocene slip rate for the San Simeon fault zone, south-central coastal California, *in* Alterman, I.B., McMullen, R.B., Cluff, L.S., and Slemmons, D.B., eds., Seismotectonics of the Central California Coast Ranges: Geological Society of America Special Paper 292, p. 133-150.

Harris, R.A., and Segall, P., 1987, Detection of a locked zone at depth on the Parkfield segment of the San Andreas Fault: Journal of Geophysical Research, v. 92, p. 7945-7962.

Henrys, S.A., Levander, A.R., and Meltzer, A.S., 1993, Crustal structure of the offshore southern Santa Maria basin and Transverse Ranges, southern California, from deep seismic reflection data: Journal of Geophysical Research, v. 98, no. B5, p. 8,335-8,348.

Hornafius, J.S., 1984, Paleomagnetism of the Monterey Formation in the western Transverse Ranges, California: University of California, Santa Barbara, Phd dissertation, 442 p.

———1985, Neogene tectonic rotation of the Santa Ynez Range, western Transverse Ranges, California, suggested by paleomagnetic investigation of the Monterey Formation: Journal of Geophysical Research, v. 90, no. B14, p. 12503-12522.

———1991, Facies analysis of the Monterey Formation in the northern Santa Barbara Channel: American Association of Petroleum Geologists Bulletin, v. 75, no. 5, p. 894-909.

Hornafius, J.S., and Luyendyk, B.P., 1995, Seismic images of the North Channel fault near Santa Barbara, CA: Southern California Earthquake Center, 1995 Annual Meeting, p. 63.

Hornafius, J.S., Luyendyk, B.P., Terres, R.R., and Kamerling, M.J., 1986, Timing and extent of Neogene rotation in the western Transverse Ranges, California: Geological Society of America Bulletin, v. 97, p. 1476-1487.

Hoskins, E.G., and Griffiths, J.R., 1971, Hydrocarbon potential of Northern and Central California offshore: American Association of Petroleum Geologists Memoir 15, p. 212-228.

Howell, D.G., Champion, D.E., and Vedder, J.G., 1987, Terrane accretion, crustal kinematics, and basin evolution, southern California, *in* Ingersoll, R.V., and Ernst, W.G., eds., Cenozoic basin development of coastal California: Rubey Volume VI, Prentice Hall, New Jersey, p. 242-258.

Howie, J.M., Miller, K.C., and Savage, W.U., 1993, Integrated crustal structure across the south-central California margin: Santa Lucia escarpment to the San Andreas Fault: Journal of Geophysical Research, v. 98, no. B5, p. 8,173-8,196.

Hutchinson, D.R., and Lee, M.W., 1989, Processing and attenuation of noise in deep seismic-reflection data from the Gulf of Maine: Marine Geophysical Researches 11, p. 51-67.

Isaacs, C.M., 1981, Lithostratigraphy of the Monterey Formation, Goleta to Point Conception, Santa Barbara coast, California, *in* Isaacs, C.M., ed., Guide to the Monterey Formation in the California coastal area, Ventura to San Luis Obispo: Pacific Section of the American Association of Petroleum Geologists, Camarillo, California, p. 9-23.

Isaacs, C.M., Keller, M.A., and Gennai, V.A., 1983, Preliminary evaluation of Miocene lithostratigraphy in the Point Conception COST well OCS-Cal 78-164 no. 1, off southern California, *in* Isaacs, C.M., and Garrison, R.E., eds., Petroleum generation and occurrence in the Miocene Monterey Formation, California: Pacific Section Society of Economic Paleontologists and Mineralogists, Los Angeles, p. 99-110.

Isaacs, C.M., Jackson, L.L., Stewart, K.C., and Scott, N. III, 1989, Analytic reproducibility and abundances of major oxides, total carbon, organic carbon, and sedimentary components of Miocene and early Pliocene cuttings from the Point Conception Deep Stratigraphic Test Well, OCS-CAL 78-164 no. 1, Offshore Santa Maria basin, Southern California: U.S. Geological Survey Open-File Report 87-75, 28 p.

Jackson, J., and Molnar, P., 1990, Active faulting and block rotations in the western Transverse Ranges, California: Journal of Geophysical Research, v. 95, p. 22073-22087.

Junger, A., 1979, Northern Channel Islands Platform, California Continental Borderland: U.S. Geological Survey Map and Report MF-991.

Kamerling, M.J., and Luyendyk, B.P., 1979, Tectonic rotations of the Santa Monica Mountains region, western Transverse Ranges, California, suggested by paleomagnetic vectors: Geological Society of America Bulletin, Part 1, v. 90, p. 331-337.

——1985, Paleomagnetism and Neogene tectonics of the northern Channel Islands, California: Journal of Geophysical Research, v. 90, no. B14, p. 12485-12502.

Larner, K., Chambers, R., Yang, M., Lynn, W., and Wai, W., 1983, Coherent noise in marine seismic data: Geophysics v. 48, p.854-886.

Larson, K.M., and Webb, F.H., 1992, Deformation in the Santa Barbara Channel from GPS measurements 1987-1991: Geophysical Research Letters, v. 19, no. 14, p. 1491-1494.

Lee, C.F., 1992, Seismic sequence stratigraphy and structural development of the southern outer portion of the California Continental Borderland: Ph.D. dissertation, University of Southern California, 296 p.

Legg, M.R., 1991, Developments in understanding the tectonic evolution of the California Continental Borderland, *in* Osborne, R.H., ed., Shepard Commemorative Volume, From Shoreline to Abyss: Society of Economic Paleontologists and Mineralogists, Special Publication no. 46, p. 291-312.

Lettis, W.R, DiSilvestro, L., Hanson, K.L, and Shiller, J.I., 1990, The San Simeon/Hosgri pull-apart basin south-central coastal California: Friends of the Pleistocene Pacific Cell, 1990 Fall Field trip, Field Trip Guidebook, Neotectonics of South-Central Coastal California.

Lettis, W.R., and Hanson, K.L., 1991, Crustal strain partitioning: Implications for seismic-hazard assessment in western California: Geology, v. 19, p. 559-562.

Liddicoat, J.C., 1990, Tectonic rotation of the Santa Ynez Range, California, recorded in the Sespe Formation: Geophysical Journal International, 102, p. 739-745.

Lonsdale, P., 1989, Geology and tectonic history of the Gulf of California, *in* Winterer, E.L., Hussong, D.M., and Decker, R.W., eds., The Eastern Pacific Ocean and Hawaii: Boulder, Colorado, Geological Society of America, The Geology of North America, v. N, p. 499-521.

—— 1991, Structural patterns of the Pacific floor offshore of peninsular California, Gulf and Peninsular Provinces of the Californias, *in* Dauphin, P., Ness, G., and Sinoneit, B., eds., Gulf and Peninsular Provinces of the Californias: American Association of Petroleum Geologists Memoir 47, p. 87-126.

Luyendyk, B.P., 1991, A model for Neogene crustal rotations, transtension, and transpression in southern California: Geological Society of America Bulletin, v. 103, p. 1528-1536.

Luyendyk, B.P., and Hornafius, J.S., 1987, Neogene crustal rotations, fault slip, and basin development in southern California, *in* Ingersoll, R.V. and Ernst, W.G., eds., Cenozoic Basin Development of Coastal California: Ruby Colloquium, VI, Univ. of Calif. Los Angeles, Prentice-Hall, p. 259-283.

Luyendyk, B.P., Kamerling, M.J., and Terres, R.R, 1980, Geometric model for Neogene crustal rotations in Southern California: Geological Society of America Bulletin v. 91, p. 211-217.

Luyendyk, B.P., Kamerling, M.J., Terres, R.R., and Hornafius, J.S., 1985, Simple shear of southern California during Neogene time suggested by paleomagnetic declinations: Journal of Geophysical Research, v. 90, no. B14, p. 12454-12466.

McClay, K.R., and Buchanan, P.G., 1992, Thrust faults in inverted extensional basins, *in* McClay, K.R., ed., Thrust tectonics: Chapman and Hall, p. 93-104.

McCrory, P.A., Wilson, D.S., Ingle, J.C. Jr., and Stanley, R.G., 1995, Neogene geohistory analysis of Santa Maria basin, California, and its relationship to transfer of central California to the Pacific plate, *in* Keller, M.A., ed., Evolution of Sedimentary Basins/Onshore Oil and Gas Investigations-Santa Maria Province: U.S. Geological Survey Bulletin 1995-J, p. J1-J38.

McCulloch, D.S., 1987, Regional geology and hydrocarbon potential of offshore central California, *in* Scholl, D. W., Grantz, A., and Vedder, J.G., eds., Geology and resource potential of the Continental Margin of Western North America and adjacent ocean basins-Beaufort Sea to Baja California: Circum-Pacific Council for Energy and Mineral Resources Earth Science Series, v. 6, Houston, Texas, p. 353-395.

———1989a, Evolution of the offshore central California margin, *in* Winterer, E.L., Hussong, D.M., and Decker, R.W., eds., The Eastern Pacific Ocean and Hawaii: Boulder, Colorado, Geological Society of America, The Geology of North America, v. N, p. 439-470.

———1989b, Geologic map of the south-central California continental margin, *in* Greene, H.G., and Kennedy, M.P., eds., 1989, Geology of the south-central California continental margin, California Continental Margin Geologic Map series, Area 4 of 7: California Division of Mines and Geology.

McCulloch, D.S., Beyer, L.A., and Childs, J.R., 1989, Free-air gravity anomaly map of offshore Santa Maria basin, California, and adjacent areas: U.S. Geological Survey Open-File Report 89-322.

McCulloch, D.S., and Chapman, R.H., 1977, Residual magnetic intensity maps along the California Coast from 37°30' N lat to 34°30' N lat: in cooperation with the California Division of Mines and Geology: U.S. Geological Survey Open-File Report 77-79, 14 aeromagnetic maps at scale 1:125,000.

McDougall, K., Barron, J.A., Kling, S., and Poore, R.Z., 1979, Biostratigraphy and paleoecology of foraminiferas, radiolarians, and diatoms, *in* Cook, H.E., ed., Geologic studies of the Point Conception deep stratigraphic test well OCS-CAL 78-164 no.1 outer continental shelf, southern California, United States: U.S. Geological Survey Open-File Report 79-1218, p. 129-140.

McGroder, M., Millson, C., and Gardner, D., 1994, Timing and geometry of left-slip faulting and compressional folding in Hondo field, western Santa Barbara Channel: Association Round Table: American Association of Petroleum Geologists Bulletin, v. 78, no. 4, p. 670, abstract.

McIntosh, K.D., Reed, D.L., Silver, E.A., and Meltzer, A.S., 1991, Deep structure and structural inversion along the central California continental margin from EDGE seismic profile RU-3: Journal of Geophysical Research, v. 96, no. B4, p. 6459-6473.

McLean, H, 1991, Distribution and juxtaposition of Mesozoic lithotectonic elements in the basement of the Santa Maria basin, California, *in* Keller, M.A., ed., Evolution of Sedimentary Basins/Onshore Oil and Gas Investigations-Santa Maria Province: U.S. Geological Survey Bulletin 1995-B, p. B1-B12.

McLean, H., Howell, D.G., and Vedder, J.G., 1976, Miocene strata on Santa Cruz and Santa Rosa Islands—A reflection of tectonic events in the southern California borderland, *in* Howell, D.G., ed., Aspects of the geological history of the California Borderland: Pacific Section, American Association of Petroleum Geologists, Miscellaneous Publication 24, p. 241-255.

McWayne, E.H., and Sorlien, C.C., 1994, History of faulting and folding in western Santa Barbara Channel, California: Supplement to EOS, Transactions American Geophysical Union, v. 75, no. 44, p. 622.

McWilliams, M.O., and Howell, D.G., 1982, Exotic terranes of western California: Nature, v. 297, p. 215-217.

Meltzer, A.S., 1988, Crustal structure and tectonic evolution: central California: Rice University Ph.D. thesis, 284 pp.

Meltzer, A.S., and Levander, A.R., 1991, Deep crustal reflection profiling offshore southern central California: Journal of Geophysical Research, v. 96, no. B4, p. 6475-6491.

Miles, G.A., and Rigsby, C.A., 1990, Lithostratigraphy and depositional environments of the Vaqueros and upper Sespe/Alegria Formations, Hondo field, Santa Barbara Channel, California, *in* Keller, M.A., and McGowen, M.K., eds. Miocene and Oligocene petroleum reservoirs of the Santa Maria and Santa Barbara-Ventura basins, California: Society of Economic Paleontologists and Mineralogists Core Workshop No. 10, p. 39-87.

Miller, K.C., 1993, Crustal structure along the strike of the offshore Santa Maria basin, California: Tectonophysics, v. 219, p. 57-69.

Miller, K.C., Howie, J.M., and Ruppert, S.D., 1992, Shortening within underplated oceanic crust beneath the central California margin: Journal of Geophysical Research, v. 97, no. B13, p. 19961-19980.

Mitra, S., 1990, Fault-propagation folds: geometry, kinematic development, and hydrocarbon traps: American Association of Petroleum Geologists Bulletin v. 74, no. 6, p. 921-945.

——1993, Geometry and kinematic evolution of inversion structures: American Association of Petroleum Geologists v. 77, no. 7, p. 1159-1191.

Molnar, P., 1992, Brace-Goetze strength profiles, the partitioning of strike-slip and thrust faulting at zones of oblique convergence, and the stress-heat flow paradox of the San Andreas Fault, *in* Fault mechanics and transport properties of rocks: Academic Press Ltd., p. 435-459.

Molnar, P., and Gipson, J.M., 1994, Very long baseline interferometry and active rotations of crustal blocks in the western Transverse Ranges, California: Geological Society of America Bulletin, v. 106, p. 594-606.

Mount, V.S., and Suppe, J., 1987, State of stress near the San Andreas fault: Implications for wrench tectonics: Geology, v. 15, p. 1143-1146.

——1992, Present-day stress orientations adjacent to active strike-slip faults: California and Sumatra: Journal of Geophysical Research, v. 97, no. B8, p. 11995-12013.

Namson, J., and Davis, T, 1988, Structural transect of the western Transverse Ranges, California: Implications for lithospheric kinematics and seismic risk evaluation: Geology, v. 16 p. 675-679.

——1990, Late Cenozoic fold and thrust belt of the southern Coast Ranges and Santa Maria basin, California: American Association of Petroleum Geologists Bulletin, v. 74, no.4, p. 467-492.

——1992, Late Cenozoic thrust ramps of southern California, Final Report for 1991 Contract, Southern California Earthquake Center.

Nicholson, C., Seeber, L., Williams, P., and Sykes, L.R., 1986, Seismic evidence for conjugate slip and block rotation within the San Andreas Fault system, southern California: Tectonics v. 5, no. 4, p. 629-648.

Nicholson, C., Sorlien, C.C., Atwater, T., Crowell, J.C., Luyendyk, B.P., 1994, Microplate capture, rotation of the western Transverse Ranges, and initiation of the San Andreas transform as a low-angle fault system: Geology, v. 22, p. 491-495.

Nicholson, C., Sorlien, C.C., and Legg, M.R., 1993, Crustal imaging and extreme Miocene extension of the inner California Continental Borderland: Geological Society of America Abstracts With Programs, v. 25, no. 6, p. A-418.

Nicholson, C., Sorlien, C.C., and Luyendyk, B.P., 1992, Deep crustal structure and tectonics in the offshore southern Santa Maria basin, California: Geology, v. 20, no 3, p. 239-242.

Omarzai, S.K., 1992, Monterey Formation of California at Shell Beach (Pismo Basin): Its lithofacies, paleomagnetism, age, and origin, *in* Schwalbach, J.R., and Bohacs, K.M., eds., Sequence stratigraphy in fine-grained rocks: Examples from the Monterey Formation: Pacific section Society of Economic Paleontologists and Mineralogists.

PG&E, 1988, Final report of the Diablo Canyon long term seismic program: Pacific Gas and Electric Company, Docket nos. 50-275 and 50-323.

Page, B.M., 1981, The southern Coast Ranges, *in* Ernst, W.G. ed., The geotectonic development of California, Rubey Volume I: Prentice-Hall, Englewood Cliffs, New Jersey p. 329-417.

Patterson, R.H., 1979, Tectonic geomorphology and neotectonics of the Santa Cruz Island Fault, Santa Barbara County, California: University of California, Santa Barbara, Masters thesis, 140 pages.

Payne, C.M., Swanson, O.E., and Schell, B.A., 1979, Investigation of the Hosgri Fault offshore southern California, Point Sal to Point Conception: U.S. Geological Survey Open-File Report 79-1199, part 1.

Pinter, N., Lueddecke-Pinter, S., and Keller, E.A., 1995, Short-term and long-term activity on the Santa Cruz Island fault, California: Geological Society of America Annual Meeting p. A375, abstract.

Pinter, N., and Sorlien, C.C., 1991, Evidence for latest Pleistocene to Holocene movement on the Santa Cruz Island fault, California: Geology v. 19, p. 909-912.

Roush, J.M., 1983, Marine geology of the western extension of the Transverse Ranges: Point Conception to Point Arguello: California State University, Northridge, Masters thesis, 151 p.

Scholl, D.W., 1960, Relationships of the insular shelf sediments to the sedimentary environments and geology of Anacapa Island, California: Journal of Sedimentary Petrology, v. 30, no. 1, p. 123-139.

Sedlock, R.L., and Hamilton, D.H., 1991, Late Cenozoic tectonic evolution of southwestern California: Journal of Geophysical Research, v. 96, p. 2325-2351.

Severinghaus, J., and Atwater, T., 1991, Cenozoic geometry and thermal state of the subducting slabs beneath western North America, *in* Wernicke, B.P., ed., Basin and Range extensional tectonics near the latitude of Las Vegas, Nevada: Boulder, Colorado, Geological Society of America Memoir 176, p. 1-22.

Shaw, J.H., and Suppe, J., 1994, Active faulting and growth folding in the eastern Santa Barbara Channel, California: Geological Society of America Bulletin, v. 106, p. 607-626.

Shelton, J.W., 1984, Listric normal faults: An illustrated summary: American Association of Petroleum Geologists Bulletin, v. 68, p. 801-815.

Shen, Z-K., and Jackson, D.D., 1993; Global positioning system reoccupation of early triangulation sites: Tectonic deformation in the southern Coast Ranges: Journal of Geophysical Research, v. 98, no B6, p. 9931-9946.

Sorlien, C.C., 1994a, Structure and Neogene evolution of offshore Santa Maria basin and western Santa Barbara Channel, California: University of California, Santa Barbara, Ph.D dissertation, 228 p.

——1994b, Faulting and uplift of the northern Channel Islands, California, *in* Halvorson, W.L., and Maender, G.J., eds., the Fourth Channel Islands Symposium: Update on the Status of Resources: Santa Barbara Museum of Natural History, Santa Barbara, California, p. 281-296.

Sorlien, C.C., Kamerling, M.J., and Mayerson, D., 1996, Map restoration of an early Pliocene horizon along the Hosgri-Purisima-Lompoc fault system, central California margin: American Association of Petroleum Geologists, Annual Convention, San Diego, California, Official Program, v. 5, p. A72-73, abstract.

Sorlien, C.C., Nicholson, C., Luyendyk, B.P., and Legg, M.R., 1993, Miocene collapse of the California continental margin: Geological Society of America Abstracts With Programs, v. 25, no. 6, p. A-311

Sorlien, C.C., Seeber, L., Pinter, N., and Geiser, P.A., 1995, Listric faults and related folds, uplift, and slip: Supplement to EOS, Transactions American Geophysical Union, v. 76, no. 46, p. F-625.

Stanley, R.G., Cotton, M.L., Bukry, D., Filewicz, M.V., Valin, Z.C., and Vork, D.R., 1994, Stratigraphic revelations regarding the Rincon Shale (Lower Miocene) in the Santa Barbara coastal area, California: American Association of Petroleum Geologists Bulletin v. 78, no. 4, p. 675-676 (abstract).

Stanley, R.G., Johnson, S.Y., Swisher, C.C. III, Mason, M.A., Obradovich, J.D, Cotton, M.L., Filewicz, M.V., Vork, D.R., 1996, Age of the Lospe Formation (early Miocene) and origin of the Santa Maria basin, California, *in* Keller, M.A., ed., Evolution of Sedimentary Basins / Onshore Oil and Gas Investigations-Santa Maria Province, U. S. Geological Survey Bulletin 1995-M, p. M1-M37.

Stanley, R.G., Johnson, S. Y., Tuttle, M.L., Mason, M.A., and Swisher, C.C. III, Cotton Thornton, M.L., Vork, D.R., Filewicz, M.V., Cole, R.B., and Obradovich, J.D., 1991a, Age, correlation, and origin of the type Lospe Formation (Lower Miocene), Santa Maria basin, Central California: American Association of Petroleum Geologists Bulletin v. 75, no. 2, p. 382 (abstract).

Stanley, R.G., Vedder, J.G., McLean, H., Cotton Thornton, M.L., Vork, D.R., Filewicz, M. V., Johnson, S.Y., Tuttle, M.L., Mason, M.A., and Swisher, C.C. III, 1991b, Three stratigraphic revelations in the Santa Maria province, California, and their paleogeographic and paleotectonic significance: Geological Society of America abstracts with programs, 23, no. 5, p.476.

Steritz, J.W., and Luyendyk, B.P., 1994, Hosgri Fault zone, offshore Santa Maria basin, California, *in* Alterman, I.B., McMullen, R.B., Cluff, L.S., and Slemmons, D.B., eds., Seismotectonics of the central California Coast Ranges: Geological Society of America Special Paper 292, p. 191-209.

Stock, J., and Molnar,P., 1988, Uncertainties and implications of the late Cretaceous and Tertiary position of the North America relative to the Farallon, Kula, and Pacific plates: Tectonics, v. 7, p. 1339-1384.

Stuart, C.J., 1976, Source terrane of the San Onofre Breccia—Preliminary notes, *in* Howell, D.G., ed., Aspects of the Geological History of the California Borderland: Pacific Section, American Association of Petroleum Geologists, Miscellaneous Publication 24, p. 309-325

———1979, Lithofacies and origin of the San Onofre Breccia, coastal southern California, *in* Stuart, C.J., ed., A guidebook to Miocene lithofacies and depositional environments, coastal southern California and northwestern Baja California: Society of Economic Paleontologists and Mineralogists, Pacific Section, p 25-42.

Suppe, J., 1983, Geometry and kinematics of fault-bend folding: American Journal of Science, v. 283, p. 684-721.

Suppe, J, Chou, G.T., and Hook, S.C, 1992; Rates of folding and faulting determined from growth strata, *in* McClay, K.R., ed., Thrust tectonics: Chapman and Hall, p. 105-121.

Suppe, J., and Medwedeff, D.A., 1990, Geometry and kinematics of fault-propagation folding: Eclogae geol. Helv. 83/3 p. 409-454.

Sylvester, A.G., and Darrow, A.C., 1979, Structure and Neotectonics of the western Santa Ynez system in southern California: Tectonophysics 52 p. 389-405.

Tennyson, M.E., 1989, Pre-transform early Miocene extension in western California: Geology, v. 17, p. 792-796.

———1992, Preliminary geologic map of Santa Maria 30'x60' quadrangle, California, U.S. Geological Survey Open-File Report 92-0189.

Tennyson, M.E., and Beeman, W.R., 1993, California, a digital compilation in progress: American Association of Petroleum Geologists Bulletin, v. 77, no. 4, p. 718 (abstract).

Tennyson, M.E., Keller, M.A., Filewicz, M., Thornton, M.L., and Vork, D., 1990, Early Miocene sedimentation and tectonics in western San Luis Obispo County, central California: American Association of Petroleum Geologists Bulletin v. 74, no. 4, p. 777, (abstract).

Trehu, A., 1991, tracing the subducted oceanic crust beneath the central California continental margin: Results from ocean bottom seismometers deployed during the 1986 Pacific Gas and Electric EDGE experiment: Journal of Geophysical Research, v. 96, no. B4, p. 6493-6506.

Turner, D.L., 1970, Potassium-argon dating of Pacific coast Miocene foraminiferal stages, *in* Bandy, O.L., ed., Radiometric dating and paleontologic zonation: Geological Society of America Special Paper 124, p. 91-129.

Underwood, M.B., Laughland, M.M., Shelton, K.L., and Sedlock, R.L., 1995, Thermal-maturity trends within Franciscan rocks near Big Sur, California: Implications for offset along the San Gregorio-San Simeon-Hosgri fault zone: Geology, v. 23, no. 9, p. 839-842.

Up de Graff, J.E., and Luyendyk, B.P., 1989, Gravity study of the boundary between the western Transverse Ranges and Santa Maria basin, California: Journal of Geophysical Research, v. 94, no. B2, p. 1817-1825.

U.S Geological Survey National Ocean Survey, 1989, Santa Maria Quadrangle, 1:250,000 scale topographic-bathymetric map, 1x2 degree quagrangle 34120-A1-TB-250.

Vedder, J.G., 1987, Regional geology and petroleum potential of the southern California borderland, *in* Scholl, D.W, Grantz, A., and Vedder, J.G., eds., Geology and resource potential of the continental margin of western North America and adjacent ocean basins, Beafort Sea to Baja California: Circum-Pacific Council for Energy and Mineral Resources, Houston, Texas, p. 403-447.

———1990, Maps of California Continental Borderland showing compositions and ages of samples acquired between 1968 and 1979: U.S. Geological Survey Miscellaneous Field Studies Map MF-2122.

Vedder, J.G., McLean, H., Stanley, R.G., and Wiley, T.J., 1991, Paleogeographic implications of an erosional remnant of Paleogene rocks southwest of the Sur-Nacimiento fault zone, southern Coast Ranges, California: Geological Society of America Bulletin, v. 103, p. 941-952.

Weaver, D.W., ed., 1969, assisted by Doerner, D.P., and Nolf, B., Geology of the Northern Channel Islands: A.A.P.G. and S.E.P.M. Pacific Section, Special Publication: Pacific Sections, American Association of Petroleum Geologists and Society of Economic Paleontologists and Mineralogists, 200 pages.

Weaver, D.W., and Doerner, D.P., 1969, Lower Tertiary stratigraphy, San Miguel and Santa Rosa islands, *in* Weaver, D.W., assisted by Doerner, D.P., and Nolf, B., Geology of the Northern Channel Islands: American Association of Petroleum Geologists and Society of Economic Paleontologists and Mineralogists Pacific Section, Special Publication, p. 30-47.

Weigand, P.W., and Savage, K.L., 1993, Review of the petrology and geochemistry of the Miocene Conejo volcanics of the Santa Monica Mountains, southern California, *in* Weigand, P.W., Fritsche, A.E., and Davis, G.E., Depositional and volcanic environments of middle Tertiary rocks in the Santa Monica Mountains, southern California: Pacific Section, Society of Economic Paleontologists and Mineralogists (Society for Sedimentary Geology), book 72, p. 93-112.

Wernicke, B, and Axen, G.J., 1988, On the role of isostasy in the evolution of normal fault systems: Geology, v. 16, p. 848-851.

Whidden, K.J., Lund, S.P., and Bottjer, D.J., 1993, Paleomagnetic evidence for large-scale block rotations north of the Santa Ynez fault: An extension of the western Transverse Ranges domain of ~90° rotations in southern California: Supplement to EOS, Transactions of the American Geophysical Union, v. 74, no. 43, p. 586.

Willingham, C.R., 1978, Geophysical evidence for 15 km of right lateral displacement on the San Gregorio fault zone, California (abs.): EOS Transactions, American Geophysical Union, 59, p. 1210.

Willingham, C.R., Heck, R.G., and Rietman, J.D., 1991, Structural deformation in the offshore Santa Maria basin, California: American Association of Petroleum Geologists Bulletin, v. 75, no. 2, p. 385-386 (abstract).

Xiao, H., and Suppe, J., 1992, Origin of rollover: American Association of Petroleum Geologists Bulletin, v. 76, no. 4, p. 509-529.

Yeats, R.S., 1976, Extension versus strike-slip origin of the southern California borderland, *in* Howell, D.G., editor: Aspects of the geological history of the California Borderland: Pacific Section, American Association of Petroleum Geologists, Miscellaneous Publication 24, p. 455-485

——1983, Large-scale Quaternary detachments in Ventura basin, southern California: Journal of Geophysical Research, v. 88, no. B1, p. 569-583.

——1988, Late Quaternary slip rates on the Oak Ridge Fault, Transverse Ranges, California: Implications for seismic risk: Journal of Geophysical Research, v. 93 no. B10, p. 12137-12150.

Yerkes, R.F., Greene, H.G., Tinsley, J.C., and Lajoie, K.R., 1981, Seismotectonic setting of the Santa Barbara Channel area, southern California: U.S. Geological Survey Map MF-1169 and accompanying report.

Yerkes, R.F., and Lee, W.H.K., 1987, Late Quaternary deformation in the western Transverse Ranges, *in* Recent reverse faulting in the Transverse Ranges, California: U.S. Geological Survey Professional Paper 1339, p. 71-82.

Yilmaz, O., 1987, Seismic data processing: Investigations in Geophysics Volume 2: Society of Exploration Geophysicists.

Yin, A., and Dunn, J.F., 1992, Structural and stratigraphic development of the Whipple-Chemehuevi detachment fault system, southeastern California: Implications for the geometrical evolution of domal and basinal low-angle normal faults: Geological Society of America Bulletin, v. 104, p. 659-674.

Chapter Z

Structure and Tectonincs of the Central Offshore Santa Maria and Santa Lucia Basins, California: Results from the PG&E/EDGE Seismic Reflection Survey

By KATE C. MILLER and ANNE S. MELTZER

U.S. GEOLOGICAL SURVEY BULLETIN 1995—Z

EVOLUTION OF SEDIMENTARY BASINS/ONSHORE OIL AND GAS INVESTIGATIONS—
SANTA MARIA PROVINCE

Edited by Margaret A. Keller

CONTENTS

PLATES

[In pocket]

FIGURES

Structure and Tectonics of the Central Offshore Santa Maria and Santa Lucia Basins, California: Results from the PG&E/EDGE Seismic Reflection Survey

By Kate C. Miller[1] and Anne S. Meltzer[2]

Abstract

Seismic reflection profiles from the offshore Santa Maria and Santa Lucia basins of central California provide insight into both the geologic evolution of the basins themselves and into tectonic models for present-day deformation along the continental margin. Seismic sequence analysis of basin strata suggests that the basins began subsiding in early Miocene time, just as a transform regime was imposed along the west coast of North America. Late Miocene to Holocene oblique plate motion has added a component of compression to the dextral slip at the plate boundary and has resulted in structural inversion of basin fill. Folding and recent sea-floor offsets suggest that current convergence is accommodated across the entire width of the continental margin. In individual basins, shortening tends to increase and structures become younger toward the south. Of the two major, through-going fault zones, the Santa Lucia Bank and Hosgri Fault Zones, only the Hosgri Fault Zone is inferred to have accommodated strike—slip motion in the Neogene. Axes of offshore subsidiary faults and folds generally strike parallel to the Santa Lucia Bank and Hosgri Fault Zones, suggesting that oblique convergence within the broader transform zone is decoupled into transcurrent motion along weak strike-slip faults and into shortening along fault normal structures. The data image numerous reverse-separation faults that offset acoustic basement and the overlying Neogene sediments but typically lack definitive fault-plane reflections beneath acoustic basement.

INTRODUCTION

Investigation of the offshore geology of the California margin provides insight into the tectonic evolution of the San Andreas transform system. At the plate tectonic scale, the late Oligocene to Holocene development of this system is well established from analysis of sea-floor magnetic anomalies (Atwater, 1970, 1989; Atwater and Molnar, 1973; Stock and Molnar, 1988). This work shows that the arrival of the Pacific-Farallon ridge-transform system at the North American continental margin created a new transform plate boundary between the Pacific and North American Plates. Since the ridge encountered the trench in late Oligocene time, the transform boundary has grown several hundred kilometers to form the modern San Andreas Fault System. Examination of offshore geologic structure in the vicinity of the offshore Santa Maria and Santa Lucia basins reveals the consequences of this family of plate-boundary processes on a local scale.

Early geologic mapping onshore and initial mapping from reflection seismic data offshore (Hoskins and Griffiths, 1971; Page and others, 1979, and references therein) showed that the structural evolution of the transform zone has been complex. In addition to the San Andreas Fault, a number of inferred strike-slip faults including the offshore Hosgri and Santa Lucia Bank Fault Zones (fig. 1) dissect the margin. An early Miocene extensional episode associated with the developing transform regime (McCulloch, 1987) led to basin subsidence along the margin and the formation of the offshore Santa Maria basin. Later, a shortening episode that began 5 to 3 Ma, and persists to the present, resulted in faulting and folding both offshore in the basin (McCulloch, 1987) and onshore in the California Coast Ranges (Cox and Engebretson, 1985; Page and Engebretson, 1984; Page and others, 1979).

In recent years, the role of compression as a mechanism of deformation within transform regimes with a component of oblique convergence has become an important area of research. Many folds and thrusts in the central California margin strike parallel to the San Andreas Fault Zone rather than at a 30° angle to the fault, as might be expected in a purely strike-slip regime (for example, see Sylvester, 1988). Mount and Suppe (1987) and Zoback and others (1987) explain fault-normal compression as a consequence of oblique convergent plate motion at a mechanically weak transform boundary. In their view, deformation adjacent to the San Andreas Fault is decoupled into a pure strike-slip component and a pure compressional component. The compressional component is accommodated in a wide zone of reverse faults and folds that strike parallel to the San Andreas Fault Zone. Crouch and oth-

[1]Department of Geological Sciences, University of Texas at El Paso, El Paso, TX 79968-0555, (915)-747-5424, miller@geo.utep.edu.

[2]Department of Earth & Environmental Sciences, Lehigh University, Bethlehem, PA, 18015.

Manuscript approved for publication May 20, 1999

ers (1984) suggest that the reverse faults near the surface sole into a subhorizontal detachment at the base of the seismogenic zone in the offshore Santa Maria basin. The Hosgri Fault Zone (fig. 1) is among those faults interpreted by Crouch and others as a high-angle reverse fault that flattens at depth.

We use regional multi-channel seismic reflection data acquired during the 1986 PG&E (Pacific Gas and Electric Co.)/EDGE seismic experiment as a database for investigating the tectonic evolution of the upper 5 to 7 km of the crust in offshore central California. These seismic lines cross the primary structural features of this region: the Hosgri Fault Zone, the offshore Santa Maria basin, the Santa Lucia Bank Fault Zone, and the Santa Lucia basin (fig. 1). We are able to place age constraints on deformational events within the offshore region by using the techniques of seismic sequence analysis (Vail and others, 1977) in conjunction with stratigraphic information from wells in the offshore Santa Maria basin. This approach allows us to place constraints on the timing of basin subsidence, age, and type of motion on the Santa Lucia Bank and Hosgri Fault Zones, and on the nature and timing of compressional deformation across the continental shelf. We evaluate current models of margin evolution in light of these results.

ACKNOWLEDGMENTS

The seismic profiles PG&E-1, PG&E-2, and PG&E-3 were provided by Woody Savage at Pacific Gas and Electric Company. This work was supported by Pacific Gas and Electric Company, the NSF-MRL program through the Center for Materials Research at Stanford University (Miller's work), and NSF grants EAR-8707466 and OCE-8812840 (Meltzer's work). Data processing was done at the facilities of the Stanford Exploration Project, the Houston Advanced Research Center, and the Rice University Geophysical Computing Center.

REGIONAL GEOLOGY AND TECTONICS

Relative plate motions

Shallow crustal features of Tertiary age in the central California offshore region record the transition from subduction to transform motion along the California margin. This process began 30 to 28 Ma when the Pacific-Farallon spreading ridge reached the North America Plate (Atwater, 1970; Engebretson and others, 1985; Stock and Molnar, 1988). This event resulted in the formation of two triple junctions and the initiation of dextral slip in a developing transform system between them. The transform system has grown since that time to its present length of more than 1,100 km. Initial transform motion probably occurred along offshore faults, but the main locus of slip moved inland to the San Andreas Fault by 10 to 6 Ma (Graham, 1978). An element of convergence was superimposed on the transform regime as recently as 3 Ma and possibly as early as 6 to 5 Ma as a result of a clockwise change in Pacific–North America relative plate motion (Cox and Engebretson, 1985; Harbert and Cox, 1989; Cande and others, 1992). Present-day convergence is occurring at a rate of 2 to 7 mm/yr across the San Andreas Fault, while motion along the San Andreas and other strike-slip faults accounts for approximately 40 mm/yr of Pacific–North America Plate motion (DeMets and others, 1987; Jordan and Minster, 1988; Argus and Gordon, 1991). The smaller convergence rate is obtained when the Sierra Nevada microplate is considered separately from the rest of North America (Argus and Gordon, 1991).

Offshore structural framework

The primary structural elements of the central California offshore area were first recognized by Hoskins and Griffiths (1971) and later examined in more detail by McCulloch, (1987). Two major structural discontinuities, the Hosgri and Santa Lucia Bank Fault Zones (fig. 1) form the eastern and western boundaries of the intervening offshore Santa Maria basin. Discontinuities in the magnetic field at the faults suggest that discrete basement blocks may be juxtaposed across the faults (McCulloch, 1987; Page and others, 1979). Strike-slip movement has been documented along the trend of the Hosgri Fault Zone and its northward extension, the San Gregorio Fault, but the amount and timing of right-slip movment is the subject of some controversy. Hall (1975) and Graham and Dickinson (1978) estimate that 80 to 115 km of slip has occurred along the Hosgri since early to middle Miocene time. By contrast, Sedlock and Hamilton (1991) question most of this slip and argue that Neogene and Quaternary slip along the system amounts to less than 5 km. A significant component of strike-slip movement along the Santa Lucia Bank Fault Zone is inferred, based on the long linear trace of the fault and the apparent high angle of the fault in cross section (McCulloch, 1987). A recent tectonic model proposed by Sedlock and Hamilton (1991) suggests that the amount of dextral slip along the Santa Lucia Bank Fault Zone is potentially large. In a recent reconstruction of the tectonic evolution of southwestern California, they have attributed nearly 700 km of right-lateral slip to the Santa Lucia Bank Fault Zone and other offshore faults since early Miocene time. However, there are no piercing points with which to document offshore slip magnitude.

Both the offshore Santa Maria basin and the Santa Lucia basin are elongate, coast-parallel basins filled with Tertiary sediments. The east and west boundaries of the Santa Maria basin are faults where Franciscan Complex(?) basement is inferred to be juxtaposed against early Miocene to Holocene strata. The Santa Lucia basin lies west of the Santa Lucia Bank Fault Zone and sits above the Santa Lucia high. Tertiary basin fill onlaps acoustic basement eastward. In general, the sediment fill thins to the west and is truncated by erosion at the basin margins. The following details of the structural evolution of these basins are based on our interpretation of the seismic reflection data from the PG&E/EDGE survey.

Regional Stratigraphy

The stratigraphy of the offshore Santa Maria basin is known primarily from oil exploration well penetrations. Whereas many of these well data are still proprietary, sufficient data are available in the recent literature to establish the main elements of the basin stratigraphy. In particular, a recent synthesis of lithologic and biostratigraphic data from more than 50 wells in the central and southern part of the basin by Clark and others (1991) has produced a preliminary chronostratigraphy for the OCS P-406-1 well that can be correlated to stratigraphy onshore and to the southern part of the basin. In addition, log data and lithologic information are publicly available for the Oceano P-060-1 well (McCulloch,

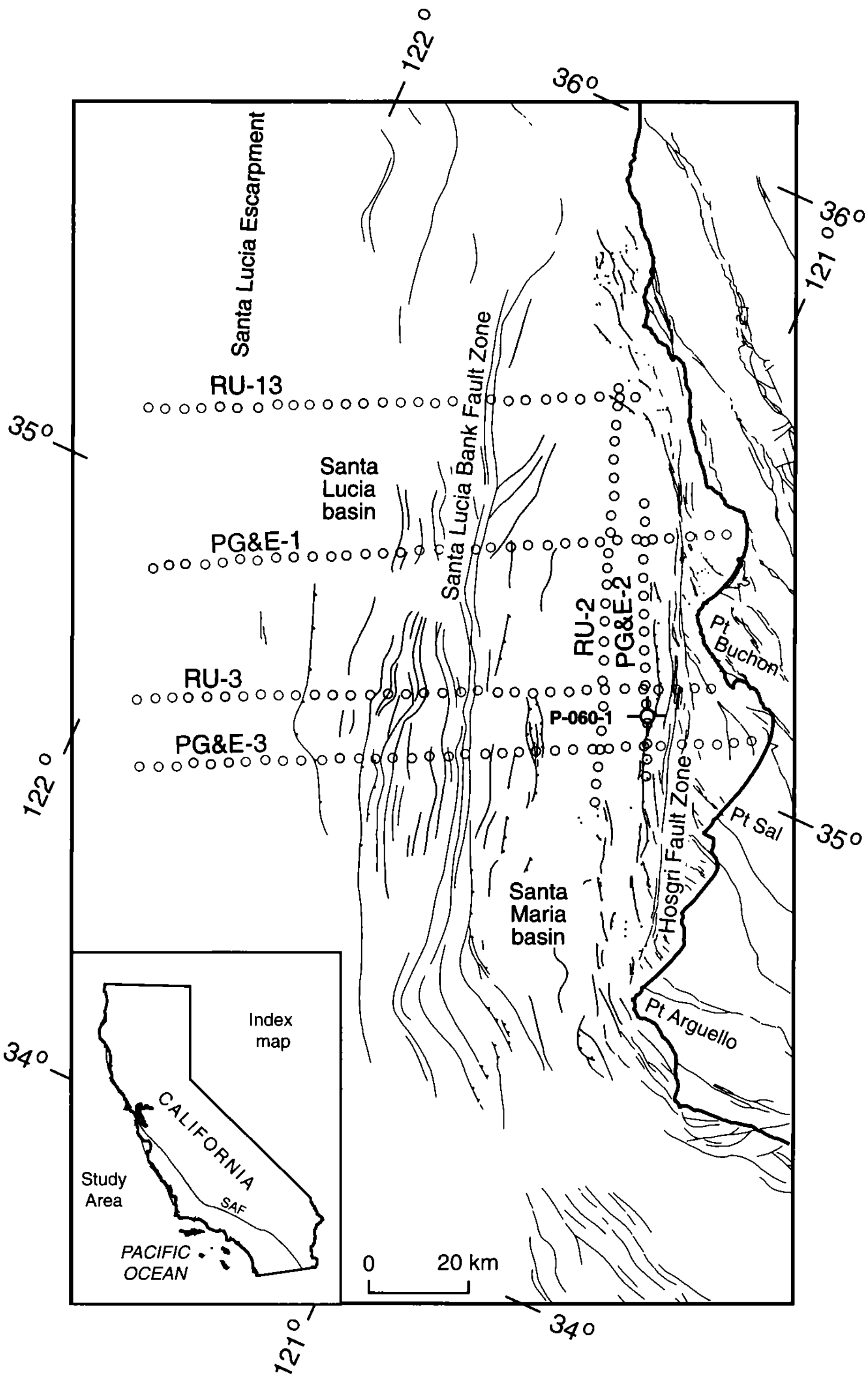

Figure 1. Structure of central California offshore and coastal areas. Shaded regions indicate (west to east) Santa Lucia Escarpment, Santa Lucia basin and offshore Santa Maria basin. Basin outlines follow McCulloch (1987). Fault and fold trends (thin lines) follow Pacific Gas and Electric (1988). Location of seismic reflection profiles (lines of circles) is superimposed on geology. Location of the Oceano P-060-1 well is marked by dry-hole symbol. Index map shows state outline, study area, and trend of San Andreas Fault Zone (SAF).

1987, and references therein, Ogle and others, 1987) that lies a few tens of meters east of seismic line PG&E-2 (fig. 1). Here, we review the basin stratigraphy established so far, so that established formation names can be assigned to the seismic stratigraphic sequences we have delineated on the reflection data. Figure 2 correlates the regional stratigraphy to a synthetic seismogram from the Oceano P-060-1 well and our seismic stratigraphic sequences.

Well data show that the central offshore Santa Maria basin contains early Miocene to Holocene marine sediments that unconformably overlie Mesozoic Franciscan basement rocks. Immediately above basement lie early Miocene volcanic rocks that are correlative with part of the Obispo Formation of the onshore Santa Maria basin (Clark and others, 1991). The Oceano P-060-1 well (fig. 2) penetrates tuff, ash, and intrusive rock of this formation at a depth of approximately 2,050 m (McCulloch, 1987). In some areas of the central offshore Santa Maria basin, volcanic rocks are overlain by sediments that can be correlated with the mudstones and dolostones of the Point Sal Formation found both onshore and in the southern part of the basin (Clark and others, 1991). However, in the P-060-1 well, the volcanic rocks are immediately overlain by 600 m of siliceous shales and

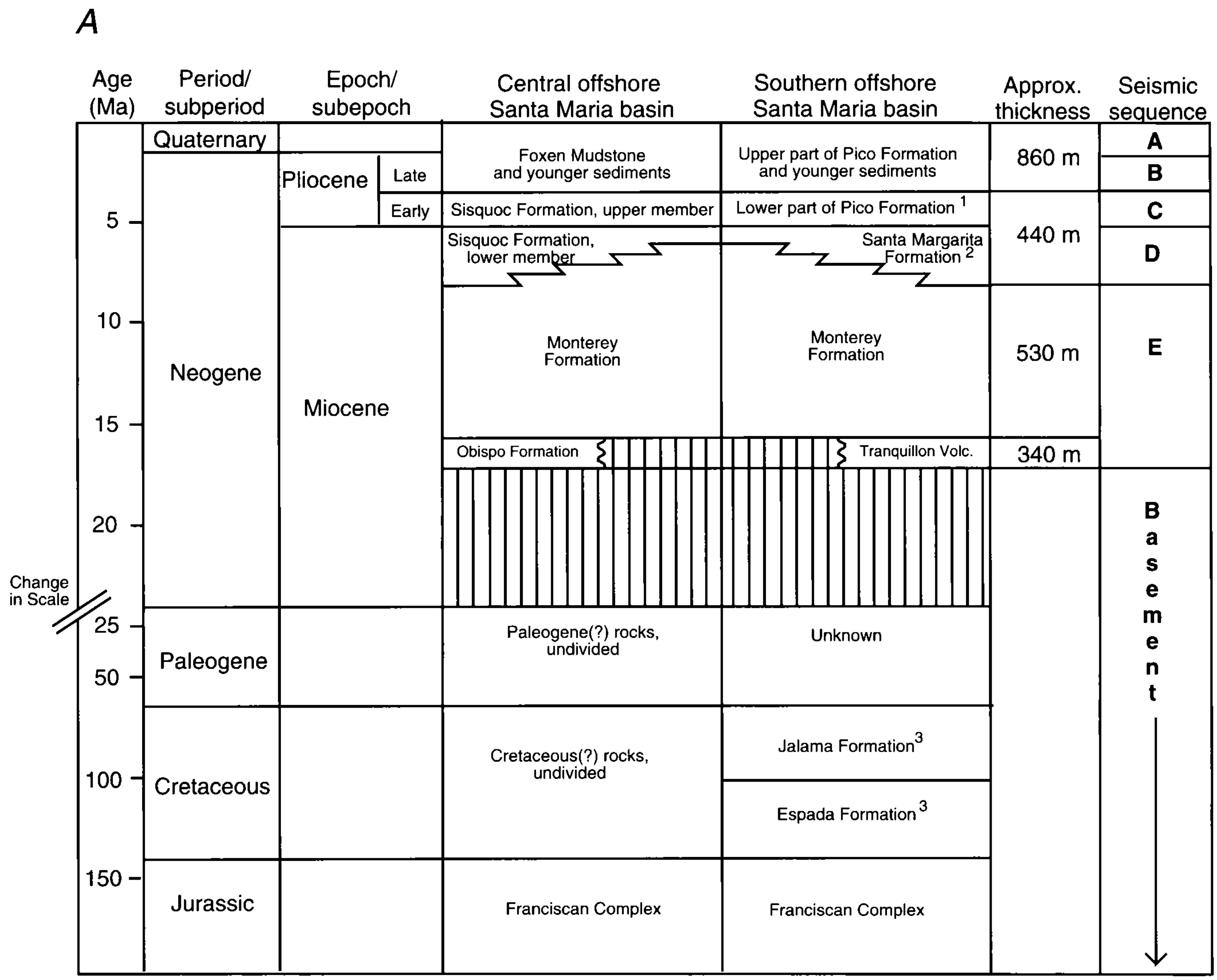

1 Stratigraphic equivalent of upper member of the Sisquoc Formation

2 Stratigraphic equivalent of lower member of the Sisquoc Formation

3 Unit of Dibblee (1950)

Figure 2. Correlation of seismic sequences to regional stratigraphy. A, Correlation chart. Age and formation names follow Clark and others (1991). Correlation to southern Santa Maria basin is based on McCulloch and others (1979), Isaacs and others (1983) and Crain and others (1985). Thicknesses based on Oceano P-060-1 well stratigraphy modified from Ogle and others (1987). B, Correlation of reflection units A through E in synthetic seismogram derived from sonic log in Oceano P-060-1 well to those in PG&E-2 seismic profile. Franciscan rocks offshore may be younger than Jurassic (Page, 1981).

cherts of the Miocene Monterey Formation (McCulloch, 1987; Ogle and others, 1987).

Siltstones, siliceous mudstones, and claystones of the late Miocene and early Pliocene Sisquoc Formation conformably overlie the Monterey Formation. Within the Sisquoc Formation is an unconformity at the Miocene/Pliocene boundary (placed at earliest Delmontian, or 5.3 Ma by Clark and others (1991), hereafter referred to as the Miocene-Pliocene boundary unconformity), which is used to divide the formation into upper and lower members (Clark and others, 1991). A second unconformity in the basin occurs at the boundary between the Sisquoc Formation and the overlying Foxen Mudstone (placed at the early-late Pliocene boundary or 3.4 Ma, by Clark and others (1991), hereafter referred to as the early-late Pliocene boundary unconformity). The Foxen consists of poorly consolidated clays with occasional siltstone, sandstone, and limestone streaks (Clark and others, 1991). Pleistocene sediments equivalent to the onshore Paso Robles Formation are rarely recognized offshore because offshore wells are drilled on structural highs, where Pleistocene sedi-

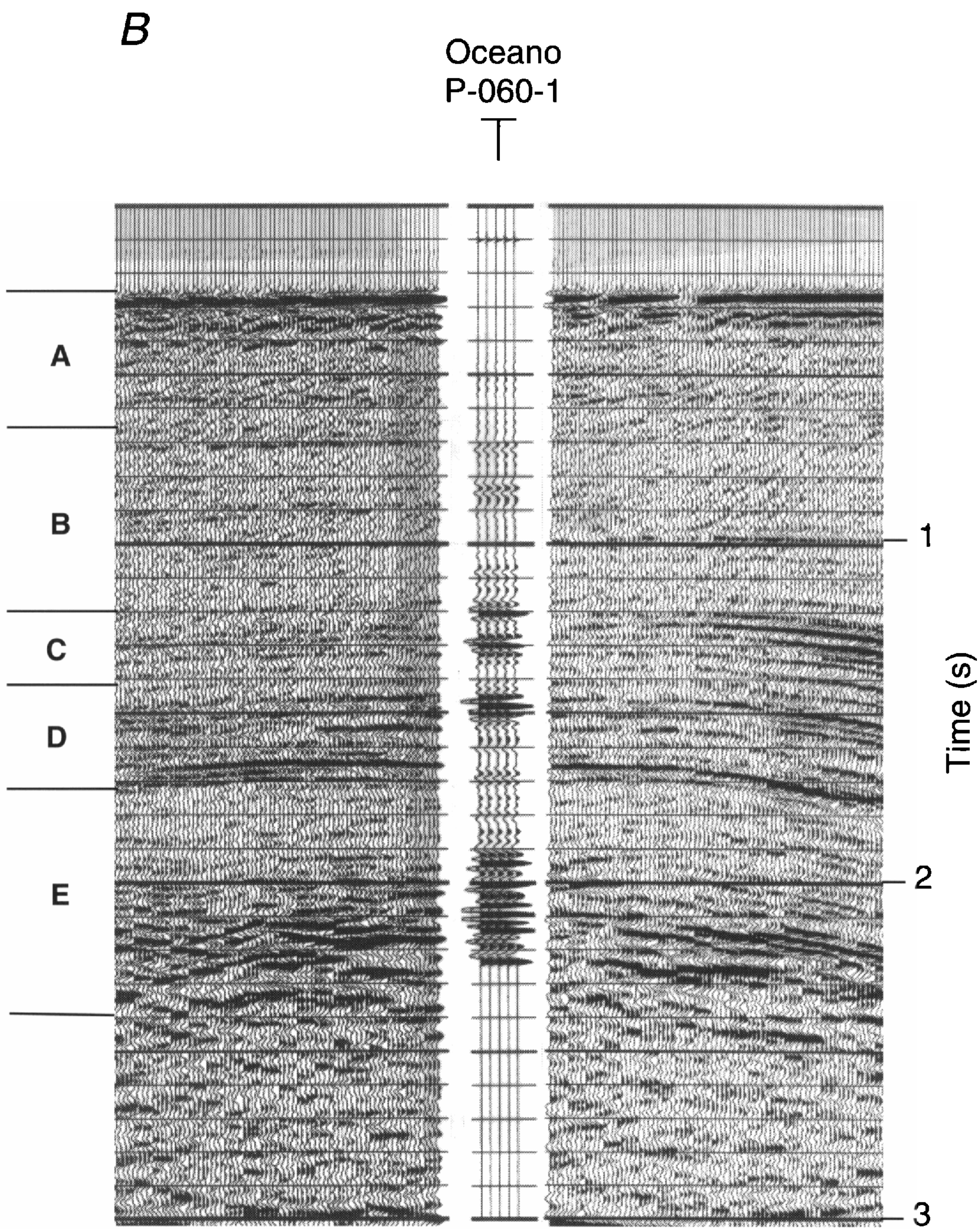

ments are thin and sample recovery near the ocean floor is limited (Clark and others, 1991). Pleistocene sediments are not recognized in the Oceano P-060-1 well (for example, see Ogle and others, 1987), but probably occur throughout the offshore area.

DATA ANALYSIS

We examined basin evolution in the central California offshore region by using the upper 4 s of seismic reflection data from the PG&E/EDGE seismic survey. All the data have been scaled with automatic gain control and migrated with a 45-degree finite-difference time migration algorithm. To constrain the timing of deformational events we have identified seismic sequences within the basins. The presence of two cross lines (PG&E-2 and RU-2) in the offshore Santa Maria basin allows us to tie individual sequences between dip lines to evaluate the development of structures along strike. In this paper, we combine individual analyses of the PG&E and the RU lines (see Meltzer and Levander, 1991; Miller, 1993) with a synthetic seismogram derived from well data in order to present a complete interpretation of the data set. A more detailed picture of the tectonic evolution of the continental shelf emerges as a result.

Consistent patterns in north-south structural variation emerge from the line-by-line examination of the data: 1, Sediments in both basins are thicker to the south; 2, folding and faulting are increasingly well developed to the south; and 3, shortening is observed in progressively younger sediments southward. The Hosgri Fault Zone dips steeply to near vertically along the length of the basin and appears to break into multiple strands to the south. The Santa Lucia Bank Fault Zone dips more moderately. With a few exceptions, reflections from faults that offset basin sediments and basement blocks cannot be traced more than a few tenths of a second below the basement-sediment interface.

Interpretation Methods

We date seismic sequences by matching them to a synthetic seismogram from the Oceano P-060-1 well and the published stratigraphic correlations for the well (McCulloch, 1987, and references therein; Ogle and others, 1987). Since seismic line PG&E-2 nearly crosses the well location, formations can be tied to seismic sequences accurately at this point in the basin. Five sequences (labelled A through E in fig. 2) have been identified within the offshore Santa Maria basin. In terms of regional stratigraphic correlations, sequence E corresponds to the stratigraphic sequence that locally includes the Miocene Obispo Formation or its stratigraphic equivalent the Tranquillon Volcanics of Dibblee (1950) and the Monterey Formation. The synthetic seismogram shows that the Obispo correlates with the particularly reflective region of the seismic record below 2.1 s but above basement rocks. Sequences D and C correspond to the marine siltstones and shales of the upper and lower members of the Sisquoc Formation. Sequence B probably corresponds to the Pliocene Foxen Mudstone. Finally, Sequence A may represent Quaternary sediments. Basement rocks below Sequence E are interpreted to be the Franciscan Complex with local occurrences of overlying Paleogene sedimentary and volcanic rocks. This interpretation is based on well data and the seismic velocity model of Howie and others (1993). Thus the D-C sequence boundary represents the Miocene-Pliocene boundary unconformity and the C-B sequence boundary represents the early-late Pliocene boundary unconformity recognized by Clark and others (1991).

Our recent acquisition of sonic log data from the Oceano P-060-1 well has resulted in somewhat different correlations of established formations to seismic sequences than those that are previously published by Meltzer and Levander (1991) and Miller (1993). Previously, sequence E had been correlated to Obispo and Point Sal Formations only. Sequence D had been correlated to the Monterey Formation and sequences C and B to the Sisquoc Formation only. We also pick a different top of the Sisquoc Formation than that published by Ogle and others (1987). The synthetic seismogram to seismic tie indicates that the top of the Sisquoc Formation as published by Ogle and others is the top of the lower member of the Sisquoc Formation (the D-C sequence boundary). Our interpretation is more consistent with Clark and others' (1991) synthesis of central Santa Maria basin well data.

In this paper we treat migrated seismic reflection data as if they represent a true geological cross section except for a time-to-depth conversion using a simplified stacking velocity field. In the presence of large velocity variation, this can be a poor assumption, as the seismic image may be distorted relative to true subsurface geometries. Although we do not present depth-converted interpretations, we do take lateral heterogeneity in the velocity field into account in our discussion. The abundance of well data, stacking velocity, and seismic refraction velocity information in this region means that the velocity field is relatively well known (for example, see Howie and others, 1993; Willingham and others, unpub. data, 1997[3]). The most significant velocity variations occur where uplifted basement blocks are juxtaposed against basin sediment. However, within the stratigraphic sequences defined here, stacking velocity estimates indicate little lateral variation in velocities. Thus estimates of fault dip at uplifted basement blocks are probably less reliable than observations of thinning and thickening sediments on the seismic record. Interpreted seismic records with approximately 2:1 vertical exaggeration assuming a velocity of 2,300 m/s are presented in plates 1 and 3.

---

[3]Willingham, C.R., Reitman, J.D., Shiller, G.I., Heck, R.G., and DiSilvestro, L.A., Seismic images of the Hosgri Fault Zone offshore, south-central California, *planned for publication as a chapter in* Keller, M.A., ed., Evolution of sedimentary basins/onshore oil and gas investigations—Santa Maria province: U. S. Geological Survey Bulletin 1995.

This is the approximate velocity of Sisquoc Formation rocks in the Oceano well's sonic log. A velocity of 2,300 m/s was also used for converting travel times to thicknesses in the following sections.

Offshore Santa Maria basin

Six profiles (fig. 1, pls. 1, 2) cross some part of the offshore Santa Maria basin. Four (RU-13, PG&E-1, RU-3 and PG&E-3) cross the basin in the dip direction, and the other two (RU-2 and PG&E-2) traverse the basin along its strike. The RU-13 profile (pl. 1*A*) is the northernmost crossing of the offshore Santa Maria basin. At the northern end of the offshore Santa Maria basin, the seismic profile shows that the sedimentary section is relatively thin, averaging ~0.9 km (0.8 s). The sediments lie above a generally west-dipping basement that is abruptly offset by the moderately dipping Santa Lucia Bank Fault Zone. Occasional reverse-separation faults having minor displacement appear to offset the basement in the eastern half of the transect. This profile does not quite reach the Hosgri Fault Zone, the eastern boundary of the basin. Thickening of the strata of the E sequence as they approach the Santa Lucia Bank Fault Zone, suggests that this fault was the initial site of extension within the basin. Significant subsidence of the eastern part of the basin began with the deposition of the D sequence, as is evident from the thicker accumulation of D strata to the east. The D strata thin westward across a basement high and then thicken toward the Santa Lucia Bank Fault Zone suggesting that the fault continued to be an important locus of subsidence during this time. Some apparent reverse motion occurred at the Santa Lucia Bank Fault Zone during the deposition of sequence D, as both the E and D sequences are gently folded and thinned within an anticline at the fault, while strata of sequence C onlap the folded material. Sequences B and A are unaffected by folding at the Santa Lucia Bank Fault.

To the south on the PG&E-1 profile (pl. 1*B*), an undulating basement topography, formed by normal-separation fault offset during extension, can be seen along with a thicker sedimentary section. In addition to basement highs at the east and west boundaries of the basin, three other highs are readily distinguished in the basin interior. Sequences D and C thin significantly across these highs, while sequence E onlaps and, in some places, is truncated by the highs. This sediment geometry suggests that early extensional faults, located at basement block boundaries, controlled the location of early deposition within the basin. Basin subsidence was greatest near the Hosgri Fault Zone, where sediment thickness exceeds 2.2 km (2 s). This observation contrasts with RU-13 where the basin is deepest adjacent to the Santa Lucia Bank Fault Zone. A period of shortening during sequence C deposition affected sediments along the PG&E-1 transect, which is somewhat later than along RU-13. Deformation is concentrated at the edges of basement highs, where sediments of the lower three sequences are gently folded. This geometry suggests structural inversion in which normal faults initiated during basin formation began to accommodate shortening through basement block uplift. Onlapping relations within sequence C, as well as a relatively undeformed top-of-sequence boundary, suggest that the compressional episode waned during sequence C deposition, although uplift at the basement high immediately west of the Hosgri Fault Zone continued until somewhat later. Sediments of sequences B and A are undeformed. At the Santa Lucia Bank Fault Zone, some evidence exists for recent compression where a fault scarp offsets the sea floor, truncating sequences B and A.

On the RU-3 profile (pl. 1*C*) 30 km to the south, the thick sedimentary section seen adjacent to the Hosgri Fault Zone on PG&E-1 now persists across much of the basin. Just as to the north, the lower three sequences thin across present-day basement highs that must also have been high at the time of deposition. On the northern two profiles, sequences B and A form a west-dipping blanket of sediments, but on RU-3 their depositional pattern is also controlled by another inversion structure, an emergent fold informally referred to as the Queenie structure (Clark and others, 1991). Onlap of sequences B and A onto the structure suggests that it formed prior to the deposition of sequence C. Faulting and folding along the transect is largely pre-Pliocene except near the Hosgri Fault Zone where strata of sequence B have been upturned. The eastern strand of the fault is nearly vertical, but a strand immediately to the west dips east and apparently accommodates some apparent reverse motion.

The most southerly E-W profile, PG&E-3 (pl. 1*D*), reveals younger and greater shortening. Folding at the Queenie structure is more fully developed. A large uplifted basement block immediately west of the structure acts as a buttress for the fold. Evidence for younger compression is seen in an anticline immediately west of the Hosgri Fault Zone, where some sequence B strata are folded above the feature. The Hosgri Fault Zone consists of numerous strands, some of which dip east, cutting through the section. By contrast, the Santa Lucia Bank Fault Zone is primarily a single, moderately east-dipping (45-60°) fault.

Profiles PG&E-2 and RU-2 (pl. 1*E, F*), along the strike of the basin, both show that the basin sediments thicken to the south and that shortening affects progressively younger sediments. North of its tie to PG&E-1, RU-2 crosses a relatively thin sedimentary sequence of ~0.9 km (0.8 s). South of this juncture, the basin deepens considerably to ~2.2 km (2.0 s). Sediments younger than sequence C are unaffected by minor reverse faults within the basement rocks to the north, whereas farther south the lower part of the B sequence eventually is involved in folding. These general observations also hold for PG&E-2, except that the observed sedimentary section is considerably thicker due to the profile's proximity to the Hosgri Fault Zone.

These data suggest that the Santa Maria basin evolved as a shelf basin during Miocene time and later underwent structural inversion in a late Miocene to Holocene compressional regime. These events affected the northern and southern parts of the basin differently, with the greatest subsidence and shortening occurring to the south. As observed by earlier workers (for example McCulloch, 1987), early normal faults offset basement and controlled deposition within the basin. Later these same faults were reactivated to accommodate shortening through structural inversion. Throughout the basin, evidence of the main episode of shortening begins with the D-C sequence boundary, the late Miocene to early Pliocene unconformity placed by Clark and others (1991) at the Miocene-Pliocene boundary or approximately 5.3 Ma. In the northern part of the basin, this period of shortening caused only minor folding in basin strata above small-offset high-angle reverse-separation faults that originate within basement at the north end of the basin. Here, strata of sequence C and younger are undeformed, except near the Hosgri Fault Zone. To the south, increasingly younger sediments are involved in larger magnitude folds. On the PG&E-3 profile, strata in the Pliocene-age sequence B are deformed east of the PG&E-2 line tie, and strata of sequence A are gently folded above the Hosgri Fault Zone. These observations suggest that the northern part of the study area was primarily affected by an intial compressional pulse associated with a plate motion change at 6-5 Ma, whereas areas to the south and east have experienced additional deformation since that time. Active shortening continues today in this region, as attested by both the seismic reflection data and two 1969 earthquakes with thrust mechanisms and local magnitudes of 5.4 (Gawthrop, 1978).

Offshore Santa Lucia basin

The Santa Lucia basin is separated from well control in the offshore Santa Maria basin by the Santa Lucia Bank, a basement high. Furthermore, sediment deposition and deformation is significantly more complex within this basin than in the offshore Santa Maria basin to the east. Because of these additional uncertainties, we have only attempted to identify two sequences west of the Santa Lucia Bank Fault Zone. Because the unconformity between the two sequences in the Santa Lucia basin and that between sequences C and B in the offshore Santa Maria basin both separate more intensely deformed strata from mildly deformed to undeformed strata, we infer that both the unconformities and the strata they separate are of similar age to those seen in the offshore Santa Maria basin. We interpret the lower sequence as being equivalent to sequences E through C, while the upper sequence would correspond to sequences B and A in the offshore Santa Maria basin.

Four profiles, RU-13, PG&E-1, RU-3 and PG&E-3 cross the Santa Lucia basin (fig. 1; pls. 3, 4) in the dip direction. Profile RU-13 (pl. 3*A*) provides the northernmost crossing of the Santa Lucia basin. There basin strata are relatively thin, reflecting as much as ~0.8 km (0.75 s) of sediments. On the eastern edge of the basin the lower sequence currently onlaps the underlying basement rock while to the west it downlaps onto the basement rock. At its eastern boundary against the Santa Lucia Bank, sediments of the lower sequence have been uplifted and truncated by erosion at the sea floor. Sediments of the upper sequence downlap against the underlying sequence. Gentle folds within the upper sequence are erosionally truncated at the sea floor. Offsets in the basement suggest that it has been disturbed by at least three small thrust faults that have deformed some of the overlying sediments as well. Fault-plane traces cannot be followed into the underlying basement rock; their presence here is only inferred.

On the next profile to the south, PG&E-1 (pl. 3*B*), the sedimentary section thickens significantly while folding and faulting of the strata are more pronounced. Along this transect, the eastern basin boundary is formed by a series of reverse separation faults that dip 45° to 60° eastward and ultimately juxtapose basin sediments against basement rocks of the Santa Lucia Bank. Sediments at the western edge of the basin have been uplifted and truncated by erosion at the sea floor. Generally west-dipping basement topography is broken up by a number of thrust faults that offset basement rocks and can be traced upwards into the lowermost seismic sequence. Fault-plane reflections beneath the basement-sediment interface are difficult to identify. The lower sequence is deformed by thrust faults, particularly to the east where faults offset the sea floor. Folding and faulting intensity diminishes westward. The upper sequence is gently folded above underlying folds and faults in the lower sequence and basement. At the eastern margin of the basin, sediments of the lower sequence are folded and truncated at the sea floor by erosion.

Along the RU-3 traverse, 30 km farther south (pl. 3*C*), folding and faulting intensify. The eastern basin boundary is a gently west-dipping unconformable contact between basement and the lower seismic sequence. The west-dipping basement topography of the two northern transects is disrupted by a series of uplifted and downdropped blocks along RU-3. These blocks show uplift of as much as 1.1 km (1 s) along steeply dipping (70°-90°) faults. In addition, the basement has been displaced by a number of small-offset reverse-separation faults that also deform the overlying sediments. Beyond the western end of the basin, the presence of layering in the basement rocks suggests that the basement is internally deformed by west-vergent folds and thrust faults. A fault scarp at the sea floor (A, pl. 3C) suggests Quaternary uplift of the westernmost block of basin strata. In the central part of the basin, a thick and internally deformed lower sequence is abruptly truncated to the east by an uplifted basement block (B, pl. 3*C*). Sediments on the east side of this block are similarly truncated. These geometries suggest that the near-vertical boundaries of this basement block are possible sites of strike-slip motion. Folding of lower sequence strata immediately above the block boundaries suggests that block-boundary faults may also have accommodated some reverse motion. Most of the movement at the edges of this block must have occurred prior to the deposition of the upper sequence, as its strata continue across the block. Immediately east of this basement block, strata of the upper sequence onlap those of the lower sequence. To the west, the upper sequence thickens and downlaps onto the lower sequence, suggesting that subsidence in the central part of the basin was significant during the period of upper sequence deposition.

The pattern of repeated reverse-separation faulting within basement and sediments continues 10 km to the south on transect PG&E-3 (pl. 3*D*). Basement rock is offset in a number of places by reverse-separation faults that also fold or offset sediments of the lower sequence. Toward the east side of the basin, the faults approach vertical and then become east vergent. The one vertical fault (A, pl. 3*D*) may also accommodate some strike-slip motion. Evidence for this is the vertical discontinuity in reflections of the lower sequence that occurs at the fault. As on RU-3, the eastern basin boundary is a west-dipping unconformity between basement and strata of the lower sequence. The upper sequence is more deformed on PG&E-3 than on any of the profiles to the north. Strata are folded and faulted near underlying thrust faults. Offsets at the sea floor indicate that a number of these faults may have been active in the Quaternary. Despite folding, the original depositional geometry (as inferred from RU-13) of onlap to the east and downlap to the west is still preserved in the upper sequence. As on RU-3, layering in basement rocks beyond the west end of the basin shows west-vergent thrusting within the underlying accretionary wedge.

Interpretation of the seismic reflection data suggests that the Santa Lucia basin is a small shelf basin that initially formed during early Miocene time and was later deformed by two episodes of shortening. Strata of the lower seismic sequence, which are interpreted to be of Miocene age, were deposited on a gently west-dipping basement. Sediment geometry on line RU-13 closely reflects this initial stage of deposition. Strike-slip faulting, also of Miocene age, locally disrupts basement rocks and the overlying strata of the lower sequence. These inferred strike-slip faults are difficult to trace in the north—south direction because they may have small displacement or they may merge eastward into the Santa Lucia Bank Fault Zone. Strike-slip motion must have ceased before the beginning of the Pliocene, because sediments of the upper sequence are not cut by inferred strike-slip faults.

In the late Miocene and early Pliocene, an episode of convergence led to displacement of basement along high-angle reverse-separation faults and to folding and faulting of the lower sequence. Strata of the upper sequence were deposited unconformably over the lower sequence as the compressional episode waned. Fault scarps at the sea floor, along with folding and faulting of the upper sequence, suggest that a second episode of compression has affected the south end of the basin in the Quaternary. Seismicity data and focal mechanism solutions (Gawthrop, 1978) also are consistent with present-day thrust faulting in the vicinity of the Santa Lucia basin.

An alternate interpretation for the origin of the Santa Lucia basin suggests it may be a slope basin of Late Cretaceous to Neogene age. On the basis of an analysis of the RU-3 profile, McIntosh and others (1991) chose this interpretation over a shelf-basin origin. On profiles RU-3 and PG&E-3 the lower basinal sediments are partially folded into the underlying accretionary wedge complex. In addition, the sediments at the western edge of the basin have been uplifted and truncated by erosion. These structural geometries are typical of slope basins forming at currently active margins (for example, see Moore and Karig, 1976). Finally, the proximity of the basin to the continental slope of a former subduction margin favors a slope-basin origin.

Examination of the north-south variation in Santa Lucia basin structure casts some doubt on the slope-basin interpretation. In particular, the nearly undisturbed basin strata on RU-13 suggest that initial basin subsidence was not accompanied by compressional deformation of the underlying accretionary wedge, as is expected in the slope-basin model. Instead, folding and faulting would be the result of the compression that has affected the California margin since the late Miocene to early Pliocene. Deformation was simply more intense at the south end of the basin than at the north. Without well data and an additional north-south seismic transect that ties RU-13 to the other lines, we cannot make the definitive age ties necessary for distinguishing between shelf and slope origins. Nevertheless, the north-south variation in deformation intensity is at least consistent with that observed in the neighboring offshore Santa Maria basin.

IMPLICATIONS FOR PRESENT-DAY TECTONICS

The geometry of compressional structures observed in the upper crustal data from the PG&E/EDGE survey has an impact on efforts to understand the tectonics and seismic hazards of the California margin. The seismic sequence analysis shows that initial shortening within the basin correlates with the most recent change in Pacific–North America Plate motion and that at least some shortening continues to occur within the oblique-slip regime that characterizes the present-day San Andreas transform zone. Below, we examine the implications that these data have for recent tectonic models of the margin.

In a strike-slip stress regime, shortening is commonly accommodated with faults and folds arranged in an en echelon pattern, with axes at an orientation oblique (normally at approximately 30°) to major through-going strike-slip faults (for example, see Sylvester, 1988). Shortening is accommodated at constraining bends along the main strand of the strike-slip fault, whereas extension is accommodated at releasing bends. This style of faulting may explain extensional structures in the offshore area (McCulloch, 1987), but it does not explain the strike of shortening structures observed in the offshore basins and in other parts of central California. In the offshore region, folds and reverse faults strike in a northwesterly direction, subparallel to the trends of the Hosgri and San

Andreas Faults (fig. 1). This differs significantly from the oblique trend expected in a theoretical strike-slip stress regime.

A mechanical model for the state of stress near strike-slip faults having low shear stress (Mount and Suppe, 1987; Zoback and others, 1987) may explain the unexpected strike of folds and thrusts within the offshore Santa Maria and Santa Lucia basins. This model was first proposed for a region adjacent to the San Andreas Fault in central California, where not only do reverse faults and folds occur, but measurements indicate that the maximum principal stress is normal to the transform (Mount and Suppe, 1987; Zoback and others, 1987). Mount and Suppe (1987) and Zoback and others (1987) show that if the transform is weak, then the stress in the near field rotates so that the maximum principal stress is approximately normal to the fault and the shear stress along the fault is small. The fault-parallel strike of offshore structures suggests that they fit into this kind of stress model. We interpret this as evidence that the weak portion of the transform regime extends into the offshore region and perhaps that offshore strike-slip faults such as the Hosgri Fault may also be weak.

Significant controversy accompanies the question of exactly how this fault-normal shortening is accommodated at depth. For example, Crouch and others (1984) have suggested that high-angle reverse faults observed near the surface, both onshore and offshore, flatten into an aseismic detachment zone at 12 to 15 km depth. This decollement is thought to coincide with the top of an oceanic crustal layer that is now known to underlie the margin. A number of regionally extensive faults, including the Hosgri are inferred to sole into this detachment. In this interpretation the Hosgri may once have been a strike-slip fault but now is predominantly a thrust fault.

Although the PG&E/EDGE seismic data image the boundary between Franciscan Complex rocks and underplated oceanic crust (McIntosh and others, 1991; Meltzer and Levander, 1991; Miller and others, 1992) they lack evidence that would permit the extension of reverse faults that offset basin strata to the deeper parts of the crust. Numerous reverse faults have already been identified on the basis of reflection terminations at the top of basement rocks and within the Tertiary strata of the offshore Santa Maria and Santa Lucia basins (pl. 1-4). However, the basement rocks lack the continuity needed to follow fault planes based on the termination method, and fault-plane reflections can rarely be followed very far into the basement. Exceptions to this observation include a possible subhorizontal fault-plane reflection beneath the Queenie structure (pl. 1*C*, *D*). Without fault-plane reflections to rely on, there is no direct way to prove or disprove the occurrence of crustal-scale thrust faults required by the model of Crouch and others (1984).

The suggestion that a major through-going fault such as the Hosgri might be a thrust fault has prompted a number of investigators to reprocess seismic data to improve both steep dip imaging and imaging in the face of large-velocity contrast. A full prestack depth migration of the Hosgri Fault Zone performed on line RU-3 (Lafond and Levander, 1993) shows 75° of east dip on the Hosgri and suggests that the fault is near vertical at this location. Through interpretation and depth conversion of many seismic reflection records across the Hosgri Fault Zone, Willingham and others (unpub. data, 1997[3]) find that the Hosgri is steeply dipping (> 60°) to subvertical and that, in the southern part of the Santa Maria basin, it is sometimes associated with auxiliary thrusts. None of their data point to flattening of the Hosgri Fault Zone itself at depth. These more detailed studies are all in agreement with our observations on the complete PG&E/EDGE dataset, that the Hosgri Fault Zone is steeply dipping to subvertical.

CONCLUSIONS

Seismic reflection data from the 1986 PG&E/EDGE experiment cross two basins, the Santa Lucia and offshore Santa Maria basins of central California. These basins initially formed in early Miocene time in the transtensional tectonic regime imposed by the onset of transform motion along the North American continental margin. Faults inferred to have accommodated some of this transform motion (and extension) include the Hosgri and Santa Lucia Bank Fault Zones, which appear as near-vertical boundaries of the offshore Santa Maria basin on the seismic data. These data show that the Santa Lucia Bank Fault Zone commonly has dips ranging from 30° to 60° that make it a poor candidate for accommodation of large amounts of strike-slip as suggested by Sedlock and Hamilton (1991). However, the data do support the presence of at least one other minor strike-slip fault further west, within the Santa Lucia basin.

A late Miocene to early Pliocene shortening episode has folded and faulted sediments within both basins. The age of strata affected by compression decreases southward, while the amount of shortening within both basins increases to the south. Since both the northern and southern sectors of the two basins should have experienced similar stress fields, the variable amounts of shortening seen in these two sectors suggests a heterogeneous strain field in central California. Shortening not seen in the northern sector of offshore central California must be accommodated elsewhere along the margin.

The age of onset of compression coincides with a late Miocene to early Pliocene change in Pacific–North America Plate motion that added a component of compression to right-lateral slip along the plate boundary. Shortening due to oblique plate motion continues today in the offshore. The PG&E/EDGE data indicate that active folding and reverse faulting affects much of the southern sector of the Santa Lucia basin but is limited to minor perturbations of very shallow strata adjacent to the Hosgri and Santa Lucia Bank Fault Zones in the offshore Santa Maria basin.

This seismic reflection survey supplies additional data for evaluating tectonic models for present-day deformation along the California margin. A model presented by Crouch and others (1984) proposes that folding and high-angle reverse faulting observed within the sedimentary section is accommodated at depth by flattening of faults into a decollement located at the base of the seismogenic zone. These workers cite the Hosgri as a major through-going fault that manifests this behavior. Whereas there is some seismic evidence for flattening of a fault plane at a shallow depth beneath the Queenie structure, these data lack reflections that might be interpreted as evidence for a flattening of fault planes beneath other convergent structures including the Hosgri Fault Zone.

REFERENCES CITED

Argus, D.F., and Gordon, R.G., 1991, Current Sierra Nevada–North America motion from very long baseline interferometry: implications for the kinematics of the western United States: Geology, v. 19, p. 1085-1088.

Atwater, T., 1970, Implications of plate tectonics for the Cenozoic tectonic evolution of western North America: Geological Society of America Bulletin, v. 81, p. 3513-3536.

Atwater, T., 1989, Plate tectonic history of the northeast Pacific and western North America, *in* Winterer, E.L., Hussong, D.M., and Decker, R.W., eds., The eastern Pacific Ocean and Hawaii, vol. N *of* The geology of North America: Geological Society of America, Boulder, Colo., pp. 21-72.

Atwater, T., and Molnar, P., 1973, Relative motion of the Pacific and North American plates deduced from sea-floor spreading in the Atlantic, Indian, and South Pacific oceans: Stanford, Calif., Stanford University Publications in Geological Sciences, v. 13, p. 136-148.

Clark, D.H., Hall, N.T, Hamilton, D.H., and Heck, R.G., 1991, Structural analysis of late Neogene deformation in the central offshore Santa Maria basin, California: Journal of Geophysical Research, v. 96, p. 6435-6458.

Cox, A., and Engebretson, D., 1985, Change in motion of Pacific plate at 5 Myr BP: Nature, v. 313, p. 472-474.

Crain, W.E., Mero, W.E., and Patterson, D., 1985, Geology of the Point Arguello discovery: American Association of Petroleum Geologists Bulletin, v. 69, p. 537-545.

Crouch, J.K., Bachman, S.B., and Shay, J.T., 1984, Post-Miocene compressional tectonics along the central California margin, *in* Crouch, J.K., and Bachman, S.B., eds., Tectonics and sedimentation along the California margin: Society of Economic Paleontologists and Mineralogists, Pacific Section, Los Angeles, Calif., p. 37-54.

DeMets, C., Gordon, R.G., Stein, S., and Argus, D.F., 1987, A revised estimate of Pacific–North America motion and implications for western North America plate boundary zone tectonics: Geophysical Research Letters, v. 14, p. 911-914.

Dibblee, T.W., Jr., 1950, Geology of southwestern Santa Barbara County, California; Point Arguello, Lompoc, Point Conception, Los Olivos, and Gaviota quadrangles: California Division of Mines Bulletin 150, 95 p., 9 pls.

Engebretson, D.C., Cox, A., and Gordon, R.G., 1985, Relative motions between oceanic and continental plates in the Pacific basin: Geological Society of America Special Paper 206, 59 p.

Gawthrop, W.H., 1978, Seismicity and tectonics of the central California coastal region, *in* Silver, E.A., and Normark, W.R., eds., San Gregorio–Hosgri Fault Zone, California: California Division of Mines and Geology Special Report 137, p. 45-55.

Graham, S.A., 1978, Role of Salinian block in evolution of San Andreas Fault system, California: American Association of Petroleum Geologists Bulletin, v. 62, p. 2214-2231.

Graham, S.A., and Dickinson, W.R., 1978, Evidence for 115 kilometers of right-slip on the San Gregorio–Hosgri Fault trend: Science, v. 199, p. 179-181.

Hall, C.A., Jr., 1975, San Simeon–Hosgri Fault system, coastal California: economic and environmental implications: Science, v. 190, p. 1291-1294.

Harbert, W. and Cox, A., 1989, Late Neogene motion of the Pacific plate: Journal of Geophysical Research, v. 94, p. 3052-3064.

Hoskins, E.G., and Griffiths, J.R., 1971, Hydrocarbon potential of northern and central California offshore, *in* Cram, I.H., ed., Future petroleum provinces of the United States—their geology and potential: American Association of Petroleum Geologists Memoir 15, v. 1, p. 212-228.

Howie, J.M., Miller, K.C., and Savage, W.U., 1993, Integrated crustal structure across the south-central California margin: Santa Lucia escarpment to the San Andreas Fault: Journal of Geophysical Research, v. 98, pp. 8173-8196.

Isaacs, C.M., Keller, M.A., Gennai, V.A., Stewart, K.C., Taggart, J.E., Jr., 1983, Preliminary evaluation of Miocene lithostratigraphy in the Point Conception COST well OCS-CAL 78-164 No. 1, off Southern California, *in* Isaacs, C.M., and Garrison, R.E., eds., Petroleum generation and occurrence in the Miocene Monterey Formation, California: Society of Economic Paleontologists and Mineralogists, Pacific Section, Los Angeles, Calif., p. 99-110.

Jordan, T.H., and Minster, J.B., 1988, Measuring crustal deformation in the American west: Scientific American, v.259, no. 2, p. 48-58.

Lafond, C.F., and Levander, A.R., 1993, Migration moveout analysis and depth focusing: Geophysics, v. 58, p. 91-100.

McCulloch, D.S., 1987, Regional geology and hydrocarbon potential of offshore central California, *in* Scholl, D.W., Grantz, A., and Vedder, J.G., eds., Geology and resource potential of the continental margin of western North America and adjacent ocean basins—Beaufort Sea to Baja California: Houston, Tex, Circum Pacific Council for Energy and Mineral Resources, Earth Science Series, v.6, p. 353-401.

McCulloch, D.S., Vedder, J.G., Wagner, H.E., Brune, R.H., 1979, Geologic setting *in* Cook, H.E., ed., Geologic studies of the Point Conception deep stratigraphic test well OCS-Cal 78-164 No. 1, outer continental shelf, southern California: U. S. Geological Survey Open-File Report 79-1218, p. 10-25.

McIntosh, K.D., Reed, D.L., Silver, E.A., and Meltzer, A.S., 1991, Deep structure and structural inversion along the central California continental margin from EDGE seismic profile RU-3: Journal of Geophysical Research, v. 96, p. 6459-6474.

Meltzer, A.S. and Levander, A.R., 1991, Deep crustal reflection profiling offshore southern central California: Journal of Geophysical Research, v. 96, p. 6459-6474.

Miller, K.C., 1993, Crustal structure along the strike of the offshore Santa Maria basin, California: Tectonophysics, v. 219, p. 57-69.

Miller, K.C., Howie, J.M. and Ruppert, S.D., 1992, Shortening within underplated oceanic crust beneath the central California margin: Journal of Geophysical Research, v. 97, p. 19,961-19,980.

Moore, G.F., and Karig, D.E., 1976, Development of sedimentary basins on the lower trench slope: Geology, v. 4, p. 693-697.

Mount, V.S., and Suppe, J., 1987, State of stress near the San Andreas Fault:

implications for wrench tectonics: Geology, v. 15, p. 1143-1146.

Ogle, B.A., Wallis, W.S., Heck, R.G., and Edwards, E.B., 1987, Petroleum geology of the Monterey Formation in the offshore Santa Maria/Santa Barbara areas, *in* Ingersoll, R.V., and Ernst, W.G., eds., Cenozoic basin development of coastal California: Englewood Cliffs, N.J., Prentice-Hall Inc., p. 382-406.

Pacific Gas and Electric Co., 1988, Final report of the Diablo Canyon Long Term Seismic Program: San Francisco, Calif., U.S. Nuclear Regulatory Commission Docket 50-275 and 50-323.

Page, B.M., 1981, The southern Coast Ranges, *in* W.G. Ernst, ed., The geotectonic development of California: Englewood Cliffs, N.J., Prentice-Hall Inc., pp. 329-417.

Page, B.M., and Engebretson, D.C., 1984, Correlation between the geologic record and computed plate motions for central California: Tectonics, v. 3, p. 133-155.

Page, B.M., Wagner, H.C., McCulloch, D.S., Silver, E.A., and Spotts, J.H., 1979, Geologic cross section of the continental margin off San Luis Obispo, the southern Coast Ranges, and the San Joaquin Valley, California: Geological Society of America Map and Chart Series MC-28G.

Sedlock, R.L., and Hamilton, D.H., 1991, Late Cenozoic tectonic evolution of southwestern California: Journal of Geophysical Research, v. 96, p. 2325-2351.

Stock, J., and Molnar, P., 1988, Uncertainties and implications of the Late Cretaceous and Tertiary position of North America plate relative to the Farallon, Kula, and Pacific plates: Tectonics, v. 7, p. 1339-1384.

Sylvester, A.G., 1988, Strike-slip faults: Geological Society of America Bulletin, v. 100, p. 1666-1703.

Vail, P.R., Mitchum, R.M., and Thompson, S., 1977, Seismic stratigraphy and global changes of sea level, part 2: the depositional sequence as a basic unit for stratigraphic analysis, *in* Payton, C.E., ed., Seismic stratigraphy—applications to hydrocarbon exploration: American Association of Petroleum Geologists Memoir 26, p. 53-62.

Zoback, M.D., Zoback, M.L., Mount, V.S., Suppe, J., Eaton, J.P., Healy, J.H., Oppenheimer, D., Reasenberg, P., Jones, L.C., Raleigh, B., Wong, I.G., Scotti, O., and Wentworth, C., 1987, New evidence on the state of stress of the San Andreas Fault system: Science, v. 238, p. 1105-1111.

☆ U.S. GOVERNMENT PRINTING OFFICE: 1999 — 573-047 / 20174 Region No. 8

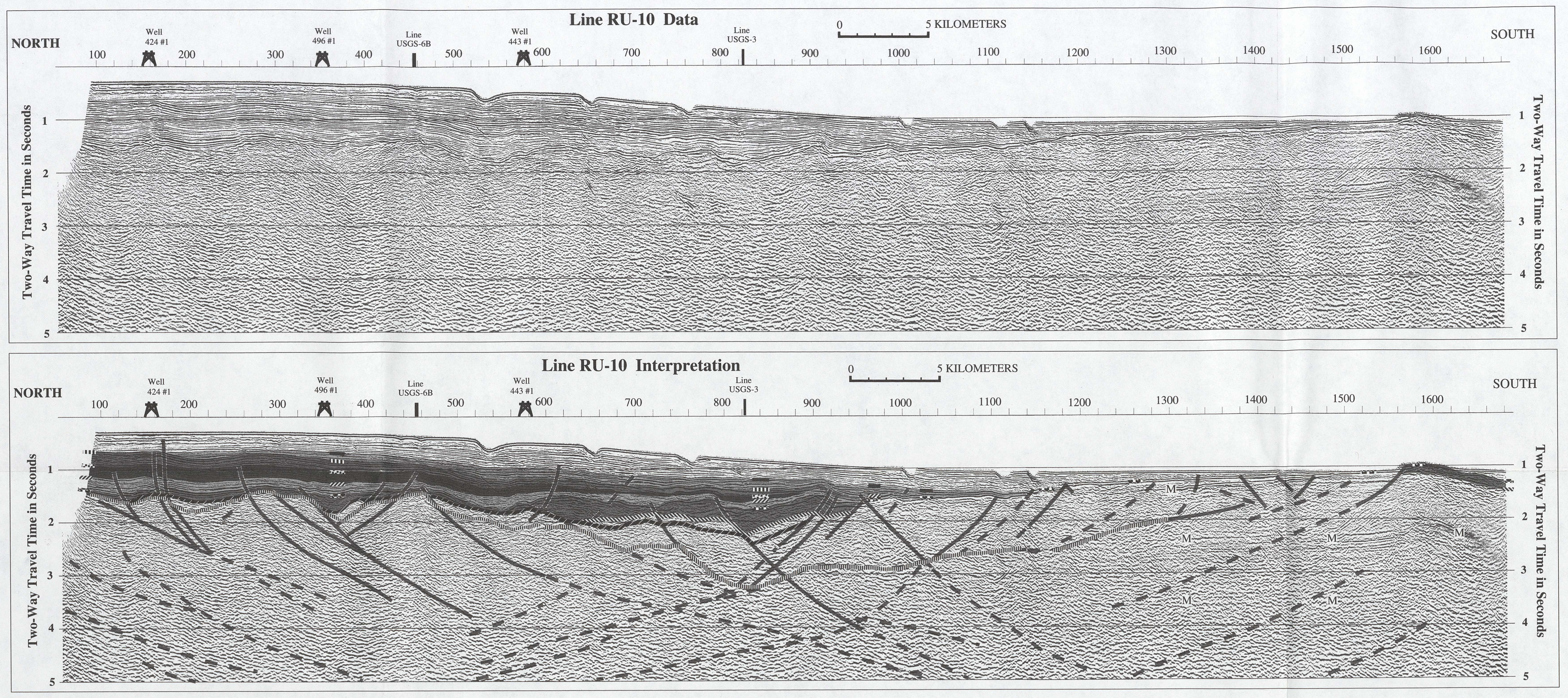

Data and interpretation of RU-10. The display is variable area, no wiggle. The wells shown were tied directly to RU-10 via USGS-103, USGS-6B, andindustry profiles. The reflection profiles on this plate are shown at the same scale except the wiggle data of USGS 3; vertical exaggeration is 1:1 at 6 km/s interval velocity. M= multiple

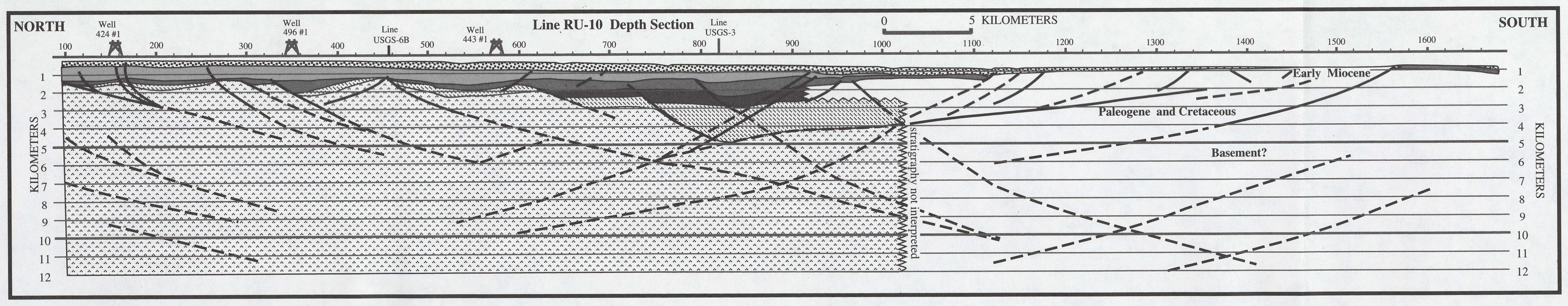

RU-10 depth section, no vertical exaggeration. The depth sections are constructed from depth migrated reflection data.

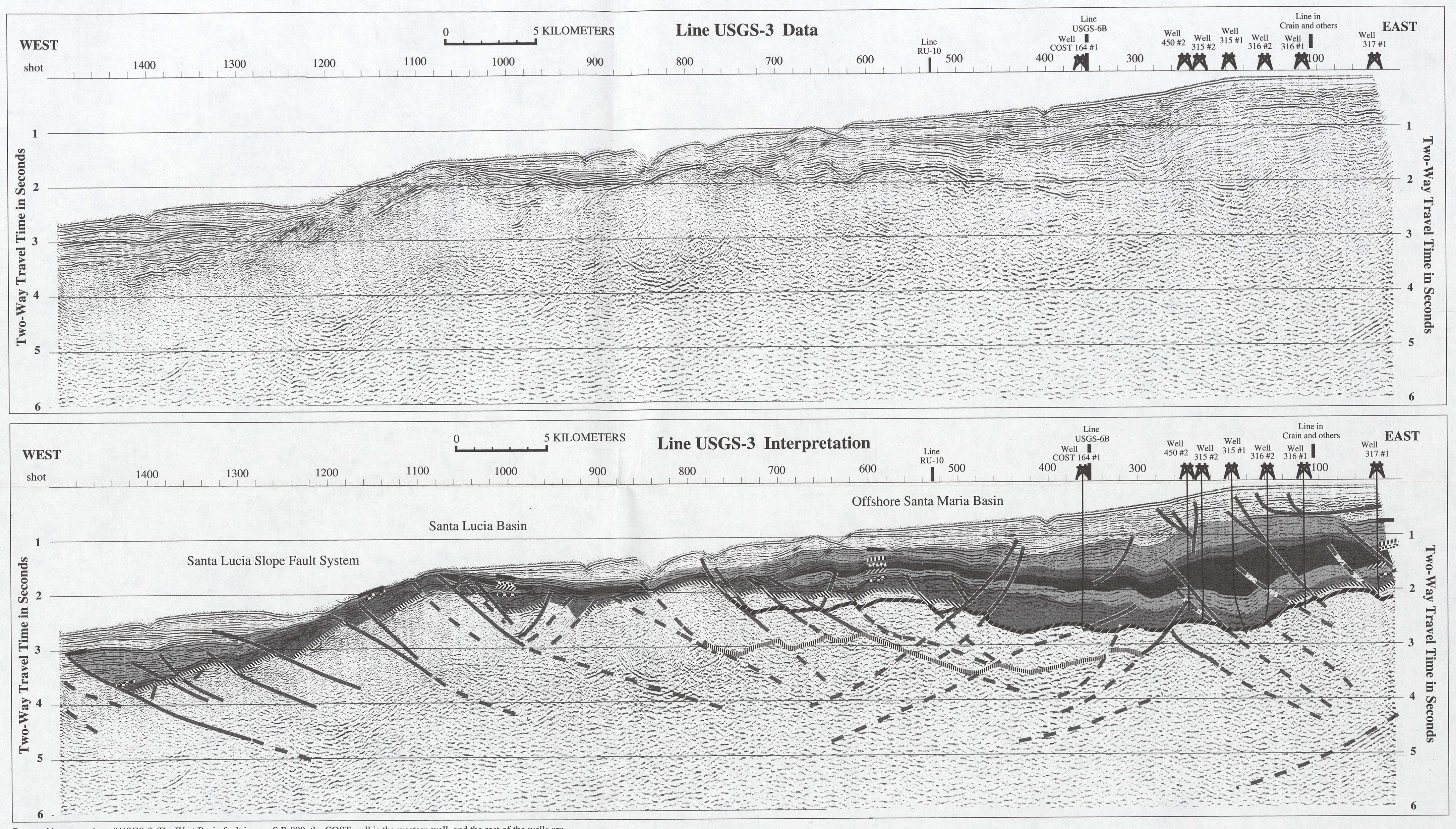

Data and interpretation of USGS-3. The West Basin fault is near S.P. 800, the COST well is the western well, and the rest of the wells are in the Pt. Arguello oil field. The well deviation is projected onto the plane of the section, wells are converted to time and placed on the section. Certain wells are a significant distance (3 km) from the profile (Fig. 2) or have limited stratigraphic information (see Table 1). In interpretation, dip is taken into account for formation tops on wells located off of the section.

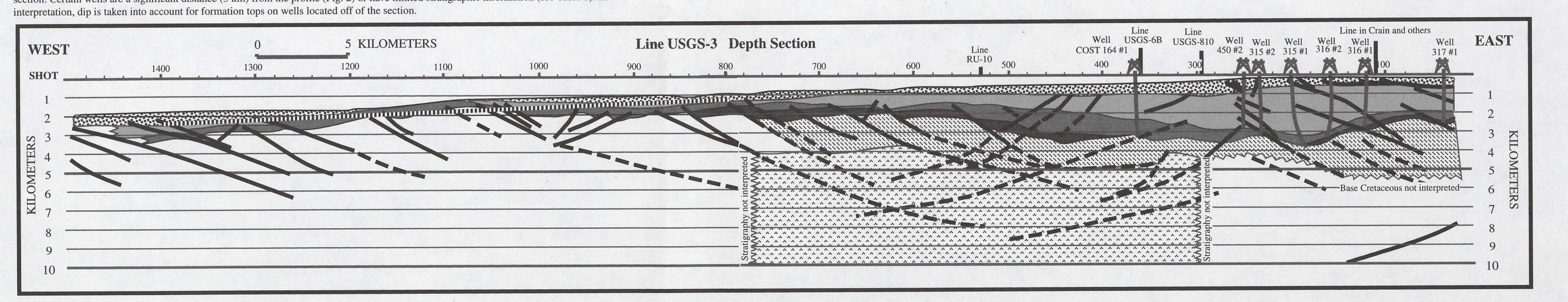

Depth section of USGS-3 with no vertical exaggeration.

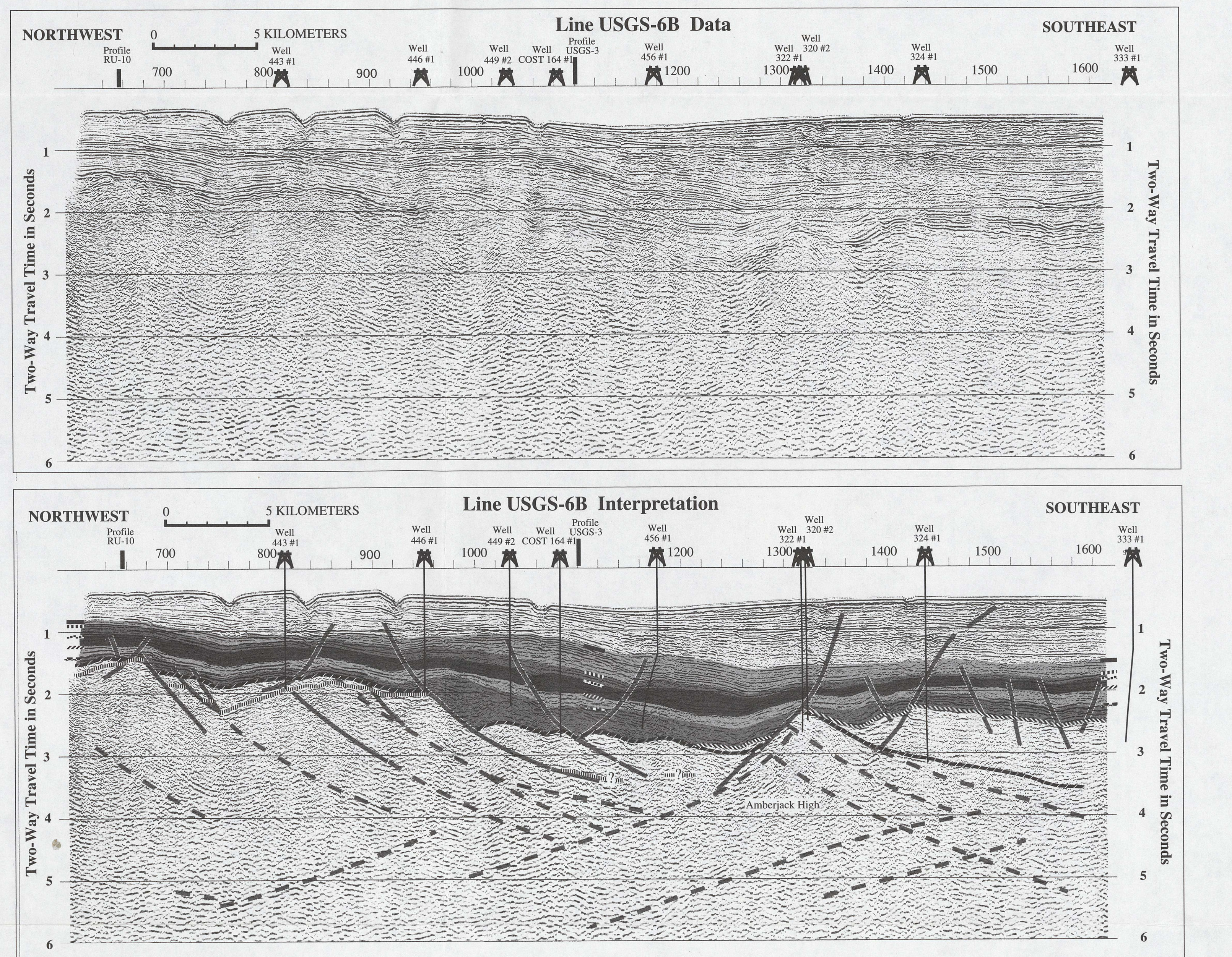

Data and interpretation of USGS-6B.

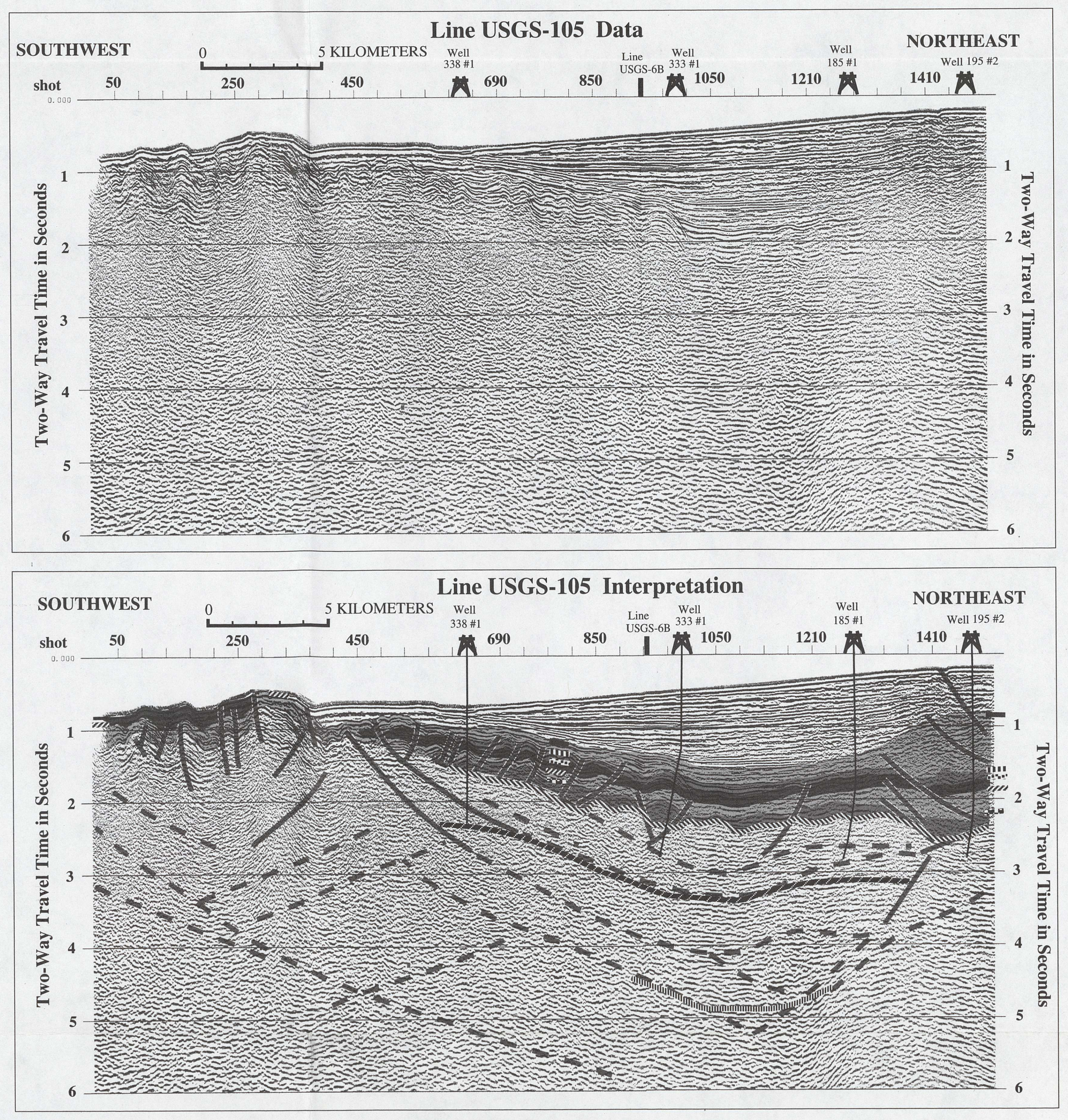

Data and interpretation of USGS-105. The vertical exaggeration is the same as for previous time profiles, or 1:1 at 6 km/s interval velocity. Less stratigraphic information was available for the two northeastern wells than for the other two wells (see Table 1).

Wiggle data part of USGS-3.

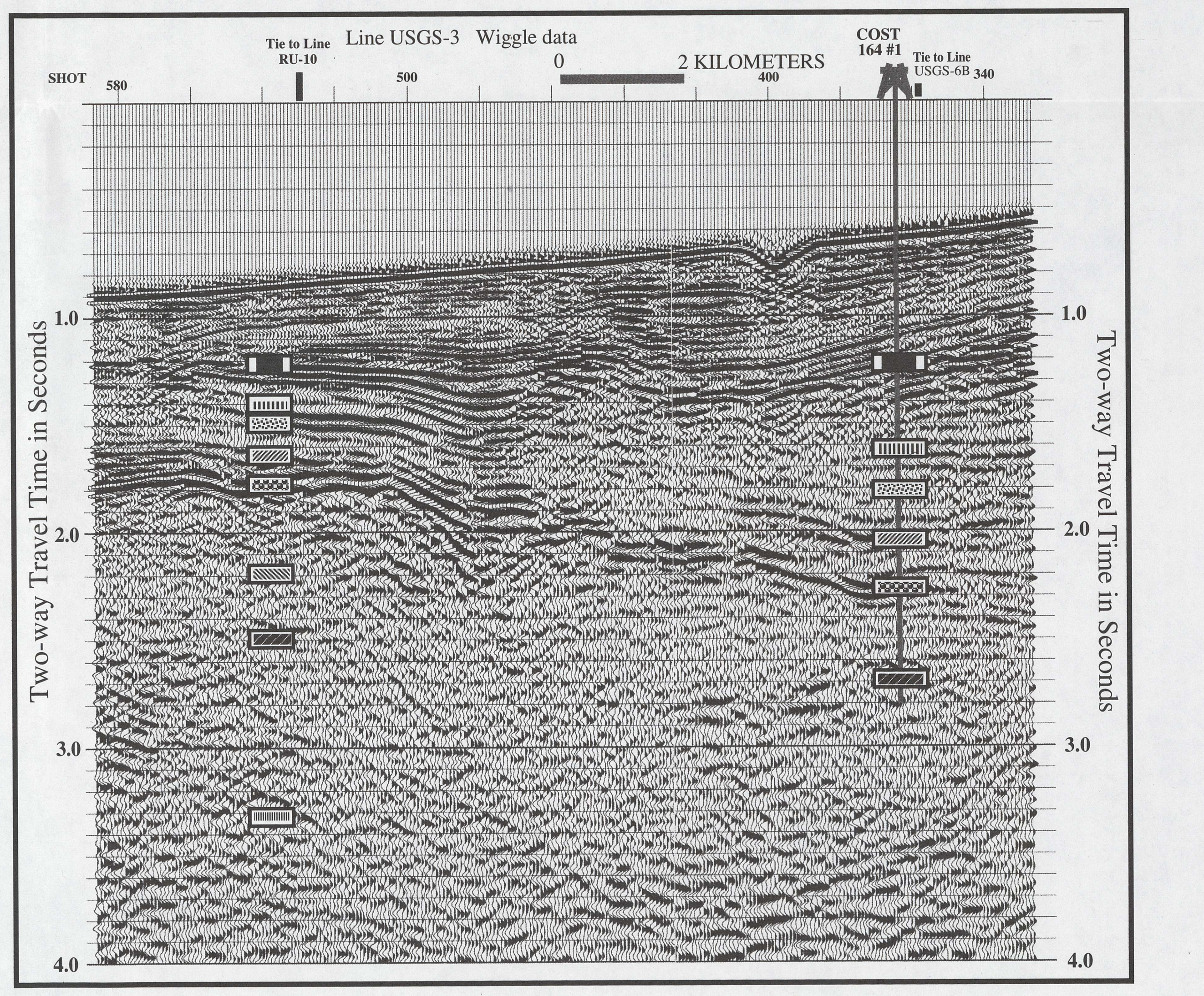

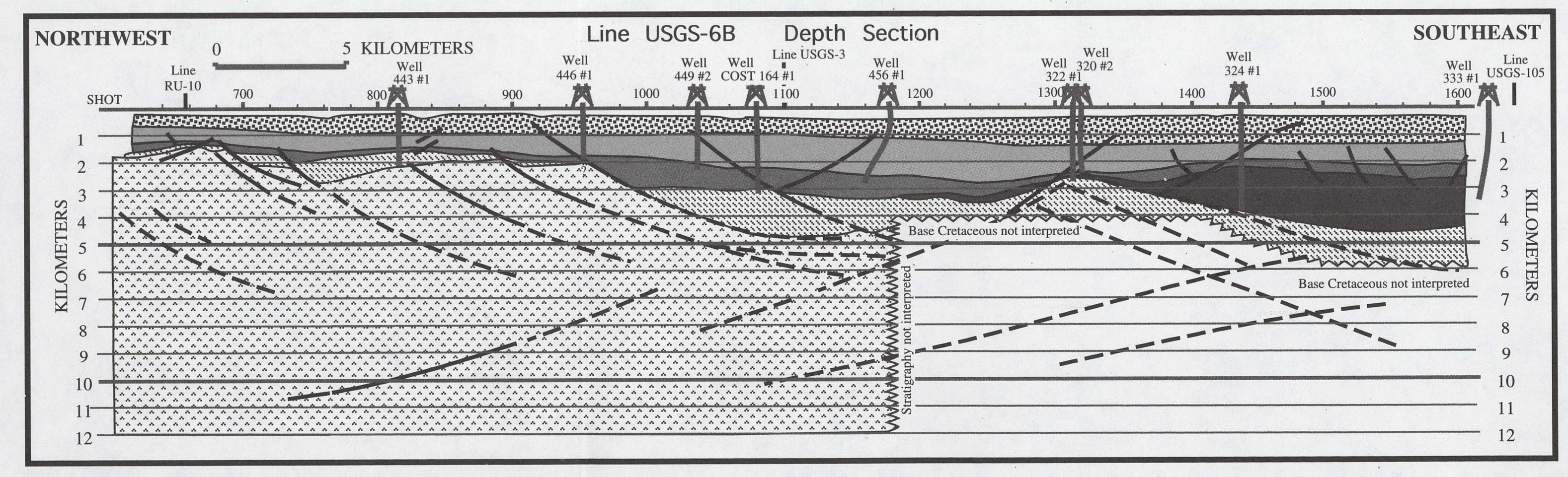

Depth section of USGS-6B with no vertical exaggeration.

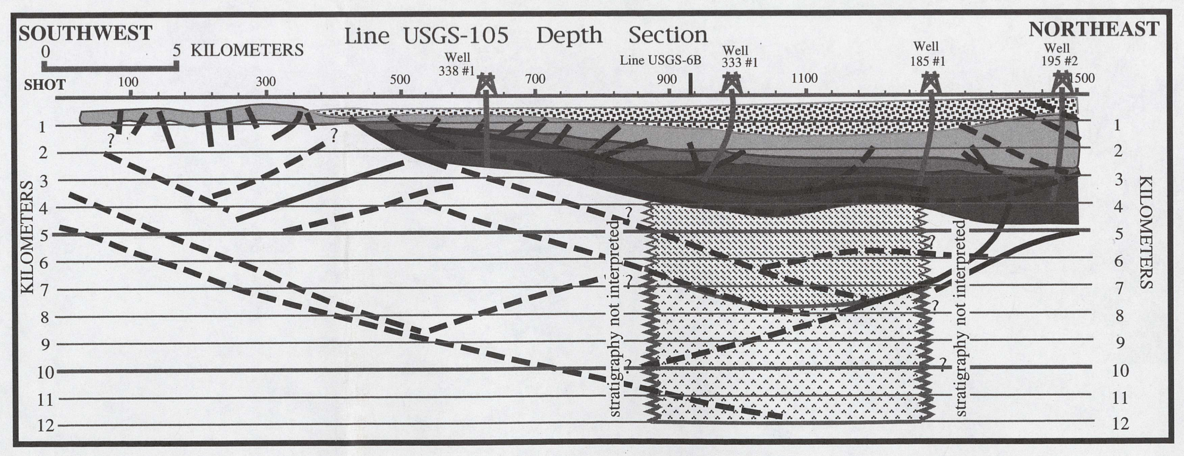

Depth section of USGS-105, no vertical exaggeration.

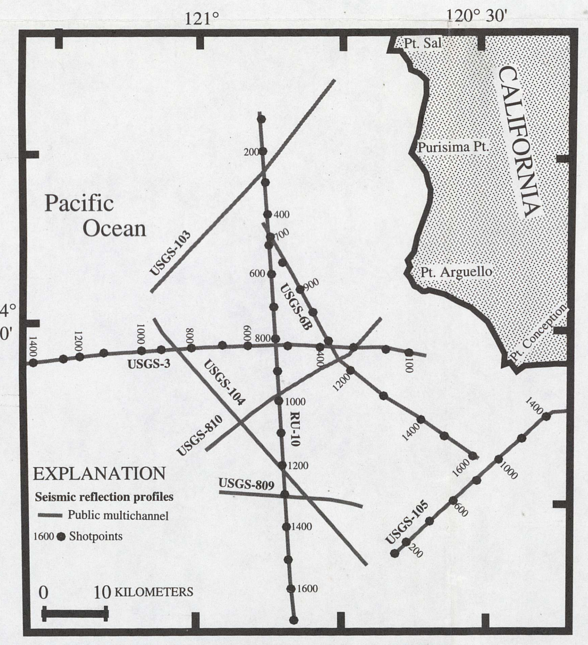

INDEX MAP SHOWING LOCATIONS OF SEISMIC REFLECTION PROFILES

EXPLANATION

Finite-difference migrations were output in both time and depth. The depth sections shown on this plate were constructed on the depth displays of the data. The time displays are shown both interpreted and uninterpreted.

Depth Sections. Shading or pattern indicatess age of strata.

- Upper Pliocene-Quaternary
- Upper Miocene-Lower Pliocene
- Lower & Middle Miocene
- Paleogene
- Cretaceous
- Basement
- Fault; interpreted on reflection or discontinuity in reflection.
- Fault; inferred on less certain reflection or discontinuity.
- Regional dip for area balance on depth section USGS-3

Interpreted time profiles. Shading indicates Formation or other sequence; thick patterned lines or curves indicate top of formation, sequence, or rocks divided by age.

- Late Pliocene-Quaternary Sediments (undivided)
- Foxen Mudstone (lower part)
- Sisquoc Formation (upper part)
- Sisquoc Formation (lower part)
- Monterey Formation (upper part)
- Monterey Formation (lower part) or older sediment or volcanic rocks
- Fault; interpreted on reflection or discontinuity in reflection.
- Fault; inferred on less certain reflection or discontinuity.
- Top Paleogene sediments (undivided)
- Top Cretaceous sediments (undivided)
- Top "Basement"
- Petroleum test well; deviation projected onto plane of profile.
- M Multiple reflection

INTERIOR—GEOLOGICAL SURVEY, RESTON, VA—1999

Sorlien, C.C., Nicholson, C., and Luyendyk, B.P., Miocene extension and post-Miocene transpression offshore of south-central California, chapter Y of Keller, M.A., ed., Evolution of sedimentary basins/onshore oil and gas investigation—Santa Maria province; U.S. Geological Survey Bulletin 1995.

SEISMIC REFLECTION PROFILES, OFFSHORE SOUTH-CENTRAL CALIFORNIA

By

Christopher C. Sorlien, Craig Nicholson, and Bruce P. Luyendyk

1999

A. RU-13

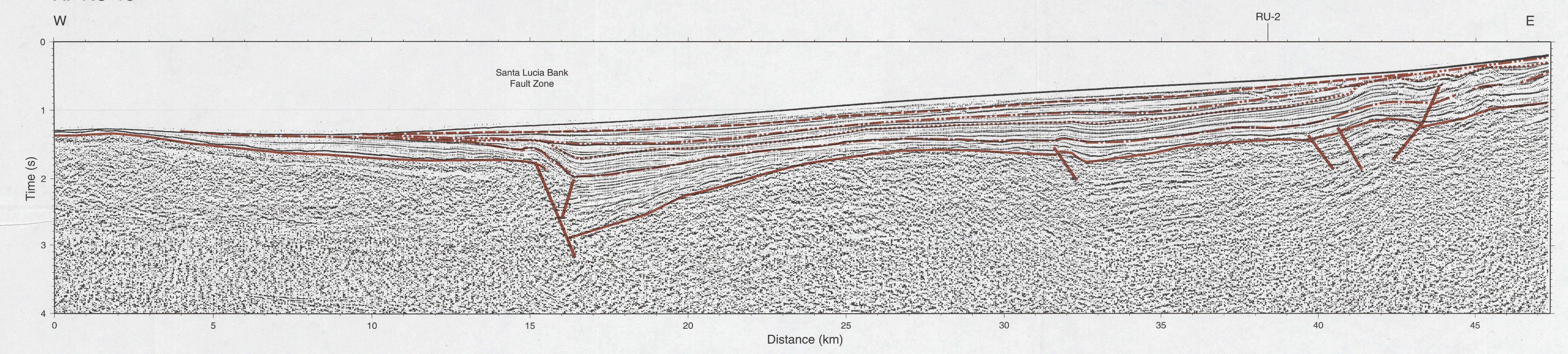

B. PG&E-1

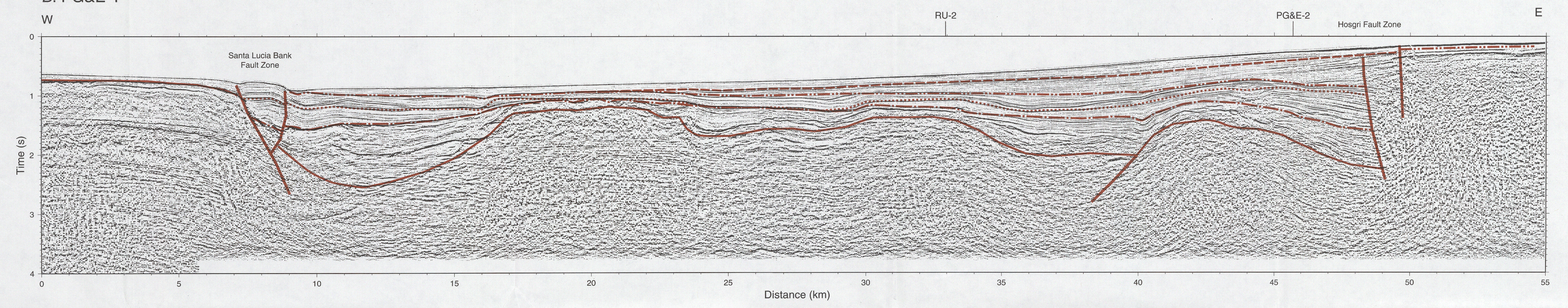

C. RU-3

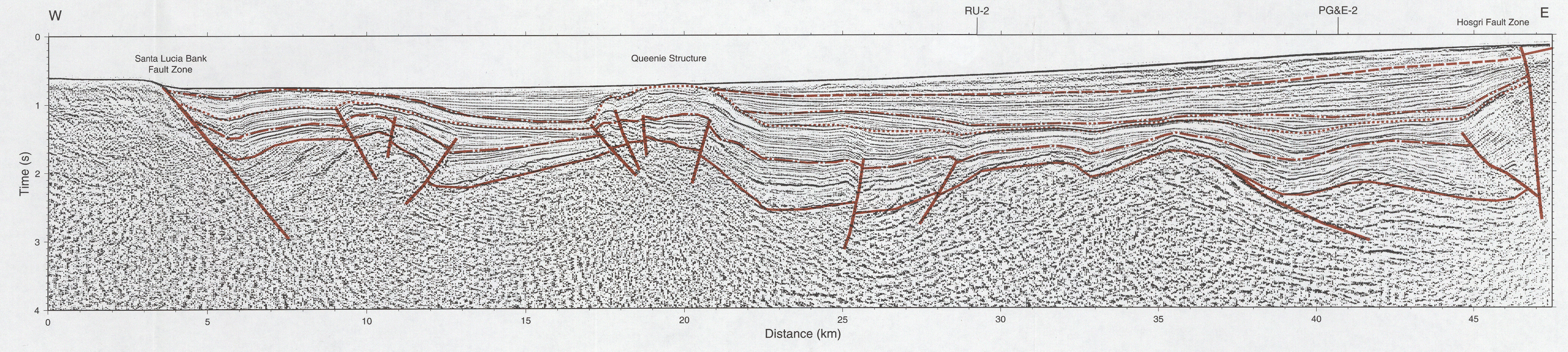

D. PG&E-3

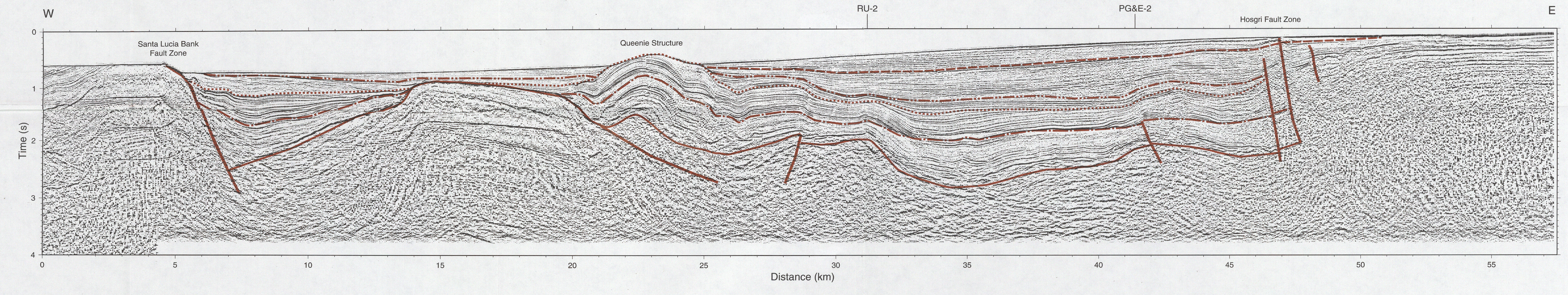

E. RU-2 , North part

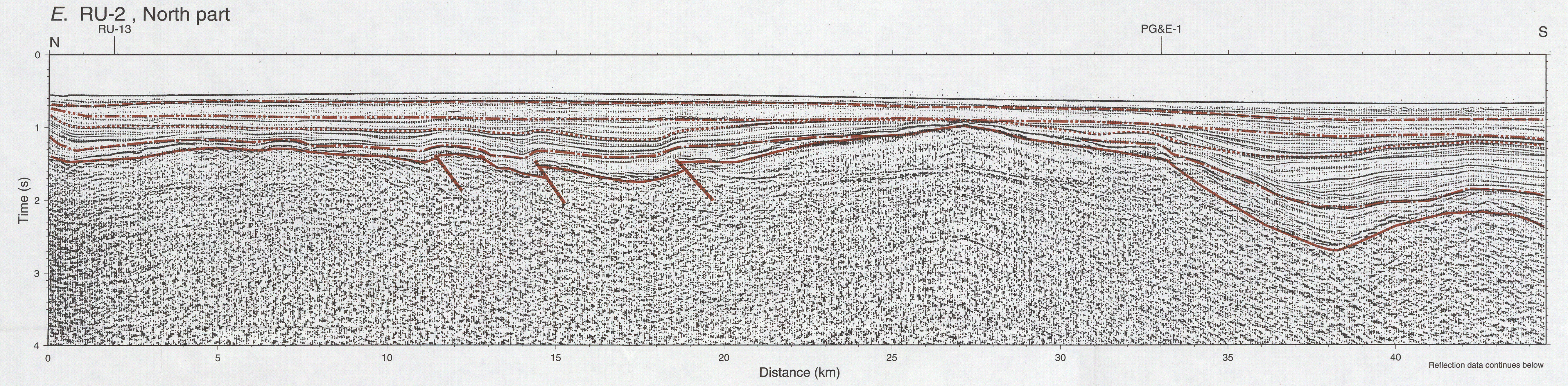

E. RU-2, South part

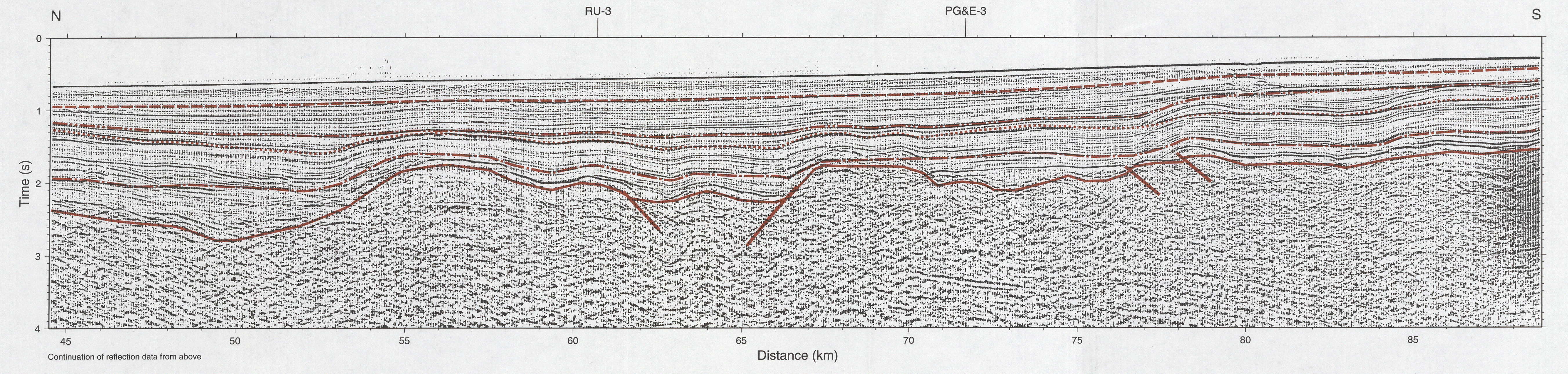

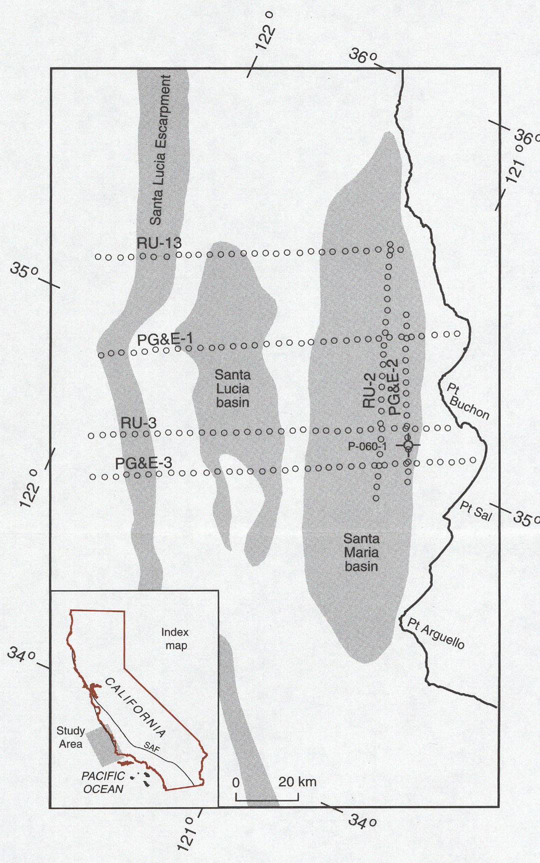

Index Map

EXPLANATION

- Base of seismic unit A
- Base of seismic unit B
- Base of seismic unit C
- Base of seismic unit D
- Base of seismic unit E and top of basement unit
- Fault

F. PG&E-2

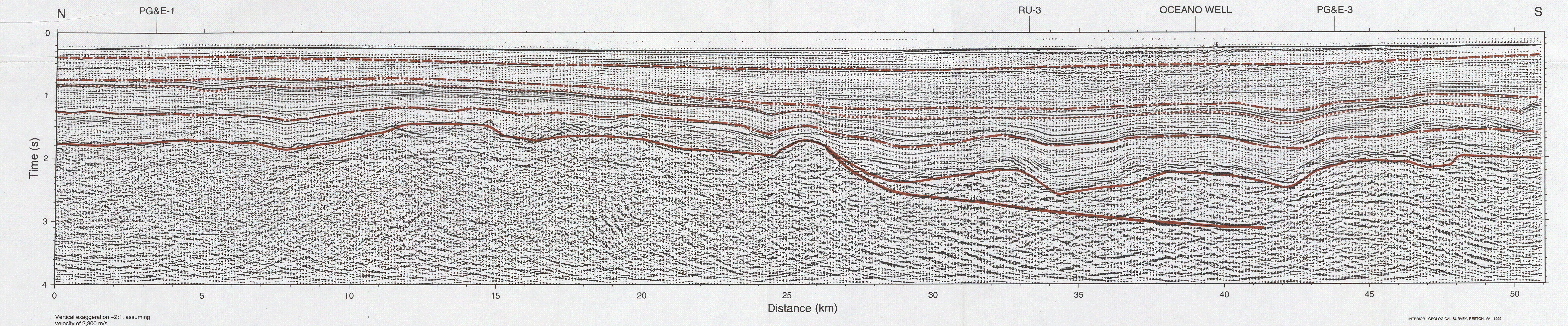

Vertical exaggeration ~2:1, assuming velocity of 2,300 m/s

INTERIOR - GEOLOGICAL SURVEY, RESTON, VA - 1999

Miller, K. C., and Meltzer, A. S., Structure and tectonics of the offshore Santa Maria and Santa Lucia basins, central California: results from the PG&E/EDGE seismic reflection survey, chapter Z of Keller, M. A., ed., Evolution of sedimentary basins/onshore oil and gas investigations—Santa Maria province: U.S. Geological Survey Bulletin 1995.

INTERPRETED MIGRATED SEISMIC REFLECTION DATA FOR OFFSHORE SANTA MARIA BASIN TRANSECTS, CALIFORNIA

By

Kate C. Miller and Anne S. Meltzer

1999

A. RU-13

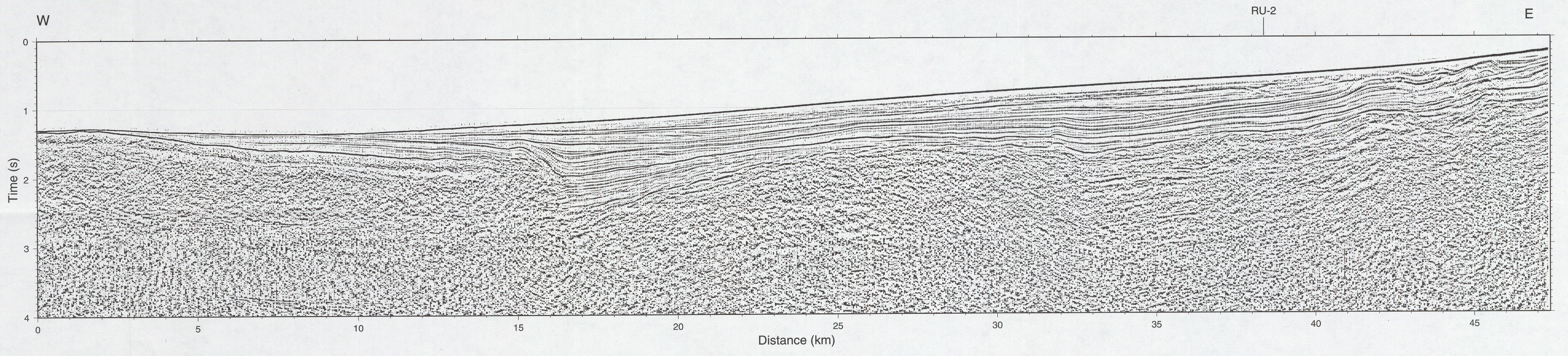

B. PG&E-1

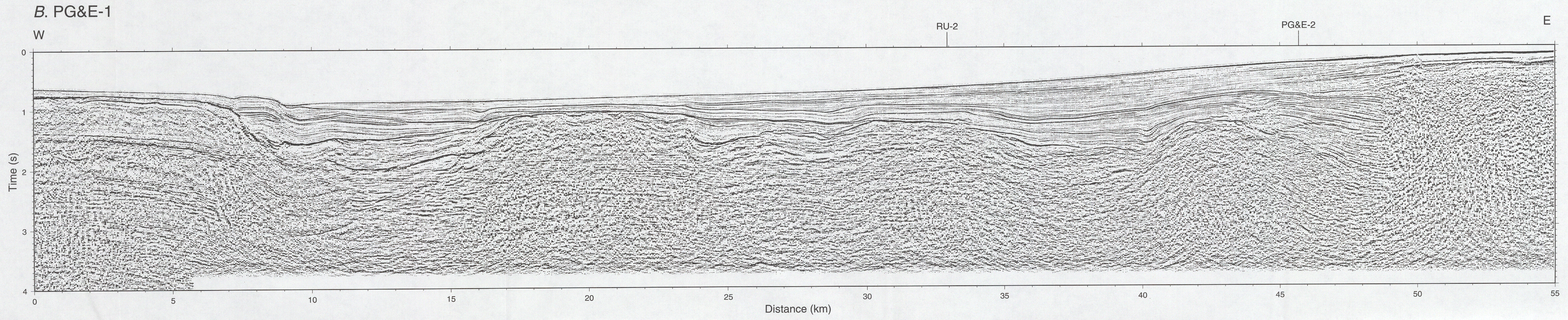

C. RU-3

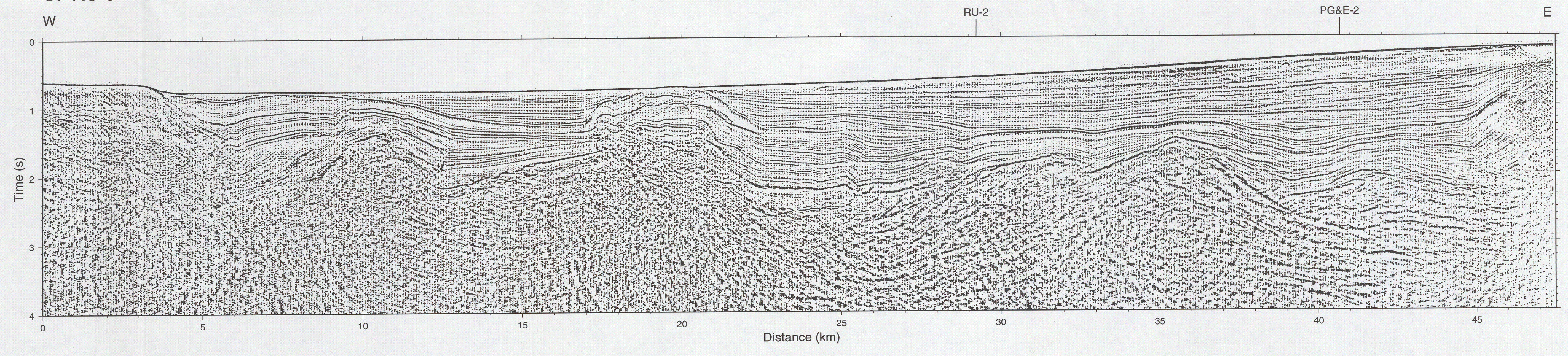

D. PG&E-3

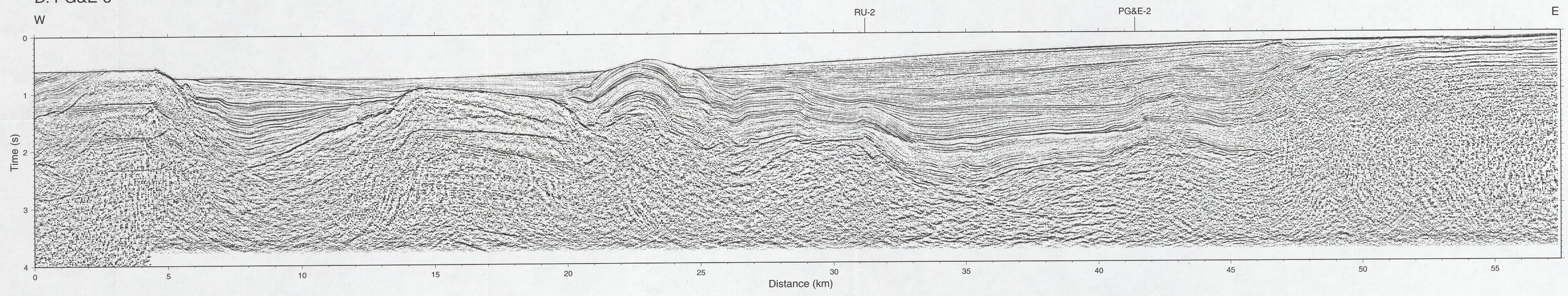

E. RU-2 , North part

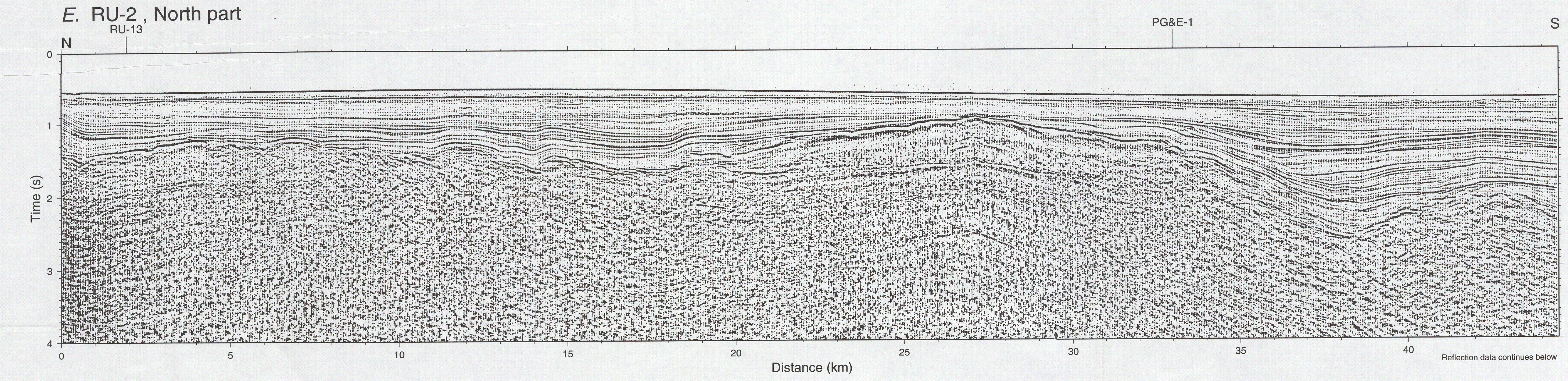

E. RU-2, South part

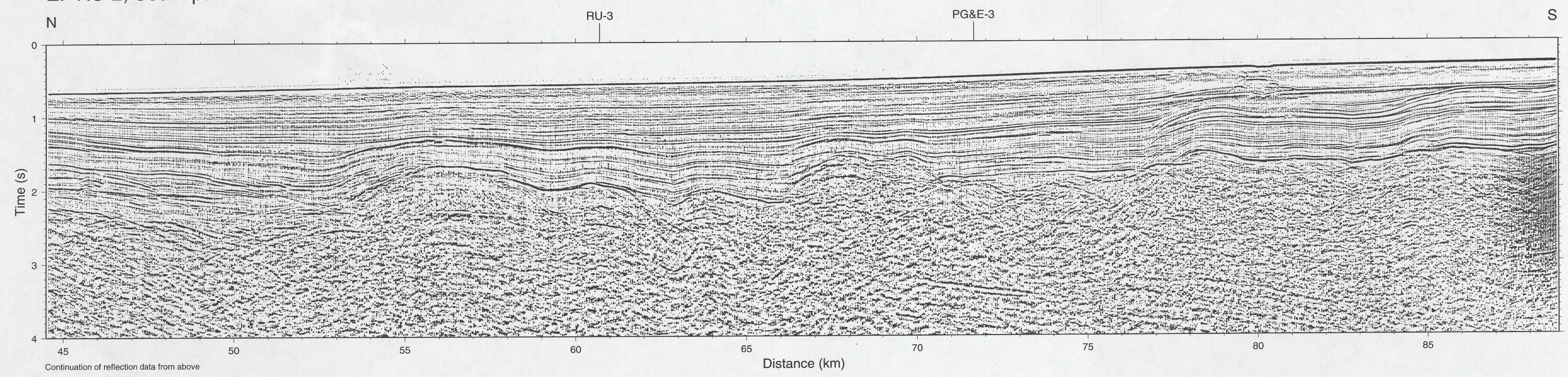

Continuation of reflection data from above

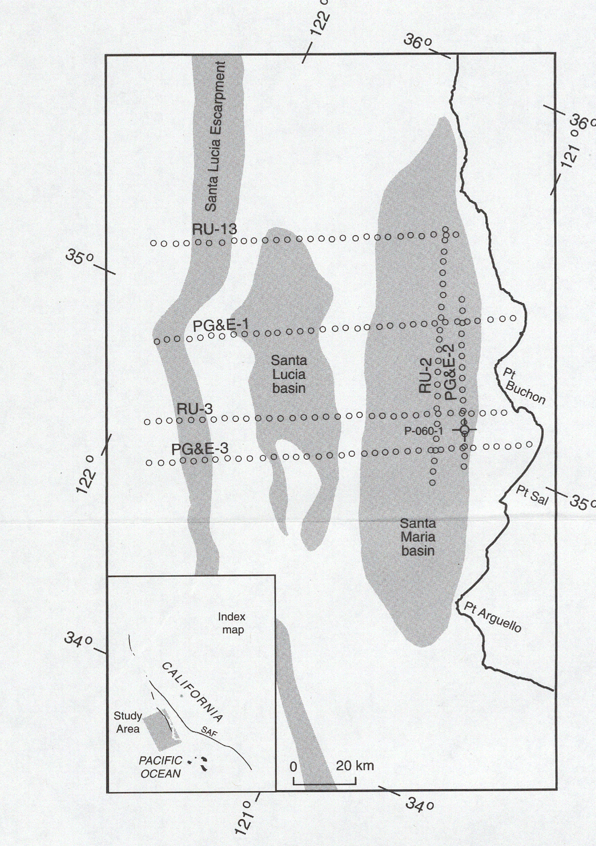

Index Map

F. PG&E-2

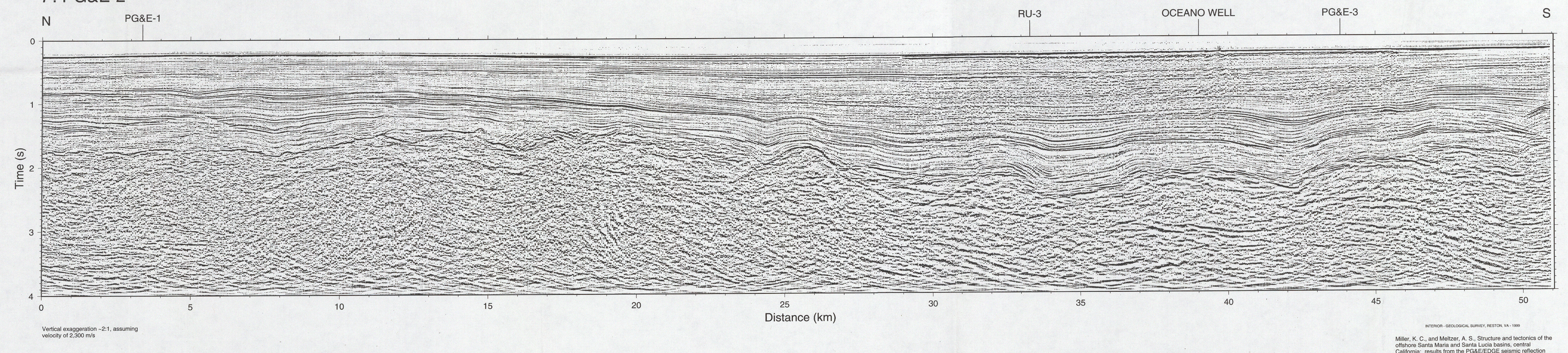

Vertical exaggeration ~2:1, assuming velocity of 2,300 m/s

INTERIOR - GEOLOGICAL SURVEY, RESTON, VA - 1999

Miller, K. C., and Meltzer, A. S., Structure and tectonics of the offshore Santa Maria and Santa Lucia basins, central California: results from the PG&E/EDGE seismic reflection survey, chapter Z of Keller, M. A., ed., Evolution of sedimentary basins/onshore oil and gas investigations—Santa Maria province: U.S. Geological Survey Bulletin 1995.

UNINTERPRETED MIGRATED SEISMIC REFLECTION DATA FOR OFFSHORE SANTA MARIA BASIN TRANSECTS, CALIFORNIA

By
Kate C. Miller and Anne S. Meltzer

1999

U.S. DEPARTMENT OF THE INTERIOR
U.S. GEOLOGICAL SURVEY

A. RU-13

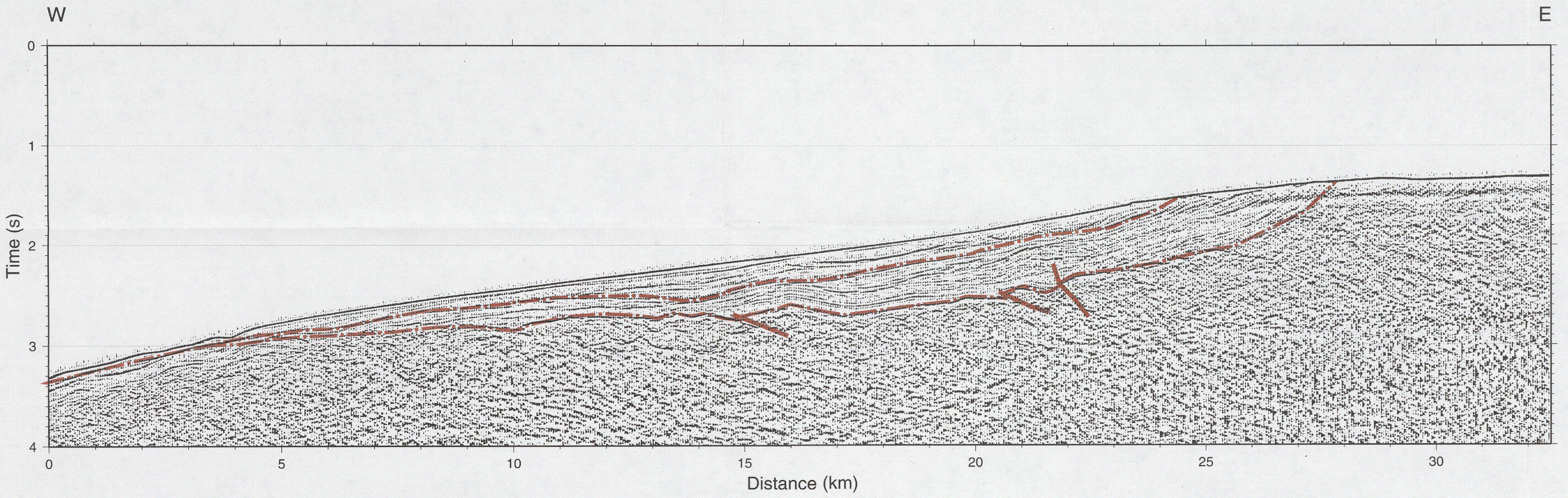

EXPLANATION

Miocene-Pliocene boundary unconformity

Top of basement unit

Fault

See index map, plates 1, 2

B. PG&E-1

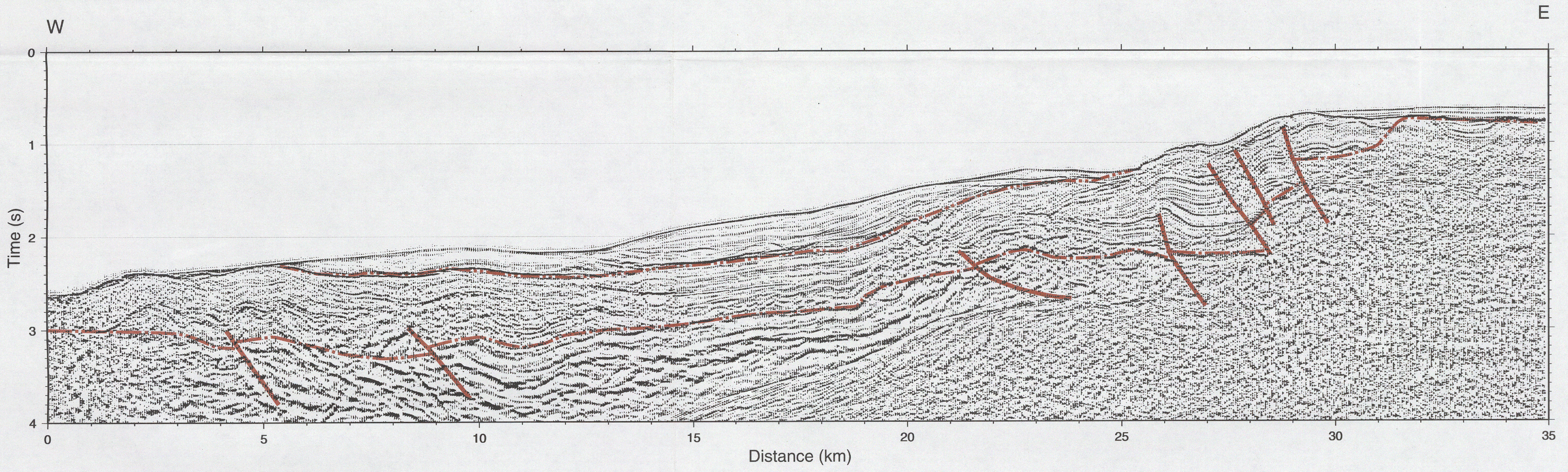

C. RU-3

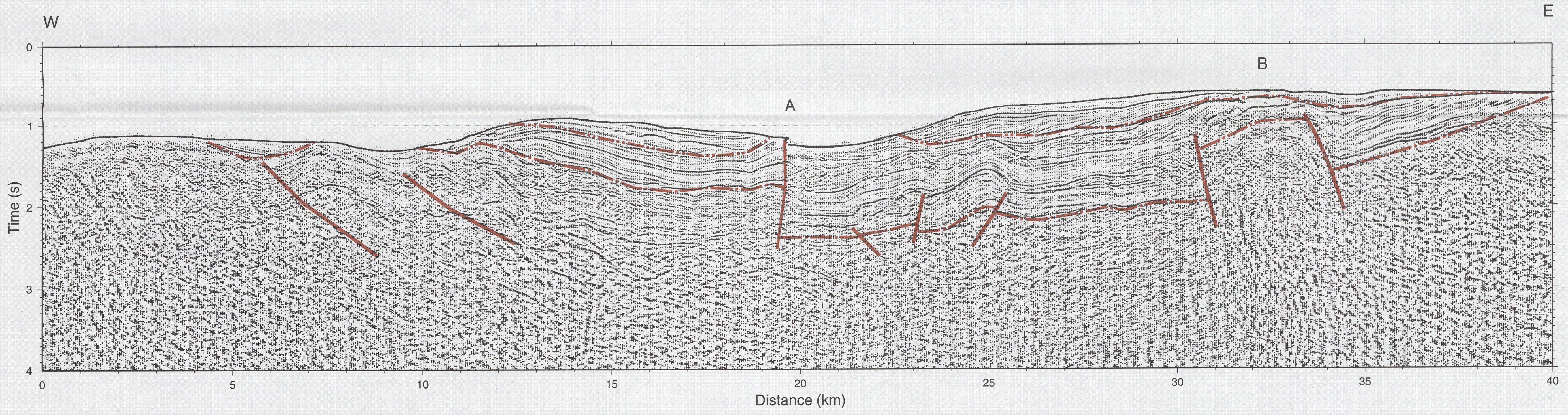

D. PG&E-3

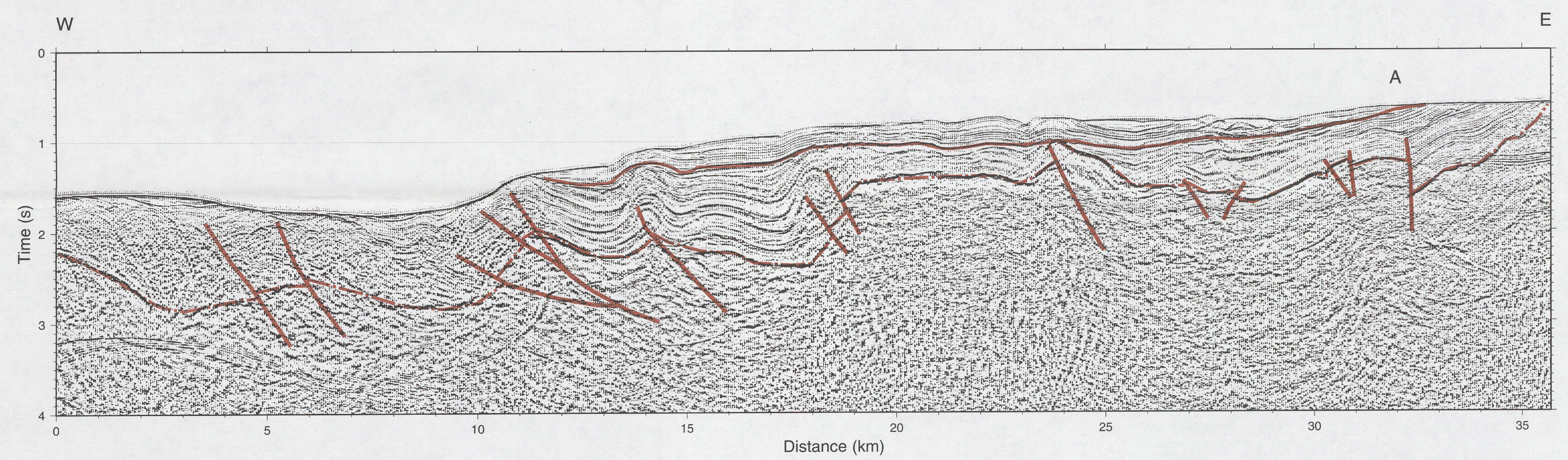

Vertical exaggeration ~2:1, assuming velocity of 2,300 m/s

INTERIOR - GEOLOGICAL SURVEY, RESTON, VA - 1999

Miller, K. C., and Meltzer, A. S., Structure and tectonics of the offshore Santa Maria and Santa Lucia basins, central California: results from the PG&E/EDGE seismic reflection survey, chapter Z of Keller, M. A., ed., Evolution of sedimentary basins/onshore oil and gas investigations—Santa Maria province: U.S. Geological Survey Bulletin 1995.

INTERPRETED MIGRATED SEISMIC REFLECTION DATA FOR OFFSHORE SANTA MARIA BASIN TRANSECTS, CALIFORNIA

By

Kate C. Miller and Anne S. Meltzer

1999

A. RU-13

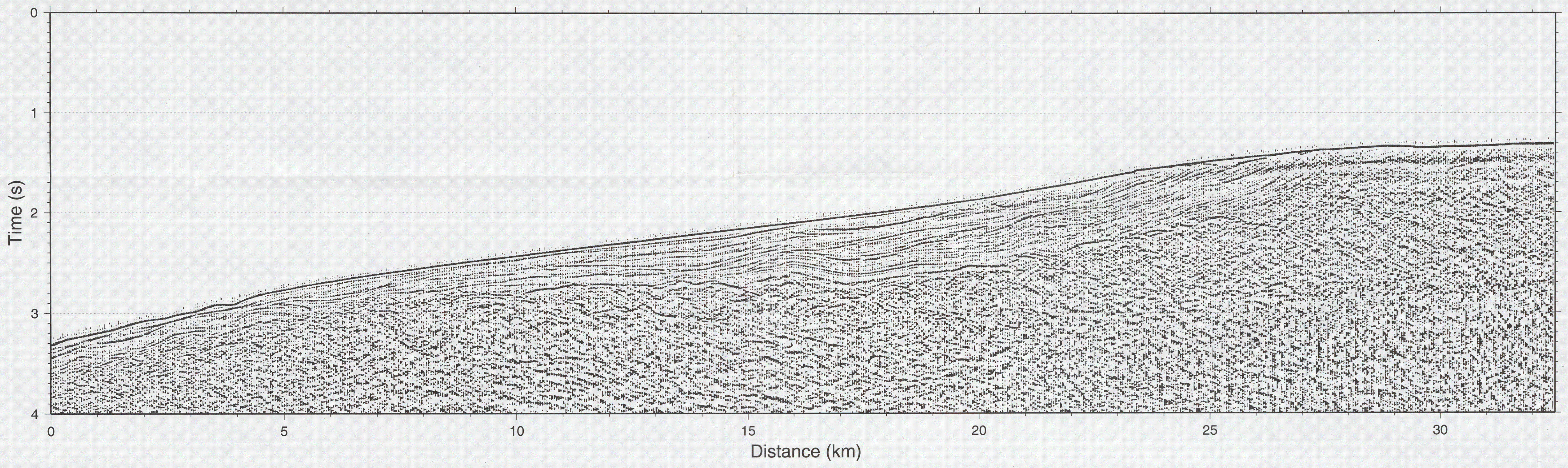

See index map, plates 1, 2

B. PG&E-1

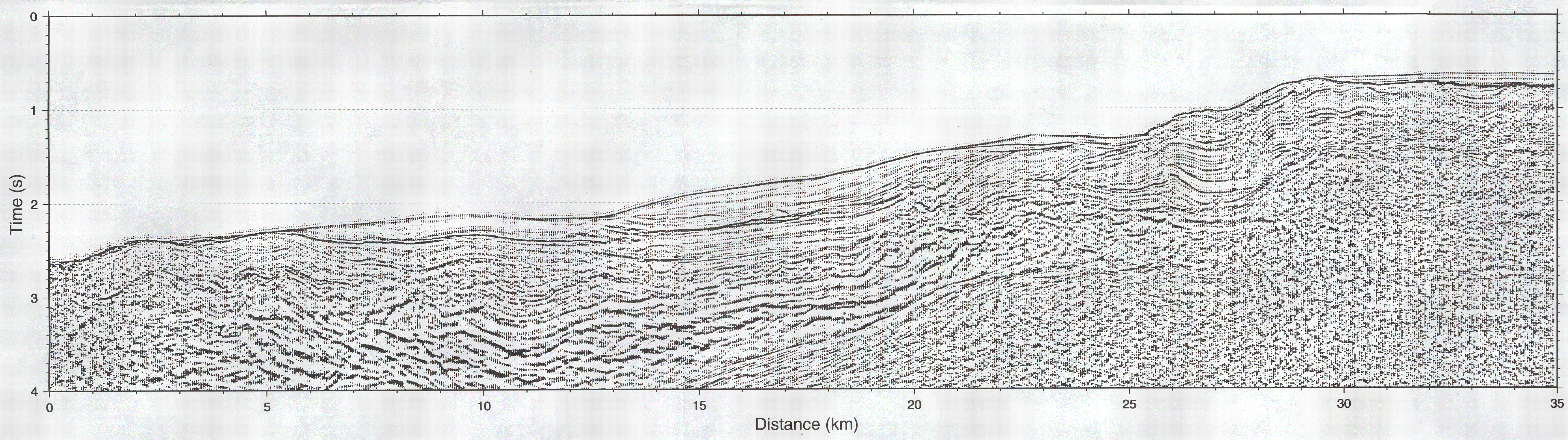

C. RU-3

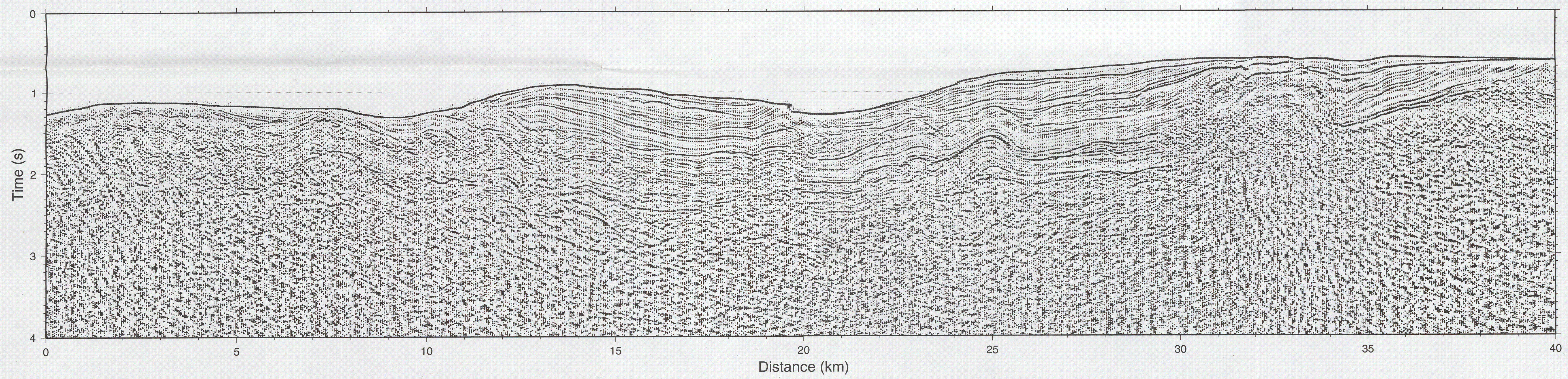

D. PG&E-3

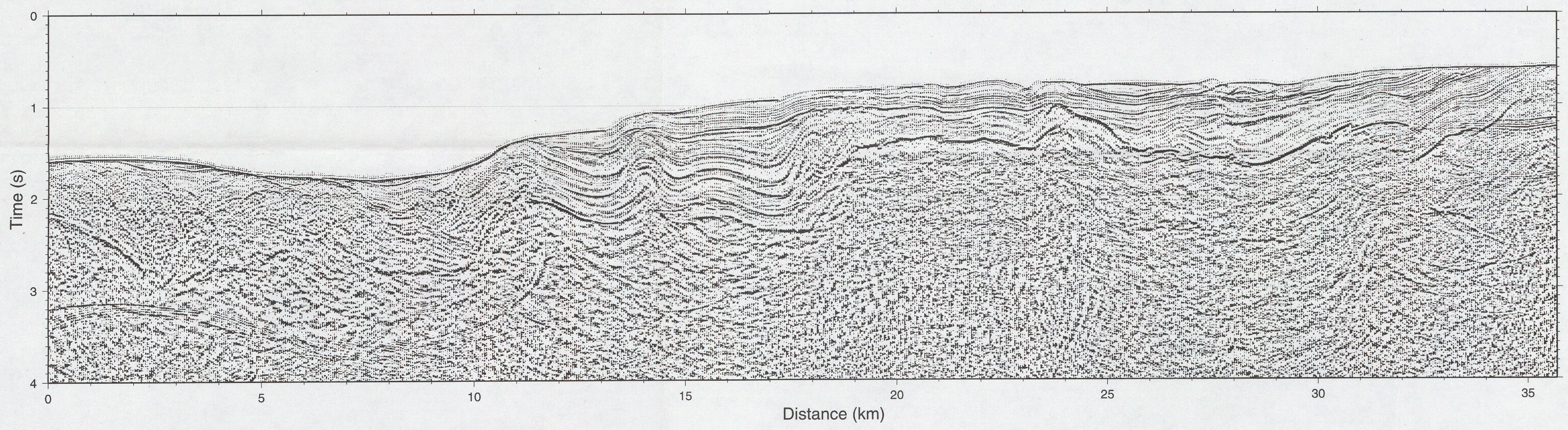

Vertical exaggeration ~2:1, assuming velocity of 2,300 m/s

INTERIOR - GEOLOGICAL SURVEY, RESTON, VA - 1999

Miller, K. C., and Meltzer, A. S., Structure and tectonics of the offshore Santa Maria and Santa Lucia basins, central California: results from the PG&E/EDGE seismic reflection survey, chapter Z of Keller, M. A., ed., Evolution of sedimentary basins/onshore oil and gas investigations— Santa Maria province: U.S. Geological Survey Bulletin 1995.

UNINTERPRETED MIGRATED SEISMIC REFLECTION DATA FOR OFFSHORE SANTA MARIA BASIN TRANSECTS, CALIFORNIA

By

Kate C. Miller and Anne S. Meltzer

1999

Selected Series of U.S. Geological Survey Publications

Books and Other Publications

Professional Papers report scientific data and interpretations of lasting scientific interest that cover all facets of USGS investigations and research.

Bulletins contain significant data and interpretations that are of lasting scientific interest but are generally more limited in scope or geographic coverage than Professional Papers.

Water-Supply Papers are comprehensive reports that present significant interpretive results of hydrologic investigations of wide interest to professional geologists, hydrologists, and engineers. The series covers investigations in all phases of hydrology, including hydrogeology, availability of water, quality of water, and use of water.

Circulars are reports of programmatic or scientific information of an ephemeral nature; many present important scientific information of wide popular interest. Circulars are distributed at no cost to the public.

Fact Sheets communicate a wide variety of timely information on USGS programs, projects, and research. They commonly address issues of public interest. Fact Sheets generally are two or four pages long and are distributed at no cost to the public.

Reports in the **Digital Data Series (DDS)** distribute large amounts of data through digital media, including compact disc-read-only memory (CD-ROM). They are high-quality, interpretive publications designed as self-contained packages for viewing and interpreting data and typically contain data sets, software to view the data, and explanatory text.

Water-Resources Investigations Reports are papers of an interpretive nature made available to the public outside the formal USGS publications series. Copies are produced on request (unlike formal USGS publications) and are also available for public inspection at depositories indicated in USGS catalogs.

Open-File Reports can consist of basic data, preliminary reports, and a wide range of scientific documents on USGS investigations. Open-File Reports are designed for fast release and are available for public consultation at depositories.

Maps

Geologic Quadrangle Maps (GQ's) are multicolor geologic maps on topographic bases in 7.5- or 15-minute quadrangle formats (scales mainly 1:24,000 or 1:62,500) showing bedrock, surficial, or engineering geology. Maps generally include brief texts; some maps include structure and columnar sections only.

Geophysical Investigations Maps (GP's) are on topographic or planimetric bases at various scales. They show results of geophysical investigations using gravity, magnetic, seismic, or radioactivity surveys, which provide data on subsurface structures that are of economic or geologic significance.

Miscellaneous Investigations Series Maps or **Geologic Investigations Series (I's)** are on planimetric or topographic bases at various scales; they present a wide variety of format and subject matter. The series also incudes 7.5-minute quadrangle photogeologic maps on planimetric bases and planetary maps.

Information Periodicals

Metal Industry Indicators (MII's) is a free monthly newsletter that analyzes and forecasts the economic health of five metal industries with composite leading and coincident indexes: primary metals, steel, copper, primary and secondary aluminum, and aluminum mill products.

Mineral Industry Surveys (MIS's) are free periodic statistical and economic reports designed to provide timely statistical data on production, distribution, stocks, and consumption of significant mineral commodities. The surveys are issued monthly, quarterly, annually, or at other regular intervals, depending on the need for current data. The MIS's are published by commodity as well as by State. A series of international MIS's is also available.

Published on an annual basis, **Mineral Commodity Summaries** is the earliest Government publication to furnish estimates covering nonfuel mineral industry data. Data sheets contain information on the domestic industry structure, Government programs, tariffs, and 5-year salient statistics for more than 90 individual minerals and materials.

The Minerals Yearbook discusses the performance of the worldwide minerals and materials industry during a calendar year, and it provides background information to assist in interpreting that performance. The Minerals Yearbook consists of three volumes. Volume I, Metals and Minerals, contains chapters about virtually all metallic and industrial mineral commodities important to the U.S. economy. Volume II, Area Reports: Domestic, contains a chapter on the minerals industry of each of the 50 States and Puerto Rico and the Administered Islands. Volume III, Area Reports: International, is published as four separate reports. These reports collectively contain the latest available mineral data on more than 190 foreign countries and discuss the importance of minerals to the economies of these nations and the United States.

Permanent Catalogs

"Publications of the U.S. Geological Survey, 1879–1961" and **"Publications of the U.S. Geological Survey, 1962–1970"** are available in paperback book form and as a set of microfiche.

"Publications of the U.S. Geological Survey, 1971–1981" is available in paperback book form (two volumes, publications listing and index) and as a set of microfiche.

Annual supplements for 1982, 1983, 1984, 1985, 1986, and subsequent years are available in paperback book form.

Keller—EVOLUTION OF SEDIMENTARY BASINS/ONSHORE OIL AND GAS INVESTIGATIONS—SANTA MARIA PROVINCE—U.S. Geological Survey Bulletin 1995–Y, Z

ISBN 0-607-92671-6

9 780607 926712

Printed on recycled paper